

Horizon 2020

Space Call - Earth Observation: EO-3-2016: Evolution of Copernicus services
Grant Agreement No. 730008

ECoLaSS

Evolution of Copernicus Land Services based on Sentinel data



D13.1

"D43.1a - Prototype Report: Improved Permanent Grassland"

Issue/Rev.: 1.0

Date Issued: 17.07.2018

submitted by:



in collaboration with the consortium partners:



submitted to:



European Commission – Research Executive Agency

This project has received funding from the European Union's Horizon 2020 Research and Innovation Programme, under Grant Agreement No. 730008.

CONSORTIUM PARTNERS

No.	PARTICIPANT ORGANISATION NAME	SHORT NAME	CITY, COUNTRY
1	GAF AG	GAF	Munich, Germany
2	Systèmes d'Information à Référence Spatiale SAS	SIRS	Villeneuve d'Ascq, France
3	JOANNEUM RESEARCH Forschungsgesellschaft mbH	JR	Graz, Austria
4	Université catholique de Louvain, Earth and Life Institute (ELI)	UCL	Louvain-la- Neuve, Belgium
5	German Aerospace Center (DLR), German Remote Sensing Data Center (DFD), Wessling	DLR	Wessling, Germany

CONTACT:

GAF AG
Arnulfstr. 199 – D-80634 München – Germany
Phone: ++49 (0)89 121528 0 – FAX: ++49 (0)89 121528 79
E-mail: copernicus@gaf.de – Internet: www.gaf.de

DISCLAIMER:

The contents of this document are the copyright of GAF AG and Partners. It is released by GAF AG on the condition that it will not be copied in whole, in section or otherwise reproduced (whether by photographic, reprographic or any other method) and that the contents thereof shall not be divulged to any other person other than of the addressed (save to the other authorised officers of their organisation having a need to know such contents, for the purpose of which disclosure is made by GAF AG) without prior consent of GAF AG. Nevertheless single or common copyrights of the contributing partners remain unconditionally unaffected.

DOCUMENT RELEASE SHEET

	NAME, FUNCTION	DATE	SIGNATURE
Author(s):	Heinz Gallaun (JR) Petra Miletich (JR) Annekatrin Metz-Marconcini (DLR) Regine Richter (GAF) Christopher Sandow (GAF) Linda Moser (GAF) Christophe Sannier (SIRS) Sophie Villerot (SIRS)	15.06.2018	
Review:	Petra Miletich (JR) Heinz Gallaun (JR) Markus Probeck (GAF) Linda Moser (GAF)	07.07.2018	
Approval:	Linda Moser (GAF)	17.07.2018	
Acceptance:	Massimo Ciscato (REA)		
Distribution:	Public		

DISSEMINATION LEVEL

DISSEMINATION LEVEL		
PU	Public	<input checked="" type="checkbox"/> X
CO	Confidential: only for members of the consortium (including the Commission Services)	

DOCUMENT STATUS SHEET

ISSUE/REV	DATE	PAGE(S)	DESCRIPTION / CHANGES
1.0	17.07.2018	63	First issue of WP43 Deliverable

APPLICABLE DOCUMENTS

ID	DOCUMENT NAME / ISSUE DATE
AD01	Horizon 2020 Work Programme 2016 – 2017, 5 iii. Leadership in Enabling and Industrial Technologies – Space. Call: EO-3-2016: Evolution of Copernicus services. Issued: 13.10.2015
AD02	Guidance Document: Research Needs Of Copernicus Operational Services. Final Version issued: 30.10.2015
AD03	Proposal: Evolution of Copernicus Land Services based on Sentinel data. Proposal acronym: ECoLaSS, Proposal number: 730008. Submitted: 03.03.2016
AD04	Grant Agreement – ECoLaSS. Grant Agreement number: 730008 – ECoLaSS – H2020-EO-2016/H2020-EO-2016, Issued: 18.10.2016
AD05	D6.1: D31.1a - Methods Compendium: Sentinel-1/2/3 Integration Strategies, (Issue 1), Issued: March 2018
AD06	D7.1: D32.1a- Methods Compendium: Time Series Preparation, (Issue 1), Issued: February 2018
AD07	D8.1 : D33.1a - Methods Compendium: Time Series Analysis for Thematic Classification (Issue 1), Issued: 29.03.2018
AD08	D9.1 : D34.1a - Methods Compendium: Time Series Analysis for Change Detection (Issue 1), Issued: 29.03.2018
AD09	D3.1 : D21.1a – Service Evolution Requirements Report (Issue 1), Issued: 09.08.2017
AD10	D2.1 : D12.1a – DWH use for 2017 (Issue 1), Issued: 29.09.2017

EXECUTIVE SUMMARY

The Horizon 2020 (H2020) project, “Evolution of Copernicus Land Services based on Sentinel data” (ECoLaSS) addresses the H2020 Work Programme 5 iii. Leadership in Enabling and Industrial technologies - Space, specifically the Topic EO-3-2016: Evolution of Copernicus services. ECoLaSS is being conducted from 2017–2019 and aims at developing and prototypically demonstrating selected innovative products and methods for future next-generation operational Copernicus Land Monitoring Service (CLMS) products of the pan-European and Global Components. This will contribute to demonstrating operational readiness of the finally selected products, and shall allow the key CLMS stakeholders (i.e. mainly the Entrusted European Entities (EEE) EEA and JRC) to take informed decisions on potential procurement of the next generation of Copernicus Land services from 2020 onwards.

To achieve this goal, ECoLaSS makes full use of dense time series of Sentinel-2 and Sentinel-3 optical data as well as Sentinel-1 Synthetic Aperture Radar (SAR) data. Rapidly evolving scientific as well as user requirements are analysed in support of a future pan-European roll-out of new/improved CLMS products, and the transfer to global applications.

This report constitutes a prototype report of the work package (WP) 43 “Improved Permanent Grassland Identification”, directly building on the methods and processing lines developed by Task 3, especially WP 33 “Time Series Analysis for Thematic Classification”, and demonstrates a grassland prototype for future potential Copernicus Land Monitoring Service (CLMS) products of the pan-European Component, which is improved compared to previous approaches such as e.g. the Copernicus HRL Grassland 2015 and will tackle improvement of the upcoming HRL Grassland 2018.

The objective of this WP is to develop a framework for an improved identification of grassland areas using Sentinel time series with the aim to develop a prototype of a European HR Grassland Layer with high thematic accuracy, optical and SAR data integration, increased spatial resolution and high automation level as well as (mid-term) increased thematic content. Together with the outcomes of the other WPs of ECoLaSS Task 3 (Automated High Data Volume Processing Lines) and Task 4 (Thematic Proof-Of-Concept), it constitutes a basis for the investigation activities of Task 5 (Operationalisation Framework).

Section 1 of the document explains the purpose and objectives of WP 43. Section 2 presents the background of Copernicus Grassland monitoring needs and the summary of related requirements. Section 3 gives a short summary and description of the demonstration sites. In section 4, an overview of the applied time series analysis methods is given based on the results and recommendations of WP 33 “Time Series Analysis for Thematic Classification”. It reviews specifically the multi-sensor data integration methods, the usage of multi-temporal time series metrics, the random forest classification approach and the validation analysis procedure. Based on these reviews, section 5 details the prototype implementation approaches, including a description of the input data, pre-processing lines, the experimental setup, and the final validation of the prototype.

The ECoLaSS project follows a two-phased approach of two times 18 months duration. This deliverable constitutes the first issue, in which preliminary results up to month 18 are presented. In the second 18-month project cycle, a second issue of this deliverable will be published, containing all final results.

Table of Contents

1	INTRODUCTION	1
2	BACKGROUND AND SUMMARY OF REQUIREMENTS	2
3	DEMONSTRATION SITES.....	3
3.1	ECoLaSS DEMONSTRATION SITES	3
3.2	DEMONSTRATION SITE WEST FOR GRASSLAND	5
4	OVERVIEW OF APPLIED METHODS.....	6
4.1	MULTI-SENSOR DATA INTEGRATION	6
4.2	MULTI-TEMPORAL SAR AND OPTICAL METRICS	6
4.2.1	Spectral Optical Indices	7
4.2.2	Multi-seasonal Features	12
4.3	RANDOM FOREST CLASSIFICATION APPROACH	13
4.4	VALIDATION ANALYSIS PROCEDURE.....	13
5	PROTOTYPE IMPLEMENTATION.....	16
5.1	DATA AND PROCESSING SETUP	16
5.1.1	Input Data and Data Integration.....	16
5.1.2	Pre-processing	19
5.1.3	Multi-temporal statistic features.....	19
5.1.4	Experimental Setup	24
5.2	CLASSIFICATION RESULTS AND VALIDATION	36
5.2.1	Feature selection results	36
5.2.2	Prototype Validation.....	37
5.2.3	HRL2015 Comparison with an Independent Data Source	39
5.3	PROTOTYPE SPECIFICATIONS	43
6	CONCLUSION AND OUTLOOK	46
REFERENCES.....		49
ANNEXE 1		52

List of Figures and Tables

Figure 3-1: European Demonstration Sites (modified from: EEA, 2015)	4
Figure 3-2: Overview of DEMO Site WEST.....	5
Figure 4-1: Confusion Matrix for Accuracy Assessment of thematic map product	14
Figure 5-1: (left): Example of grassland areas in S-1 false colour composite of bands STD_VH (R), Mean_VV (G), and CoV_VH (B) of 2017 for Huldenberg. (right): ArcGIS Basemap (25.09.2016) with LGP grassland polygons in red (2016).....	20
Figure 5-2: (left) Example of grassland areas in S-1 false colour composite of bands STD_VH (R), Mean_VV (G), and CoV_VH (B) of 2017 for area Huldenberg. (right) ArcGIS Basemap (25.09.2016) with LGP grassland polygons in red.	20
Figure 5-3: Feature importance of the forest for annual vegetation indices (median).	21
Figure 5-4: (left) Example of grassland areas in S-2 false colour composite of bands SWIR1 (R), NNIR (G), and Green (B) of 2017 for area Huldenberg. (right) ArcGIS Basemap (25.09.2016) with LGP grassland polygons in red.	22
Figure 5-5: (left) Example of grassland areas in S-2 false colour composite of bands EVI (R), TCB (G), and TCG (B) of 2017 for area Huldenberg. (right) ArcGIS Basemap (25.09.2016) with LGP grassland polygons in red.	22
Figure 5-6: Feature importance of the forest for seasonal statistical reflectance features (median).....	23
Figure 5-7: (left): Example of grassland areas in S-2 seasonal false colour composite of bands NNIR March-April (R), NNIR July-August (G), and NNIR September-October (B) of 2017 for area Huldenberg. (right): ArcGIS Basemap (25.09.2016) with LGP grassland polygons in red.....	24
Figure 5-8: Spectral signatures of the 5 grassland types: green urban areas (rose) and sports and leisure areas (red) of the UA data set, as well as grassland (agriculturally used) (green), pastures with trees (blue), and natural grasslands (yellow) of the Belgian reference data set over the course of 2017 of the 16 indices: (a) Clgreen, (b) CIRedEdge, (c) EVI, (d) MCARI/OSAVI, (e) MTCI, (f) NBR, (g) NDMI, (h) NDRE1, (i) NDRE2, (j) NDVI, (k) REP, (l) TCARI/OSAVI, (m) SAVI, (n) TCB, (o) TCG, and (p) TCW.	27
Figure 5-9: Feature importance for the combination of SAR and seasonal optical features.....	28
Figure 5-10: (left) Classification result of SAR + seasonal detailed view of 33UFS compared to (right) WV03 image (R:IR2;G:Red;B:Green) from 14.03.2017 with LGP grassland polygons in yellow (2016).....	28
Figure 5-11: (left) aggregated classification result of SAR + seasonal detailed view of 33UFS compared to (right) WV03 image (R:IR2;G:Red;B:Green) from 14.03.2017 with LGP grassland polygons in yellow (2016).	29
Figure 5-12: Feature importance for the combination of SAR, vegetation indices seasonal optical features.	30
Figure 5-13: (left) Classification result of SAR + VI + seasonal detailed view of 33UFS compared to (right) WV03 image (R:IR2;G:Red;B:Green) from 14.03.2017 with LGP grassland polygons in yellow (2016).....	30
Figure 5-14: (left) Aggregated classification result of SAR + VI + seasonal detailed view of 33UFS compared to (right) WV03 image (R:IR2;G:Red;B:Green) from 14.03.2017 with LGP grassland polygons in yellow (2016)	31
Figure 5-15: Feature importance for the combination of SAR, annual and seasonal optical features.....	32
Figure 5-16: (left) Classification result of SAR + OPT + seasonal detailed view of 33UFS compared to (right) WV03 image (R:IR2;G:Red;B:Green) from 14.03.2017 with LGP grassland polygons in yellow (2016).....	32
Figure 5-17: (left) Aggregated classification result of SAR + OPT + seasonal detailed view of 33UFS compared to (right) WV03 image (R:IR2;G:Red;B:Green) from 14.03.2017 with LGP grassland polygons in yellow (2016).	33
Figure 5-18: Feature importance for the combination of SAR, annual statistical vegetation indices, annual and seasonal optical features.....	34
Figure 5-19: (left) Classification result of SAR + OPT + VI + seasonal detailed view of 33UFS compared to (right) WV03 image (R:IR2;G:Red;B:Green) from 14.03.2017 with LGP grassland polygons in yellow (2016).	34

Figure 5-20: (left) Aggregated classification result of SAR + OPT + VI + seasonal detailed view of 33UFS compared to (right) WV03 image (R:IR2;G:Red;B:Green) from 14.03.2017 with LGP grassland polygons in yellow (2016).....	35
Figure 5-21: (left) Classification result of SAR + OPT + VI + seasonal detailed view of 33UFS compared to (right) WV03 image (R:IR2;G:Red;B:Green) from 14.03.2017 with LGP grassland polygons in yellow (2016).	38
Figure 5-22: Example of orchards. Aggregated (MMU = 1ha) classification result (left) detailed view of 33UFS for SAR + OPT + VI + seasonal compared to (right) ArcGIS Basemap (25.09.2016).....	38
Figure 5-23: Unfiltered comparison of the HRL GRA 2015 and the ECoLaSS prototype 2017: grassland in both layers (green), grassland only in the ECoLaSS prototype (red), and only in the HRL GRA 2015 (blue).	40
Figure 5-24: Filtered comparison of the HRL GRA 2015 and the ECoLaSS prototype 2017: grassland in both layers (green), grassland only in the ECoLaSS prototype (blue), and only in the HRL GRA 2015 (red).....	41
Figure 6-1: Comparison of an agricultural pixel to a grassland pixel.	47
Figure 6-2: Greenness trend and amplitudes of an agriculture and grassland pixel.	47
Figure 6-3: Overview of the MEAN spectral signature of the index Clgreen for all five grassland types (a) as well as the MEAN +/- the standard deviation for the single five grassland types: (b) green urban areas, (c) sports and leisure areas, (d) pastures with trees, (e) grassland (agriculturally used), and (f) natural grasslands.	52
Figure 6-4: Overview of the MEAN spectral signature of the index CIRedEdge for all five grassland types (a) as well as the MEAN +/- the standard deviation for the single five grassland types: (b) green urban areas, (c) sports and leisure areas, (d) pastures with trees, (e) grassland (agriculturally used), and (f) natural grasslands.	53
Figure 6-5: Overview of the MEAN spectral signature of the index EVI for all five grassland types (a) as well as the MEAN +/- the standard deviation for the single five grassland types: (b) green urban areas, (c) sports and leisure areas, (d) pastures with trees, (e) grassland (agriculturally used), and (f) natural grasslands.	54
Figure 6-6: Overview of the MEAN spectral signature of the index MCARI/OSAVI for all five grassland types (a) as well as the MEAN +/- the standard deviation for the single five grassland types: (b) green urban areas, (c) sports and leisure areas, (d) pastures with trees, (e) grassland (agriculturally used), and (f) natural grasslands.	55
Figure 6-7: Overview of the MEAN spectral signature of the index MTCI for all five grassland types (a) as well as the MEAN +/- the standard deviation for the single five grassland types: (b) green urban areas, (c) sports and leisure areas, (d) pastures with trees, (e) grassland (agriculturally used), and (f) natural grasslands.	55
Figure 6-8: Overview of the MEAN spectral signature of the index NBR for all five grassland types (a) as well as the MEAN +/- the standard deviation for the single five grassland types: (b) green urban areas, (c) sports and leisure areas, (d) pastures with trees, (e) grassland (agriculturally used), and (f) natural grasslands.	56
Figure 6-9: Overview of the MEAN spectral signature of the index NDMI for all five grassland types (a) as well as the MEAN +/- the standard deviation for the single five grassland types: (b) green urban areas, (c) sports and leisure areas, (d) pastures with trees, (e) grassland (agriculturally used), and (f) natural grasslands.	57
Figure 6-10: Overview of the MEAN spectral signature of the index NDRE1 for all five grassland types (a) as well as the MEAN +/- the standard deviation for the single five grassland types: (b) green urban areas, (c) sports and leisure areas, (d) pastures with trees, (e) grassland (agriculturally used), and (f) natural grasslands.	58
Figure 6-11: Overview of the MEAN spectral signature of the index NDRE2 for all five grassland types (a) as well as the MEAN +/- the standard deviation for the single five grassland types: (b) green urban areas, (c) sports and leisure areas, (d) pastures with trees, (e) grassland (agriculturally used), and (f) natural grasslands.	58
Figure 6-12: Overview of the MEAN spectral signature of the index NDVI for all five grassland types (a) as well as the MEAN +/- the standard deviation for the single five grassland types: (b) green urban areas, (c)	

sports and leisure areas, (d) pastures with trees, (e) grassland (agriculturally used), and (f) natural grasslands.....	59
Figure 6-13: Overview of the MEAN spectral signature of the index REP for all five grassland types (a) as well as the MEAN +/- the standard deviation for the single five grassland types: (b) green urban areas, (c) sports and leisure areas, (d) pastures with trees, (e) grassland (agriculturally used), and (f) natural grasslands.....	60
Figure 6-14: Overview of the MEAN spectral signature of the index SAVI for all five grassland types (a) as well as the MEAN +/- the standard deviation for the single five grassland types: (b) green urban areas, (c) sports and leisure areas, (d) pastures with trees, (e) grassland (agriculturally used), and (f) natural grasslands.....	61
Figure 6-15: Overview of the MEAN spectral signature of the index TCB for all five grassland types (a) as well as the MEAN +/- the standard deviation for the single five grassland types: (b) green urban areas, (c) sports and leisure areas, (d) pastures with trees, (e) grassland (agriculturally used), and (f) natural grasslands.....	61
Figure 6-16: Overview of the MEAN spectral signature of the index TCG for all five grassland types (a) as well as the MEAN +/- the standard deviation for the single five grassland types: (b) green urban areas, (c) sports and leisure areas, (d) pastures with trees, (e) grassland (agriculturally used), and (f) natural grasslands.....	62
Figure 6-17: Overview of the MEAN spectral signature of the index TCW for all five grassland types (a) as well as the MEAN +/- the standard deviation for the single five grassland types: (b) green urban areas, (c) sports and leisure areas, (d) pastures with trees, (e) grassland (agriculturally used), and (f) natural grasslands.....	63

Table 3-1: Description of the selected Demonstration Sites.....	4
Table 5-1: Used Sentinel-2 reflectance bands (adapted from Suhet, 2015).....	17
Table 5-2: VHR data available for the demonstration site WEST.....	17
Table 5-3: VIRP reference dataset codes.....	18
Table 5-4: SAR annual statistical features.....	19
Table 5-5: Used vegetation indices. (Xue and Su, 2017; Clevers et al., 2013; Wu et al., 2008).....	21
Table 5-6: Error matrix (non-area-weighted) for SAR + seasonal features grassland mapping.....	29
Table 5-7: Error matrix (non-area-weighted) for SAR + VI + seasonal features grassland mapping.....	31
Table 5-8: Error matrix (non-area-weighted) for SAR + OPT + seasonal features grassland mapping	33
Table 5-9: Error matrix (non-area-weighted) for SAR + VI + OPT + seasonal features grassland mapping	35
Table 5-10: Detailed class statistics for grassland mapping 2017 for different feature selections. Accuracy parameters are in percent (non-area-weighted).	36
Table 5-11: Internal validation results for the SAR + OPT+ VI + seasonal product (area-weighted plausibility approach).	37
Table 5-12 - Validation results for the SAR + OPT+ VI + seasonal product (area-weighted blind approach)	37
Table 5-13: Comparison between the HRL Grassland layer 2015 and the adapted VIRP 2017	39
Table 5-14: Accuracies for HRL Grassland using the adapted VIRP 2017 as Reference.....	39
Table 5-15: Comparative Grassland statistic (HRL 2015, ECoLaSS 2017) for the demonstration site West	40
Table 5-16: Types of omission errors for HRL GRA 2015 and the ECoLaSS prototype 2017	42
Table 5-17: Types of commission errors for HRL GRA 2015 and the ECoLaSS prototype 2017	42
Table 5-18: Grassland prototype specifications.....	45

Abbreviations

AGRI	Agriculture
AVHRR	Advanced Very High Resolution Radiometer
CE	Central
CI_green	Green Chlorophyll Index
CI_red_edge	Red Edge Chlorophyll Index
CLMS	Copernicus Land Monitoring Services
CORINE	Coordination of Information on the Environment
CoV	Coefficient of Variation
CRM	Crop Mask
CRT	Crop Type
DIFF	Difference Feature
DLT	Dominant Leave Type
DWH	Data Warehouse
ECoLaSS	Evolution of Copernicus Land Services based on Sentinel data
EEA	European Environment Agency
EEA39	39 European countries
EEE	Entrusted European Entities
EO	Earth Observation
ESA	European Space Agency
EVI	Enhanced Vegetation Index
GC	Ground cover
GIS	Geographic Information System
GRA	Grassland
GRD	Ground Range Detected
H2020	Horizon 2020
HR	High Resolution
HRL	High Resolution Layer
IMC	Imperviousness degree change
IMD	Imperviousness degree
IMP	Imperviousness
INSPIRE	Infrastructure for Spatial Information in the European Community
ISO	International Organization for Standardization
IW	Interferometric Wide Swath Mode
JECAM	Joint Experiment for Crop Assessment and Monitoring network
JRC	Joint Research Centre
LAEA	Lambert azimuthal equal-area projection
LC	Land cover
LGP	Grassland Reference Polygons (Landbouwgebruikspercelen ALV)
LPIS	Land Parcel Identification System
LU	Land use
LUCAS	Land Use/Cover Area frame statistical Survey
LZW	Lempel–Ziv–Welch
MA	Mali
MAX	Maximum
MCARI	Modified Chlorophyll Absorption Ratio Index
MEAN	Mean
MIN	Minimum
MMU	Minimum Mapping Unit
MODIS	Moderate Resolution Imaging Spectroradiometer
MSAVI	Modified Soil-Adjusted Vegetation Index
MSGI	Metadata Standard for Geographic Information
MTCI	MERIS Terrestrial Chlorophyll Index

MTV2	Modified Triangular Vegetation Index (2)
NBR	Normalized Burn Ratio
NDII	Normalized Difference Infrared Index
NDMI	Normalized Difference Moisture Index
NDRE	Normalized Difference Red Edge Index
NDRE1	Normalized Difference Red Edge Index (1)
NDRE2	Normalized Difference Red Edge Index (2)
NDSVI	Normalized Difference Senescence Vegetation Index
NDVI	Normalized Difference Vegetation Index
NDWI	Normalized Difference water index
NIR	Near-InfraRed, Sentinel-2 – Near-InfraRed – B8
NNIR	Sentinel-2 – Short Wavelength Infrared – B8a
NO	North
OA	Overall Accuracy
OPT	Optical
OSAVI	Optimized Soil-Adjusted Vegetation Index
PA	Producer Accuracy
PSRI	Plant Senescence Reflectance Index
REP	Red-Edge Position
RF	Random Forest
RGR	Red-Green Ratio
S-1	Sentinel-1
S-2	Sentinel-2
S-3	Sentinel-3
SA	South Africa
SAR	Synthetic Aperture Radar
SAVI	Soil-Adjusted Vegetation Index
SE	Southeast
STD	Standard deviation
SW	Southwest
SWIR	Short Wavelength Infrared
SWIR1	Sentinel-2 – Short Wavelength Infrared – B11
SWIR2	Sentinel-2 - Short – B12
TCARI	Transformed Chlorophyll Absorption Ratio Index
TCB	Tasseled Cap Brightness
TCC	Tree Cover Change
TCG	Tasseled Cap Greenness
TCW	Tasseled Cap Brightness
UA	User Accuracy
USA	United States of America
VH	Vertical transmit/Horizontal receive (polarization)
VHR	Very High Resolution
VI	Vegetation Indices
VIRP	Visually interpreted reference points
VRE1	Sentinel-2 - Vegetation Red Edge – B5
VRE2	Sentinel-2 - Vegetation Red Edge – B6
VRE3	Sentinel-2 - Vegetation Red Edge – B7
VV	Vertical transmit/Vertical receive (polarization)
WE	West
WI	Wetness Index
WP	Work Package
XML	Extensible Markup Language

1 Introduction

The Horizon 2020 (H2020) project, “Evolution of Copernicus Land Services based on Sentinel data” (ECoLaSS) addresses the H2020 Work Programme 5 iii. Leadership in Enabling and Industrial technologies - Space, specifically the Topic EO-3-2016: Evolution of Copernicus services. ECoLaSS is being conducted from 2017–2019 and aims at developing and prototypically demonstrating selected innovative products and methods for future next-generation operational Copernicus Land Monitoring Service (CLMS) products of the pan-European and Global Components. This will contribute to demonstrating operational readiness of the finally selected products, and shall allow the key CLMS stakeholders (i.e. mainly the Entrusted European Entities (EEE) EEA and JRC) to take informed decisions on potential procurement of the next generation of Copernicus Land services from 2020 onwards.

To achieve this goal, ECoLaSS makes full use of dense time series of Sentinel-2 and Sentinel-3 optical data as well as Sentinel-1 Synthetic Aperture Radar (SAR) data. Rapidly evolving scientific as well as user requirements are analysed in support of a future pan-European roll-out of new/improved CLMS products, and the transfer to global applications.

This Deliverable **D13.1 - D43.1a - Prototype Report: Improved Permanent Grassland (Issue 1)** comprises a description of the provided prototype datasets of Improved Permanent Grassland products (linked to Deliverable P43.2). It provides a detailed description of the objectives together with an explanation of the methodology, results and conclusions, as derived by WP 43. It addresses the prototype methodologies for preparation of in-situ reference and validation data sets, application of different grassland classification algorithms (as described in WP 33) in the defined demonstration site WEST covering parts of Belgium and France, accuracy assessment for the grassland product prototype results, and optimisation of the algorithms described in WP 33 based on the assessment results. As such, it is part of WP 43 of Task 4: “Thematic Proof-of-Concept/Prototype on Continental/Global Scale”, which aims at exploring and setting up a robust classification approach for an improved identification of permanent grasslands based on Sentinel-2 and Sentinel-1 time series and in-situ data for pan-European land monitoring. This report will be accompanied by the Deliverable **D13.3 - P43.2a - Data Sets of HRL Permanent Grassland Products (Issue 1)**. This report serves as documentation for the prototype dataset.

In the ECoLaSS project a prototype is defined as a prototypic / thematic proof-of-concept implementation of an improved or newly defined potential future Copernicus Land layer, building on the methods and processing lines developed in Task 3. The consortium has selected representative demonstration sites both in Europe and Africa, covering various bio-geographic regions and biomes. All prototype products and services are being prototypically implemented in a selection of these sites in the frame of the Task 4 WPs. In ECoLaSS, proofs-of-concept / prototype demonstrations are carried out with respect to five topics of relevance: (i) Time series derived indicators and variables, (ii) Incremental Updates of HR Layers, (iii) Improved permanent grassland identification, (iv) Crop area and crop status / parameters monitoring, and (v) New LC/LU products. This deliverable focusses on the prototype GRASSLAND (GRA) as part of WP 43.

This report constitutes the first issue, in which preliminary results up to month 18 are presented. In the second 18-month project cycle, a second issue of this deliverable will be published, containing all final results. It is comprised of six sections. Section 1 of the document is this introduction explaining the purpose and objectives of WP 43 as well as the document structure. Section 2 presents the background of CLMS grassland monitoring needs and the related summary of requirements. Section 3 gives a short summary and description of the demonstration sites. Section 4 gives an overview of the time series analysis methods which have been chosen based on the results and recommendations of WP 33 “Time Series Analysis for Thematic Classification”. It reviews the multi-sensor data integration methods, the use of multi-temporal time series metrics, the random forest classification approach and the validation analysis procedure. Based on these reviews, section 5 details the prototype implementation approach including a description of the input data, pre-processing lines, the experimental setup, and the final validation of the prototype.

2 Background and Summary of Requirements

After first methods have been tested by the Task 3, the demonstration activities of Task 4 show the implementation of the developed advanced processing lines for prototyping. The prototype for “improved permanent grassland” delivers new methodologies using Sentinel time series with the aim to develop a prototype of a next-generation European HR Grassland Layer with high thematic accuracy. The improvement of permanent grassland identification targets to enhance the specifications and quality of the current generation of HRL Grassland products, such as implemented by the EEA for the reference time step 2015 and presumably similar for the reference time step 2018 (to be confirmed when the Call for Tender will be published by the EEA later in 2018). The development is based on the experiences of the HRL Grassland 2015 production being the baseline for improvement, as well as high-priority user requirements that are regularly updated and documented in WP21.

The HRL Grassland 2015 is the first layer of its kind, as the previous HRL Natural Grassland with the reference year 2012 suffered from technical constraints and accuracy limitations leading to a quite restricted definition of *natural* grassland to be detected. The current HRL 2015 Grassland layer, however, shows a completely new product, comprising natural, semi-natural and managed grasslands of the EEA39 countries at 20m spatial resolution and with a minimum mapping unit of 1ha. The layer represents the full range of grassland types and covers all typical grassland landscapes of Europe.

The HRL Grassland 2015 production used a multi-seasonal, multi-temporal and multi-sensor approach. The layer was produced by using a combined optical/SAR data analysis approach based on data from the reference period 2015 +/- 1 year. Image segments derived from multi-temporal, best-suited optical EO data were utilized to classify the multi-temporal data base of both optical and SAR input data. Automatically and manually derived training samples of the main land use classes were selected and applied in a supervised multi-temporal classification approach to compute grassland maps from both sensor types. A subsequent rule-based evaluation finally defined the optimum grassland mask. Additionally, recent and historic bare soil masks helped to identify grassland areas that show a ploughing indication and therefore were excluded from the mask. The result was a pan-European grassland/non-grassland mask showing an overall thematic accuracy of 94.32% and for the grassland class a user accuracy of 85.9% and a producer accuracy of 77.8 %. These are internal validation results provided by the HRL 2015 consortium. It was based on open source VHR images in combination with the multi-temporal, multi-seasonal EO data base (e.g. Sentinel-2, Landsat) used for production.

Despite the high quality of the present pan-European HRL Grassland 2015 layer, there is potential for enhancement and improvement of the methodological approach in order to further accelerate production speed, optimise the overall and regional reliability of the classification, to reduce data gaps, increase the spatial resolution and to include further user needs. Main requirements from users for the prototype developments have been collected in WP21 and 51, as well as from current developments in Copernicus, and can be summarized as follows:

- Design a refined and sound workflow with an **improved level of automation** to allow a faster production and shorter monitoring intervals (e.g. yearly updates)
- Improve the **thematic classification accuracy**
- Fully exploit **optical Sentinel-2 time series** instead of using pre-selected, best-suited EO data scenes
- Design a fully **integrated SAR/optic** time series data analysis to benefit from the multi-sensor characteristics
- Provide a **seamless, wall-to-wall product** (maximally reduced data gaps due to cloud cover)

- Improve the status layer's detail from 20m **spatial resolution to 10m**. Product definitions consequently might have to be adapted, such as e.g. the Minimum Mapping Unit
- Investigate a **future change detection** approach to detect grassland increase and decrease
- Include **more seasonal information** with respect to the grassland's phenological/vitality behaviour that can be further exploited in order to support further **grassland discrimination** between e.g. intensively managed (frequently cut grassland) and extensively managed (more natural, extensively used or grazed grassland)

The methodologies tested for the grassland prototype development are described in the following chapters. They address the abovementioned user demands and try to provide the best trade-off between grassland classification accuracy, level of automation and time-series integration.

3 Demonstration Sites

All prototypes are implemented in selected representative demonstration sites, which cover various biogeographic regions and biomes. The Improved Primary Status Layer for Grassland is demonstrated in the WEST (Belgium) Demonstration site. In phase 2 the developed processing line on grassland identification will be implemented on the demonstration sites SOUTH-EAST and CENTRAL.

3.1 ECoLaSS Demonstration Sites

The selected larger demonstration sites (60,000/90,000km² per demonstration site) contain the 5 test sites from Task 3. These demonstration sites are relevant in Task 4 for demonstrating the proposed candidates for a Copernicus Land Service Evolution roll-out on a larger scale. As shown in Figure 3-1, the pre-selected demonstration sites West covered the Atlantic and Continental zones (Source EEA: <http://www.eea.europa.eu/data-and-maps/data/biogeographical-regions-europe-3#tab-gis-data>) of the member and associated states of the EEA-39. The ECoLaSS demonstration sites are located in the **North of Europe, in the Alpine/Central region, in the West, in the South-West and in the South-East of Europe**. All prototype products and services will be prototypically implemented in one or more demonstration sites in project phase 1, and in three demonstration sites in phase 2 (including the sites of phase 1).

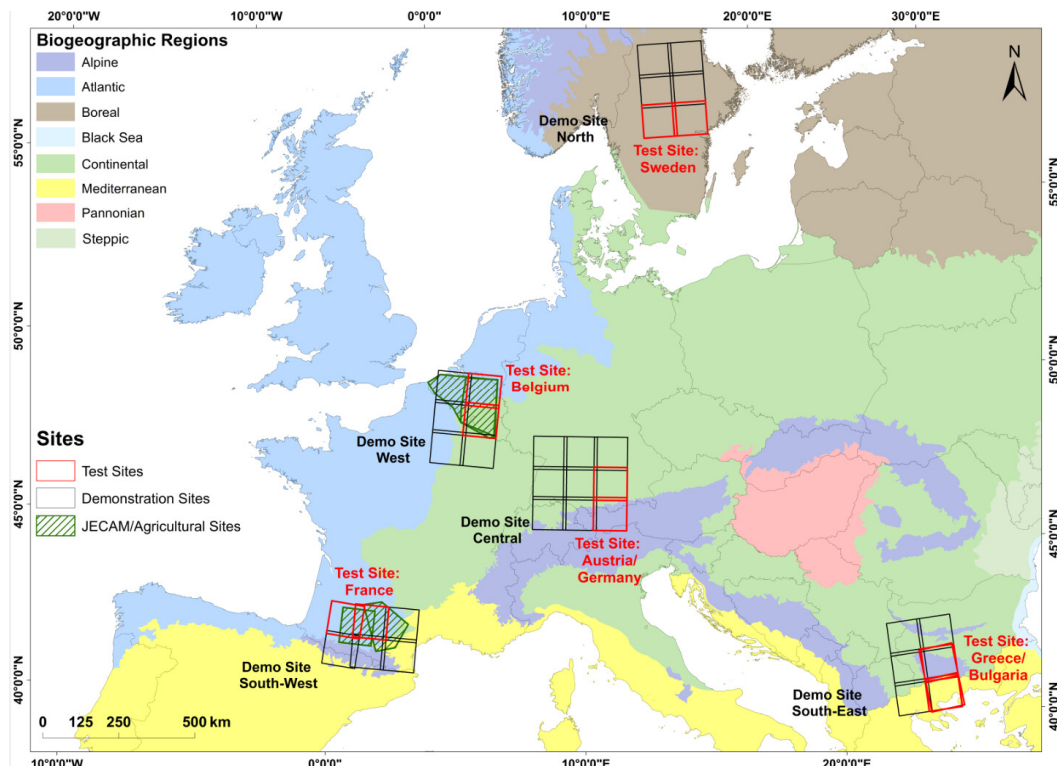


Figure 3-1: European Demonstration Sites (modified from: EEA, 2015).

A short description of the different demonstration sites is given in the following Table 3-1 below:

Table 3-1: Description of the selected Demonstration Sites

Location	Biogeographical region(s)	Countries	Distribution of CORINE land cover classes 2012 (Level 1) per demonstration site
Northern Europe	Boreal	Sweden, Norway	Artificial areas: 1,05%, Agricultural areas: 9,07%, Forest and semi-natural areas: 46,70%, Wetlands: 1,74%, Waterbodies: 41,43%
Alpine / Central Europe	Continental, Alpine	Germany, Austria, Switzerland, Italy and Czech Republic	Artificial areas: 7,71%, Agricultural areas: 47,36%, Forest and semi-natural areas: 42,83%, Wetlands: 0,19%, Waterbodies: 1,90%
West Europe	Atlantic, Continental	Belgium, France, Luxembourg	Artificial areas: 7,81%, Agricultural areas: 53,75%, Forest and semi-natural areas: 13,15%, Wetlands: 0,25%, Waterbodies: 25,04%
South-East Europe	Mediterranean, Continental, Alpine	Serbia, Macedonia, Greece, Bulgaria and Kosovo	Artificial areas: 1,84%, Agricultural areas: 23,92%, Forest and semi-natural areas: 37,83%, Wetlands: 0,11%, Waterbodies: 36,30%
South-West Europe	Atlantic, Mediterranean, Alpine	France, Spain	Artificial areas: 1,15%, Agricultural areas: 19,04%, Forest and semi-natural areas: 20,53%, Wetlands: 0,04%, Waterbodies: 59,24%

3.2 Demonstration Site WEST for Grassland

The demonstration site “West” is the primary demonstration site for prototype developments (Task 4) related to the potential future Copernicus Land High Resolution Layer (HRL) on Agricultural (AGRI), and as well for improvements of the HRL Grassland (GRA). Furthermore, the Belgium site serves as secondary demo site for the HRL Imperviousness (IMP). It contains the test site “Belgium” where methodological developments were carried out in Task 3.

Within this the demonstration site West, with an area of approximately 6500000ha, 53.75% are agriculturally used while the rest is covered by water bodies (25.04%), forests and semi-natural areas (13.15%), artificial areas (7.81%), as well as wetlands (0.25%). In this statistic the various grassland types appear under different land cover classes. Natural grasslands (CLC code 321) with 0.10% are generalised under forests and semi-natural areas, whereas pastures (CLC code 231) with 0.11% are generalised under agricultural areas. Further, green urban areas (CLC code 141) with 0.0009% and sport and leisure facilities (CLC code 142) with 0.004% are generalised under artificial areas. This shows that the demonstration site WEST is mainly comprised by natural grasslands and agricultural grasslands. A map of the selected demonstration site WEST for the HRL Grassland (GRA) prototype is provided in Figure 3-2 below.

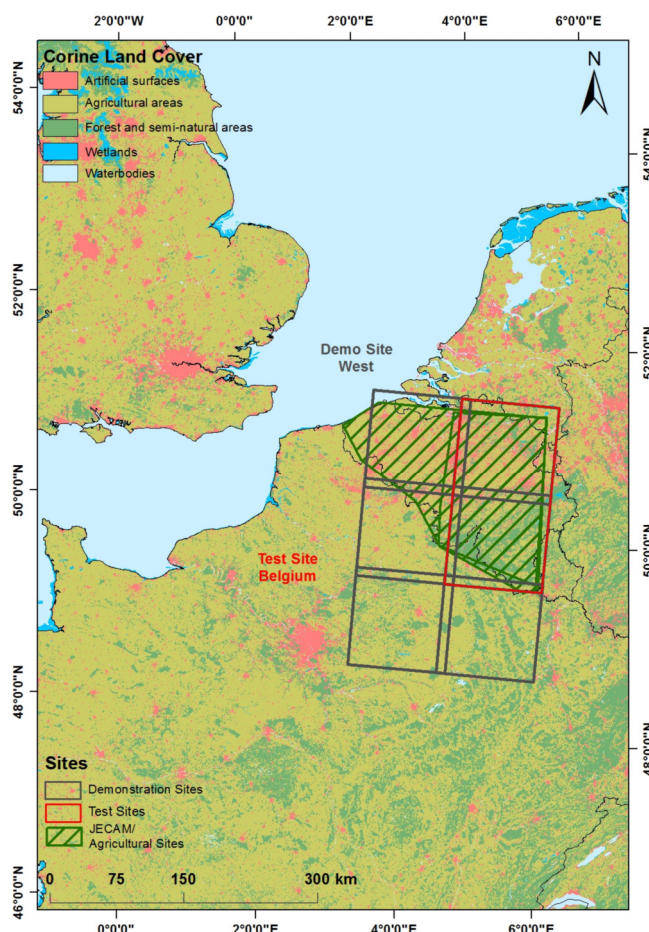


Figure 3-2: Overview of DEMO Site WEST.

4 Overview of applied methods

Grasslands are dynamic throughout the time and within its growing period, it is characterised by changing canopy density, chlorophyll status and ground cover (Zillmann et al., 2014). Nevertheless, in comparison with highly dynamic land cover classes like croplands grassland has also almost no phenology as orchards. Since grasslands and crops show significant variations throughout their growing cycle, time series representing information about phenological dynamics are required. Even using time series a unique spectral signature for grasslands is not available since other vegetation features, especially crop types, might show similar characteristics. Therefore, the aim of the prototype implementation is to identify the most suitable phenological seasons and time series indicators from optical data and SAR data time series to get the best-trade-off between minimum numbers of individual time features needed and the best corresponding classification accuracy.

4.1 Multi-sensor Data Integration

The usage of only SAR time series as alternative data, and the combination and integration of S-1 and S-2 data to both, closing data gaps due to cloud cover, or as complementary information to increase the thematic accuracy has been addressed in WP31 [AD05]. The advantages of the synergetic combination of different sensors at high spectral and spatial resolution are (i) to achieve a denser temporal resolution by filling the missing observations of S-2 data due to cloud cover with SAR data, and (ii) to create complementary information layers as input for the classification approach. Several state-of-the-art fusion methods were benchmarked and tested in WP31 [AD05] including the pixel level fusion, feature level fusion and the decision level fusion.

As described in WP31 [AD05] the image fusion on pixel level is the computationally most intensive approach because the merging is applied directly on the pixels obtained at the source images. This approach can be used to take all information into account when the sensors have similar spatial characteristics (Samadzadegan, 2004). The feature level fusion uses different extracted features derived from source data or ancillary data, which are also used for classification purposes. The feature level-fusion should be used if the features can be appropriately associated (Samadzadegan, 2004). Decision fusion methods combine results obtained through separate classifications of optical and SAR features. Indices and statistics for the classification are calculated for each data set separately and the results of the classification can be combined using logical AND functions, expert systems or probabilistic techniques. This approach should be used when the sensors are very different, additionally, it has the advantage of being less computationally intensive (Samadzadegan, 2004).

As shown in the benchmarking applications in WP31 and WP33, the integration of S-1/S-2 allows benefiting from the multi-sensor characteristics, using the information gained from both sensors in parallel for the classification process as they record complementary characteristics of the land surface. Therefore integrated S-1/ S-2 datasets were used for the prototype production.

4.2 Multi-temporal SAR and Optical Metrics

Multi-temporal features that aim at quantifying the vegetation cycle based on the images acquired by fused S-2 and S-1 images are looked at in this chapter. Their statistical properties are computed in order to select the most relevant features to study grassland cover. Several metrics can be constructed to focus on grassland, derived from both sensors, S-1 and S-2. As already described in WP 31 [AD05] temporal metrics can be summarized to different types. The first category includes statistical metrics of spectral values calculated over one or several periods such as the average, the maximum, the minimum – especially relevant to follow seasonality and phenology. The second category includes change metrics, usually derived from a temporal trajectory which represents the magnitude and the duration of the change, or the slope of the modelled trend. Third, stationary or non-stationary shape variables derived by temporal trajectories can be seen as a function of time and provide periodic patterns or transitions patterns. Final,

trend metrics can be used to find simple linear trends, seasonal trends and breakpoints to describe landscape processes. For further detailed information see WP 31 [AD05].

In the prototype implementation the above mentioned statistical metrics of spectral values calculated over one or several periods are exploited. Different multi-sensor temporal statistical metrics are derived from the synergetic use of optical and SAR data to enhance the accuracy of the classification result in comparison to optical or SAR only features (described in detail and benchmarked in WP 33 [AD07]), including seasonal optical metrics and vegetation indices.

4.2.1 Spectral Optical Indices

Many spectral indices have been defined in the past three decades. Some have been and are still widely used, such as the NDVI, while others have only been proposed as alternatives in the recent years. In the WP 31 [AD05], main spectral indices are listed focusing on vegetation and built-up discrimination in order to explore their potential contribution to the evolution of Copernicus Land Services products. Moreover, the assessment of vegetation chlorophyll at the canopy level, using remote sensing data is important for providing information about the health status of grassland ecosystem, for example, the physiological status, productivity, or phenology (Tong and He, 2017). Below paragraphs complement the description of indices in WP31 with focus on those indices which were used in the feature selection process to determine the optimal set of features for grassland identification.

Zillmann et al. (2014) concluded that the usage of seasonal statistics of various vegetation indices from multi-season images in conjunction with the spectral reflectances of the visible, near-infrared and short-wave infrared spectrum are useful for grassland discrimination. The most relevant seasonal vegetation indices features are the Normalized Difference Senescent Vegetation Index (NDSVI) average and maximum, due to the sensitivity of the index to drying and senescence events. Other useful seasonal indices used within the study are NDVI, ground cover (GC), Plant Senescence Reflectance Index (PSRI), Normalized Difference Infrared Index (NDII), NDSVI, Wetness Index (WI), and Brightness as they describe phenological differences of grasslands and croplands (Zillmann et al., 2014). Another study conducted from Yang et al. (2017) stated that the Normalized Difference Vegetation Index (NDVI), Red-Green Ratio (RGR), Enhanced Vegetation Index (EVI), Normalized Difference Infrared Index (NDII), Modified Triangular Vegetation Index II (MTV2), SWIR Reflectance and PSRI were important for distinguishing grassland and cropland. Furthermore, Tong and He (2015) tested the performance of 144 published broad- and narrowband vegetation indices for retrieving chlorophyll content for a semi-arid mixed-grass prairie ecosystem. In general, narrowband indices utilizing data from a wavelength from the red to the red-edge region (690–750nm) performed best. Broadband indices are found to be as effective as narrowband indices for chlorophyll content estimation at both leaf and canopy scales. Based on the results of the benchmarking applications in WP31 and WP33 and on findings described in above papers, the most promising indices were selected for the prototype implementation. Please note, that only a subset of these indices were finally used in the classification, based on the automated derived feature importance measures, as described in next chapters.

CI_GREEN – GREEN CHLOROPHYLL INDEX [783, 560]:

The CI_green which is adapted for the Sentinel sensor and used by (Clevers and Gitelson, 2013) can be defined as follows:

$$CI_{green} = \frac{\rho_{VRE3}}{\rho_{Green}} - 1$$

Wu et al. (2012) evaluated the potential of the CI_green index derived from MODIS data for estimating midday light use efficiency in grassland areas. They stated that the CI_green index is a good indicator of the canopy of chlorophyll content. Clevers and Gitelson (2013) pointed out that the major advantage is the linearity with chlorophyll content and absence of the saturation effect. Clevers and Kooistra (2012) confirm that green chlorophyll index accurately estimates the leaf and canopy nitrogen status content, which is consistent with findings for both crops and grassland systems.

CI_REDEDGE – RED-EDGE CHLOROPHYLL INDEX [783, 705]:

The CI_rededge which is adapted for the Sentinel sensor and used by (Clevers and Gitelson, 2013) can be defined as follows:

$$CI_{red-edge} = \frac{\rho_{VRE3}}{\rho_{VRE1}} - 1$$

Gitelson et al. (2005) stated that the CI_rededge with MERIS spectral bands was able to accurately estimate chlorophyll content in maize and soybean. Rossini et al. (2014) evaluated different models derived by vegetation indices to estimate the primary gross production for grasslands in subalpine regions. The results indicate that the CI_rededge performed better than the NDVI and the CI_green, due to their sensitivity to the chlorophyll content. The combination of CI_green and CI_rededge also seems promising accounting for both the seasonal change in the chlorophyll content and changes in radiation conditions.

EVI – ENHANCED VEGETATION INDEX

The EVI which is adapted for the Sentinel sensor and defined by (Henrich et al., 2012) can be defined as follows:

$$EVI = 2.5 * \frac{(\rho_{NIR} - \rho_{Red})}{(1 + \rho_{NIR} + 6 * \rho_{Red} - 7.5 * \rho_{Blue})}$$

where the numerical parameters are specific for the S-2 sensor. The main feature of the EVI is to incorporate background corrective term as well as atmospheric resistance concepts. The index ranges from -1 to 1, being more responsive to canopy structural variations through a de-coupling of the canopy background signal and a reduction in atmosphere influences (Huete et al., 1997 as cited in Kawamura et al. 2005).

Kawamura et al. (2005) evaluated that the MODIS-EVI was a good predictor of total biomass compared with AVHRR. These results suggest that the MODIS-EVI can reliably detect the phenology and forage quantity and quality of grassland steppe areas. Yang et al. (2009) studied the above-ground biomass in alpine grasslands using the EVI index showing a relationship between the above-ground biomass and the EVI index estimating the magnitude and spatial distribution of the above-ground biomass for alpine grasslands.

MTCI – MERIS TERRESTRIAL CHLOROPHYLL INDEX [740,705,665]:

The MTCI which is adapted for the Sentinel sensor and used by (Clevers and Gitelson, 2013) can be defined as follows:

$$MTCI = \frac{\rho_{VRE2} - \rho_{VRE1}}{\rho_{VRE1} - \rho_{Red}}$$

Foody and Dash (2007) evaluated the potential of the MTCI concerning the grassland mapping for South Dakota, USA from multi-temporal remote sensing imagery. The derived relationships between the MTCI composites of grasslands were significant. “The MTCI is positively related with plant biochemical variables such as the total chlorophyll content, which is, in turn, a function of chlorophyll concentration and leaf area index”(Foody and Dash, 2007).

NBR – NORMALIZED BURN RATIO:

The NBR which is adapted for the Sentinel sensor and defined by (Henrich et al., 2012) can be defined as follows:

$$NBR = \frac{\rho_{NIR} - \rho_{SWIR2}}{\rho_{NIR} + \rho_{SWIR2}}$$

The formula is similar to NDVI, except that it uses near-infrared (NIR) and shortwave-infrared (SWIR) wavelengths. The index shows saturation effect at denser vegetation covers. A high NBR value generally indicates healthy vegetation while a low value indicates bare ground and recently burned areas (Fernández-Manso, 2016).

Xu et al. 2014 studied the dead component of grasslands including litter and standing dead material as indicator for the grassland productivity. Since the spectral signal of dead material is similar to bare soil or soil crust. The results show that the dead component can be estimated with multispectral images using Normalized Burn Ratio (NBR) or Normalized Difference water index (NDWI).

NDMI – NORMALIZED DIFFERENCE MOISTURE INDEX:

The NDMI which is adapted for the Sentinel sensor and defined by (Henrich et al., 2012) can be defined as follows:

$$NDMI = \frac{\rho_{NIR} - \rho_{SWIR1}}{\rho_{NIR} + \rho_{SWIR1}}$$

The normalized difference moisture index (NDMI), in a similar form as NDVI but utilizing SWIR and NIR reflectance. The NIR, which is sensitive to the reflectance of leaf chlorophyll content to SWIR, which is sensitive to the absorbance of leaf moisture. The index is ranging from -1 to +1 where positive data values are typically moist areas (Gao, 1996). Meaning, the NDMI is positively related to vegetation wetness varying with vegetation growth because of water absorption in SWIR region (Wang et al., 2007).

Wang et al. (2007) used the NDVI and the NDMI index to detect warm seasons grass and cool season grass in grassland areas over the growing season. The results show that the NDMI has been found to be useful within the spring-summer period, while the NDVI is useful in the summer-fall period. In the early growing season, the NDMI showed a decrease thus it is primarily attributed to the soil moisture.

NDRE1 – NORMALIZED DIFFERENCE RED EDGE INDEX (1): [740,705]:

The NDRE1 which is adapted for the Sentinel sensor and used by (Clevers and Gitelson, 2013) can be defined as follows:

$$NDRE1 = \frac{\rho_{VRE2} - \rho_{VRE1}}{\rho_{VRE2} + \rho_{VRE1}}$$

Normalized Difference Red Edge Index (NDRE) is similar to the well-known NDVI, using the Red-Edge spectrum instead of the Red band. The main advantage is the reduced saturation effect due to a lower absorption by the chlorophyll in the red-edge and the red-edge band is very sensitive to medium to high levels of chlorophyll content (Vicente et al., 2017).

There are different normalized difference indices like the NDRE using red-edge bands in a slightly different band setting depending on the available sensor. The NDRE1 introduced by Gitelson and Merzlyak (1994) uses the 750 nm and 705 nm regions, whereas the NDRE2 version is introduced by Barnes et al. (2000) using 790 nm and 720 nm regions.

NDRE2 – NORMALIZED DIFFERENCE RED EDGE INDEX (2) [783,705]:

The NDRE2 which is adapted for the Sentinel sensor and used by (Clevers and Gitelson, 2013) can be defined as follows:

$$NDRE1 = \frac{\rho_{VRE3} - \rho_{VRE1}}{\rho_{VRE3} + \rho_{VRE1}}$$

NDVI – NORMALIZED DIFFERENCE VEGETATION INDEX:

The NDVI which is adapted for the Sentinel sensor and defined by (Henrich et al., 2012) can be defined as follows:

$$NDVI = \frac{\rho_{NIR} - \rho_{Red}}{\rho_{NIR} + \rho_{Red}}$$

The NDVI trends in this period varied with both phenology and grassland treatments such as haying and grazing, which provided additional information in grassland discrimination (Wang et al., 2007). Furter details on the NDVI are provided in WP31 [AD05]

REP – RED-EDGE POSITION LINEAR INTERPOLATION:

The REP which is adapted for the Sentinel sensor and used by (Clevers and Gitelson, 2013) can be defined as follows:

$$REP = 705 + 35 \frac{\left(\frac{\rho_{Red} + \rho_{VRE3}}{2 - \rho_{VRE1}} \right)}{\rho_{VRE2} - \rho_{VRE1}}$$

The REP index presents the maximum slope in the red-NIR region and has the advantage of being less sensitive to varying soil, atmospheric conditions and sensor view angles (Cho and Skidore, 2009).

Horler et al. (1983) have been amongst the first identifying the importance of the position of the red-edge reflection point for the detection of plant stress. Since then the REP has often been used to estimate the chlorophyll content (Clevers et al., 2013). Cho and Skidmore (2009) tested the robustness the REP by comparing the consistency of the relationships between green grass/herb biomass and the spectral predictors. The results showed that the REP is showing a strong correlation with the biomass being useful for monitoring annual changes in grass/herb biomass production in the Mediterranean mountain ecosystems. Furthermore, it could be observed that the predicted grassland map based on the Rep model showed higher similarities compared with the NDVI models.

SAVI – SOIL-ADJUSTED VEGETATION INDEX:

The SAVI which is adapted for the Sentinel sensor and defined by (Henrich et al., 2012) can be defined as follows:

$$SAVI = \frac{(\rho_{NIR} - \rho_{Red})(1 + L)}{\rho_{NIR} + \rho_{Red} + L}$$

where L is called the soil conditioning index. The values of L are fixed according to the specific environmental conditions, from 1 to 0 (Huete, 1988).

The SAVI uses coefficients based on a relationship between NIR and VIS for bare soil. Therefore, the influence of soil on the canopy reflectance can be reduced. It is less sensitive to soil reflectance at low canopy cover compared to the NDVI (Daughtry et al., 2000) increasing the interest in the development of new indices, such as the soil-adjusted vegetation index (SAVI) (Turner et al., 1999).

Magiera et al. (2017) used several vegetation indices including the SAVI index to model the biomass of mountainous grasslands by producing a species composition map. The results show that the SAVI index, the NIR band and the MSAVI index show high importance grassland vegetation change estimation due to

the strong relationship between canopy reflectance and canopy structure. The SAVI is designed to correct for soil brightness, which is beneficial for the influence of low vegetation cover (Magiera et al., 2017).

OSAVI – OPTIMIZED SOIL-ADJUSTED VEGETATION INDEX:

The OSAVI which is adapted for the Sentinel sensor and used by (Wu et al., 2008) can be defined as follows:

$$OSAVI = (1 + 0.16) \frac{\rho_{NIR} - \rho_{Red}}{\rho_{NIR} + \rho_{Red} + 0.16}$$

The OSAVI belongs to the soil-adjusted vegetation index family (Wu et al., 2008) and shows that the value of the L parameter is critical in the minimization of the soil reflectance. The OSAVI considers L = 0.16 as optimized value (Daughtry et al., 2000).

MCARI – MODIFIED CHLOROPHYLL ABSORPTION RATIO INDEX:

The MCARI which is adapted for the Sentinel sensor and simplified by (Daughtry et al., 2000) can be defined as follows:

$$MCARI = ((\rho_{VRE1} - \rho_{Red}) - (\rho_{VRE1} - \rho_{Green})) \left(\frac{\rho_{VRE1}}{\rho_{Red}} \right)$$

The MCARI measures the depth of chlorophyll absorption at VRE1 relative to the Green reflectance and the Red reflectance reducing the variability of photosynthetically active radiation (Wu et al., 2008).

Daughtry et al. (2000) demonstrated that the MCARI is still sensitive to background reflectance properties and non-photosynthesis elements effects at low chlorophyll concentrations. Furthermore, the MCARI index is influenced by the LAI-chlorophyll interaction (Wu et al., 2008).

TCARI – TRANSFORMED CHLOROPHYLL ABSORPTION RATIO INDEX:

The OSAVI which is adapted for the Sentinel sensor and used by (Wu et al., 2008) can be defined as follows:

$$TCARI = 3[(\rho_{VRE1} - \rho_{Red}) - 0.2(\rho_{VRE1} - \rho_{Green})] \left(\frac{\rho_{VRE1}}{\rho_{Red}} \right)$$

To compensate the variations of reflectance characteristics of background components and to increase the sensitivity to low chlorophyll values the transformed chlorophyll absorption ratio index can be calculated (Wu et al., 2008).

TCARI/OSAVI [705,750]:

The TCARI/OSAVI which is adapted for the Sentinel sensor and used by (Clevers and Gitelson, 2013) can be defined as follows:

$$\frac{TCARI}{OSAVI} = \frac{3[(\rho_{VRE2} - \rho_{VRE1}) - 0.2(\rho_{VRE2} - \rho_{Green})] \left(\frac{\rho_{VRE2}}{\rho_{VRE1}} \right)}{(1 + 0.16) \frac{\rho_{VRE2} - \rho_{VRE1}}{\rho_{VRE2} + \rho_{VRE1} + 0.16}}$$

Combining the TCARI with the OSAVI reduces the underlying soil reflectance properties (Wu et al., 2008). To achieve the full potential the red and the NIR spectral band where adapted with bands at 705 nm and 750 nm respectively. This adaption showed a better linearity with the canopy chlorophyll content (Clevers and Gitelson, 2013).

MCARI/OSAVI [705,750]:

The MCARI/OSAVI which is adapted for the Sentinel sensor and used by (Clevers and Gitelson, 2013) can be defined as follows:

$$MCARI/OSAVI = \frac{((\rho_{VRE2} - \rho_{VRE1}) - 0.2 - (\rho_{VRE2} - \rho_{Green})) \left(\frac{\rho_{VRE2}}{\rho_{VRE1}} \right)}{(1 + 0.16) \frac{\rho_{VRE2} - \rho_{VRE1}}{\rho_{VRE2} + \rho_{VRE1} + 0.16}}$$

Combining the MCARI with the OSAVI the underlying soil reflectance properties can be reduced (Wu et al., 2008). To achieve the full potential the red and the NIR spectral band were adapted with bands at 705 nm and 750 nm respectively. This adaption showed a better linearity with the canopy chlorophyll content (Clevers and Gitelson, 2013).

TCB – TASSELED CAP BRIGHTNESS:

The TCB which is adapted for the Sentinel sensor and defined by (Henrich et al., 2012) can be defined as follows:

$$TCB = 0.3037 \rho_{Blue} + 0.2793 \rho_{Green} + 0.4743 \rho_{Red} + 0.5585 \rho_{NIR} \\ + 0.5082 \rho_{SWIR1} + 0.1863 \rho_{SWIR2}$$

The Tasseled Cap transformation incorporates more information into vegetation indices by using six different reflectance bands. The resulting brightness, greenness, and wetness indices improve vegetation classifications because they are sensitive to phenological changes (Dymond et al., 2012). Therefore, the indices can be used to distinguish between crops grassland.

TCG – TASSELED CAP GREENNESS:

The TCG which is adapted for the Sentinel sensor and defined by (Henrich et al., 2012) can be defined as follows:

$$TCG = -0.2848 \rho_{Blue} - 0.2435 \rho_{Green} - 0.5436 \rho_{Red} + 0.7243 \rho_{NIR} \\ + 0.0840 \rho_{SWIR1} - 0.1800 \rho_{SWIR2}$$

TCW – TASSELED CAP WETNESS:

The TCW which is adapted for the Sentinel sensor and defined by (Henrich et al., 2012) can be defined as follows:

$$TCW = 0.1509 \rho_{Blue} + 0.1973 \rho_{Green} + 0.3279 \rho_{Red} + 0.3406 \rho_{NIR} \\ - 0.7112 \rho_{SWIR1} - 0.4572 \rho_{SWIR2}$$

4.2.2 Multi-seasonal Features

Multi-seasonal features can be generated from different seasons concerning those periods of the year where grassland could be identified the best, taking into account agricultural management schemes as well as grassland mowing cycles. To characterize different temporal behaviours of grasslands and other land cover classes, high-frequency acquisitions over the growing seasons are essential. Nevertheless, the temporal behaviour may vary considering different mowing practices. Schmidt et al. (2014) concluded from their study with RapidEye data from 2009 to 2011 that the NDVI composites from the early summer seasons are most important for the grassland discrimination, whereas spring, late summer and midsummer seasons also played an important role. Keil et al. (2013) stated that March, May and August (using NDVI composites) are important seasons in central Europe to discriminate crops and grasslands. After identifying the optimal acquisition period it still can be impossible to find good quality images or image composites with no cloud gaps for the entire area (Zillmann et al., 2013). Wang et al. (2010),

extracted temporal trajectories of the normalized difference vegetation index (NDVI) and the normalized difference moisture index (NDMI) to examine the temporal variation of warm-season grass and cool-season grass grasslands in a growth cycle. It was found that the spring–summer period revealed maximal spectral differences between these two grass types. The NDVI is stated to be more useful than NDMI in summer–fall. The NDVI trends in this period varied with both phenology and grassland treatments such as haying and grazing.

As pointed out in WP 33 [AD07] these seasons vary for different regions with changing climate conditions and differing management systems (Zillmann et al., 2013). The aim for the prototype production is to find the most suitable phenological season to get optimized results and the best trade-off between the minimum numbers of individual scenes needed to achieve the best corresponding classification accuracy.

4.3 Random Forest Classification Approach

The amount of images used in multi-temporal classification studies has greatly increased along with enhanced temporal sensor capacities. As pointed out in WP33 [AD07] the availability of dense time series supports the use of machine learning algorithms over the traditional statistical classification approaches due to the increasing computational capabilities necessary to process big amounts of data (Waske and van der Linden, 2008).

The Random Forest (RF) classifier first proposed by Breiman (2001) belongs along with other boosting and bagging methods as well as classification trees in general to the ensemble learning methods, which generates many classifiers and aggregates their results to calculate their response (Liaw and Wiener, 2002; Horning et al., 2010; Li et al., 2016). The random forest algorithm generates multiple decision trees with randomly drawn subsets, instead of using all variables from the available data. The subsets are drawn with replacement, meaning that one sample can be selected several times, while others may not be selected at all (Belgiu and Dragut, 2016; Ali et al., 2012). Regarding each random sample, a classification or regression tree is grown to the largest possible extent without pruning. At each node, a random sample of a predictor variable is extracted; among those, the best split is chosen. To predict new data the prediction among all trees are aggregated using majority votes. The class with the maximum vote overall decision trees is the one selected for the output product (Liaw and Wiener, 2002; Ali et al., 2012). One advantage of the classifier is the calculation of the variable feature importance.

In this context, the relative importance of variables is calculated for each feature available for both optical and SAR data. Within the forest generation, every node in the decision trees is a condition on a single feature to split the dataset. The Mean Decrease Impurity (also known as Gini importance) measure, calculates the sum of the total impurity reductions at all tree nodes where the variable appears (Breiman, 2001). Therefore, each feature importance represents the sum over the number of splits across all trees that include the feature; proportionally to the number of samples it splits (Louppe et al., 2013). One drawback of this method is that the mean decrease impurity measure is biased towards preferring variables with more categories. Another drawback is when the dataset is composed of correlating features, which can be assumed to have the same importance. Nevertheless, the first feature analysed reduces the importance of other correlating features (Louppe et al., 2013).

4.4 Validation analysis procedure

Thematic accuracy is presented in the form of an error matrix made out of the results of the samples blind and plausibility interpretation. As explained in (Selkowitz and Stehman, 2011) unequal sampling intensity resulting from the stratified systematic sampling approach should be accounted for by applying a weight factor (p) to each sample unit based on the ration between the number of samples and the size of the stratum considered:

$$\hat{p}_{ij} = \left(\frac{1}{N} \right) \sum_{x \in (i,j)} \frac{1}{\pi_{uh}^*}$$

Where i and j are the columns and rows in the matrix, N is the total number of possible units (population) and π is the sampling intensity for a given stratum.

This is because the samples from the smaller strata potentially exhibit a higher sampling intensity than those from the larger strata. Therefore, a correction for the sampling intensity will be applied to the error matrices produced following the procedure described (Selkowitz and Stehman, 2011) and applied (Olofsson et al., 2013) leading to a weighting factor inversely proportional to the inclusion probability of samples from a given stratum. Not applying this correction could result in underestimating or overestimating map accuracies.

Thematic accuracy is usually assessed based on the construction of confusion or error matrix which can be described as illustrated in Figure 4-1 for 5 thematic classes.

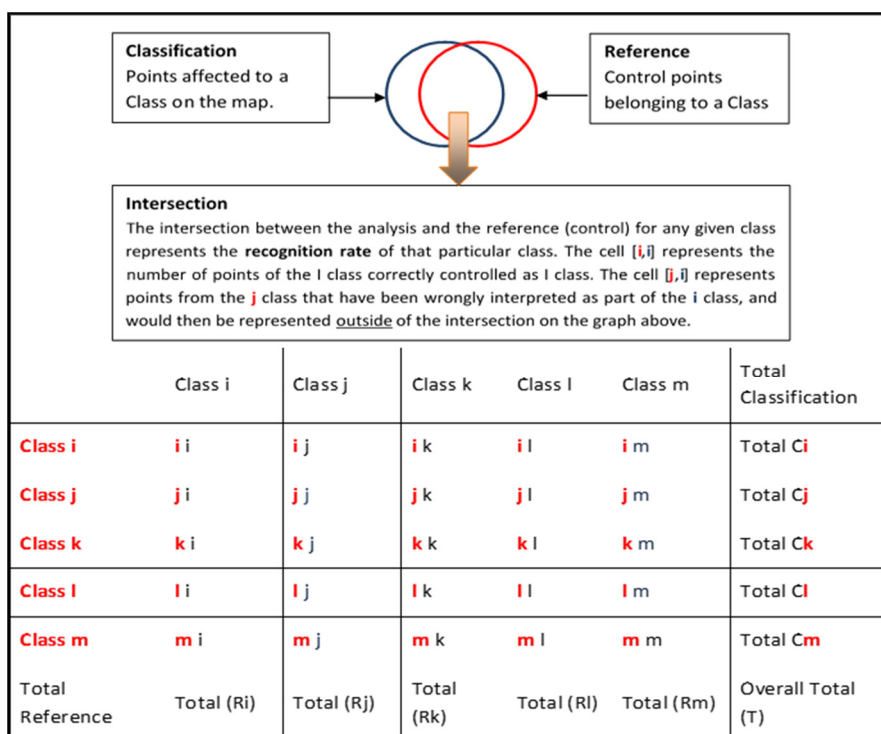


Figure 4-1: Confusion Matrix for Accuracy Assessment of thematic map product.

Let us assume α represents any given class of $[i, j, k, l, m]$, the following accuracy metrics can be calculated:

- The **Overall Accuracy** or Recognition Rate is measured by the sum of the diagonal of the Confusion Matrix divided by the total number of controlled points: OA or $R_r = \sum_{\alpha=i}^m (\alpha\alpha)/T$. The Recognition Rate or Overall Accuracy assesses the overall agreement between the classified and reference data set. However, for single class themes such as in the HRL, it does not necessarily provide a realistic assessment of the quality of the map produced because the area covered by the theme considered (Grassland in this case) can be relatively small in comparison to the rest of the area.
- Therefore, the row and column totals and the diagonal of the Matrix are used to assess two types of accuracy, the User and Producer Accuracy:
 - **Producer Accuracy** for the α class = $\alpha\alpha/C\alpha$ is a measure of **omission error**. For instance, an observation has been identified as grassland during the validation, but has been classified as another class: it has been omitted from the grassland class. The number of omission errors should be less than 15% for the Grassland Mask.
 - **User Accuracy** for the α class = $\alpha\alpha/R\alpha$ is a measure of the **commission error** (or contamination risk): errors due to the wrong allocation of an observation to a class. For instance, an observation is classified as grassland, but identified as belonging to another

class during the validation process: this observation has contaminated another class. The number of commission errors should be less than 15% for the Grassland Mask.

The standard error of the error rate estimate can be calculated as follows: $\sigma_h = \sqrt{\frac{p_h(1-p_h)}{n_h}}$ where n_h is the sample size for stratum h and p_h is the expected error rate. The 95% Confidence Interval is +/- 1.96. σ_h .

5 Prototype Implementation

This chapter shows the prototypical implementation of the Improved Primary Status Grassland Layer prototype (GRA_2017_010m_WEST_03035_V0_1). For the grassland prototype generation different technical approaches and the usability of different temporal and seasonal features are tested. The grasslands within the demonstration site comprise natural, semi-natural and managed grasslands. A prototype product covering the demo site with 10m spatial resolution and a minimum mapping unit of 1ha is produced.

Firstly, in chapter 5.1 the used data and the processing setup for the prototype production is described. To improve the optical and SAR-based grassland classification compared to the WP 33 [AD07] test results, further derived indices from high resolution optical satellite image coverages have been used. However, the occurrence of clouds specifically in northern, western and mountainous parts of Europe significantly reduces the density of the time series. Another drawback of using S-2 data only is that there are similarities of spectral characteristics of different land cover types, which may lead to uncertainties in the resulting product. Secondly, chapter 0 presents the results and the internal validation of the grassland prototype and lastly, the description of the dataset properties and its metadata, referring to P43.2 – Data Sets of HRL Permanent Grassland Products is provided in section 5.3.

5.1 Data and Processing Setup

Firstly, the integrated EO and ancillary data is described (section 5.1.1), followed by explaining the pre-processing steps (section 5.1.2), and the used multi-temporal statistical features (section 5.1.3) and finally the experimental prototype implementation setup including intermediate results (section 5.1.4).

The developed processing chain is able to process a large amount of time series input data within a reasonable amount of time to provide the multi-temporal input variables for the classification process. The achieved level of automation ensures the effective application of the process to map grasslands of almost the entirety of Europe. The optical data proved to be more suitable to characterize the vegetation status and to exclude water covered objects and urban objects, while SAR imagery proved the information to separate the grassland from cropland areas. Especially, the combination of data of the Sentinel fleet shows great potential in terms of geometric consistency and enhancement for the grassland classifications.

5.1.1 Input Data and Data Integration

SAR DATA

SAR data are acquired independently from weather and daytime conditions and generally allow a better discrimination of vegetation types due to their diverse response to different polarisation signals. Compared to the optical data microwaves are less affected by the physical-chemical characteristics of the surface, but rather by its structure such as geometry and roughness. Active energy scattered by vegetation is dependent on size, density, orientation and dielectric properties of elements compared to the size of radar wavelength helping to differ between roughness and moisture content (Rüetschi et al., 2017). SAR time series products are based on Level-1 products in Interferometric Wide swath (IW) mode and Level-1 Ground Range Detected (GRD). The IW mode is considered the main acquisition mode over land and satisfies the majority of service requirements. For each Sentinel-1 orbit, the pre-processing is calculated separately as multi-temporal filtering can only be applied to images of the same orbit. In addition, a local incidence file is calculated for each orbit stack and delivered with the data [see WP32 [AD06]. Additionally, temporal image stack statistics have been calculated which are used as input data for the time series classification processing chains.

OPTICAL DATA

The Sentinel-2 sensor system has an overall number of 12 bands from 10m to 60m spatial resolution. For the ECoLaSS processing, only the 10m and 20m bands are used, which are in total 10 bands. The list of the used bands with their central wavelengths and abbreviations is shown in Table 5-1.

Table 5-1: Used Sentinel-2 reflectance bands (adapted from Suhet, 2015).

Sentinel-2 Bands	Description	Central Wavelength (μm)	Stack number
Band 2	Blue	0.490	1
Band 3	Green	0.560	2
Band 4	Red	0.665	3
Band 5	Vegetation Red Edge (VRE1)	0.705	5
Band 6	Vegetation Red Edge (VRE2)	0.740	6
Band 7	Vegetation Red Edge (VRE3)	0.783	7
Band 8	NIR	0.842	4
Band 8A	Narrow NIR (NNIR)	0.865	8
Band 11	SWIR (SWIR1)	1.610	9
Band 12	SWIR (SWIR2)	2.190	10

S-1/S-2 DATA INTEGRATION

The integration of S-1/S-2 allows benefiting from the multi-sensor characteristics, using the information gained from both sensors in parallel for the classification process as they record complementary characteristics of the land surface. The fusion on pixel level has been applied by stacking different S-1/S-2 features into one dataset, which is used for as input for the classification approach. A high geometric accuracy at sub-pixel level is required for this approach to avoid artificial errors being introduced to the fused data set, which means the image data set need to be resampled to common pixel spacing.

VHR DATA – DATA WAREHOUSE

Copernicus Contributing Mission ADDITIONAL datasets were requested via the Data Warehouse mechanism managed by ESA and an overall quota of 13,200 km² has been granted to the ECoLaSS project for 2017 [AD10]. The demonstration site WEST is represented by an overall extension of 1300 km², encompassing 13 scenes (see Table 5-2). The ECoLaSS prototype generation is focussing on methods and prototypical developments based on multi-temporal Sentinel data and time series analysis. The VHR data was applied for the training as well as for validation.

Table 5-2: VHR data available for the demonstration site WEST.

test site BELGIUM / demonstration site WEST	
number:	13 scenes (sum 1300km ²)
timeframe:	April-October 2017 (+/- equally distributed acquisition times), and 2016 scenes
location:	same area (mainly 31UFS/31UFR),
size:	10x10 km scene subset
type:	7 VHR-1 archive, 4 VHR-1 new acquisition
DWH ID:	ADD_011a/ADD_012a

The ordered VHR data partly covers the geographic area where reference data is available. In order to cover the full phenology and dynamics of grasslands (approximate date and number of mowing events)

VHR data for the vegetation season are needed. This is important since grasslands are much more dynamic than forests or urban areas, especially when crop rotation is applied in agricultural areas.

The VHR data sets provide additional information on grassland location, mowing dynamics and phenology in order to increase the separability of grasslands from agricultural fields and broadleaf forests. A total number of 7 archive scenes and 4 new acquisitions (all 10x10km) have been ordered so far for 2017 covering 2 areas of interest.

VISUALLY INTERPRETED REFERENCE POINTS (VIRP)

For training and intermediate validation, LUCAS points covering the demonstration site are used, since they represent a regular unbiased grid of sampling points. Since the thematic information is not from the reference year 2017 and doesn't provide sufficient thematic reliability, the 3408 LUCAS points covering the demonstration site were visually interpreted based on the Sentinel-2 time series data. A Minimum Mapping Unit (MMU) of 30m x 30m has been applied in the interpretation process. Additionally, high resolution data like Bing maps (ArcGIS Basemap layer, RGB imagery) or Arc2Earth imagery (Google commercial ArcGIS plugin, RGB imagery) and if available VHR data from the Data Warehouse have been used. The land cover classes interpreted are shown in Table 5-3. The interpreted points were randomly split into training and validation data sets at a ratio of 66% training to 33% validation. Furthermore, the eight land cover classes are aggregated to grassland / non grasslands classes. With the aggregated classes the random forest model has been trained using temporal and spectral variables with the same input parameters with the number of trees set to 500 and the number of variables to the square root of the total number of input variables.

Table 5-3: VIRP reference dataset codes.

Class code	Class label
1	Cropland
2	Grassland
3	Forest and Trees
4	Shrubs
5	Artificial Surfaces & Associated Area(s)
6	Bare Area(s)
7	Waterbodies, Snow and Ice
8	Wetlands

From the training models, the Mean Decrease Impurity measure is calculated for each feature based on the aggregated classes. Finally, the output classifications are treated as thematic layers and validated against the remaining points not used for training using a point-based method. The accuracy of the experimental setup is assessed with confusion matrices and accuracy metrics.

LANDBOUWGEbruikSPERCELEN ALV, 2016 (LGP) – REFERENCE POLYGONS:

The reference data set “Landbouwgebruikspervelen ALV, 2016” (LGP) provided by the Departement Landbouw en Visserij is used for visual comparisons with the classification results. The dataset presents a polygon-wise assessment for the year 2016, differentiating between several agricultural areas including cultivation crops and grasslands. Since this reference data set was composed for agricultural purposes this reference data set does not include following grassland types:

- Grasslands in urban areas: parks, urban green spaces in residential and industrial areas, sport fields, golf courses
- Natural grasslands on military sites, airports
- Grasslands on land without use
- Semi-arid steppes with scattered Artemisia scrub

- Coastal grasslands, such as grey dunes and salt meadows located in intertidal flat areas with at least 30% graminoid species of vegetation cover

The LGP reference polygons were therefore only used for qualitative comparison with the grassland prototype.

5.1.2 Pre-processing

The ECoLaSS WEST demonstration site in Belgium is comprised of the footprints of six adjacent Sentinel-2 tiles (32UES, 32UER, 32UFS, 32UFR, 32UFQ and 32UEQ) for which Sentinel-2 and Sentinel-1 data were processed according to the outcome of WP32. The Sentinel-2 imagery had been atmospherically corrected and topographically normalized using the ESA Sen2Cor software. Furthermore, images with more than 90% cloud cover are excluded and an enhanced cloud mask is applied to the remaining images.

For each Sentinel-1 orbit, the pre-processing is calculated separately as multi-temporal filtering can only be applied to images of the same orbit. The S-1 time-series images are radiometric calibrated, radiometric terrain corrected, resampled to 10m and orthorectified. Based on pre-processed time series of VV and VH images the temporal image stack statistics are calculated. Next, the SAR images are temporally filtered by a multi-temporal speckle filtering approach reducing the speckle noise (3x3 kernels).

The large amount of scenes with strong cloud cover in the time series reinforces the need for the use of image composite-like time features. Different multi-temporal features based on the S-1 and S-2 time series from 2017 are generated. The annual features have the advantage of having included more observations to reduce biases from missing observations, whereas the seasonal features are useful to discriminate the phenological differences between vegetation types. All available images are reduced to temporal statistics including the metrics explained in the following chapter 5.1.3.

5.1.3 Multi-temporal statistic features

In the ECoLaSS WP 31 deliverable [AD05] several spectral, textural and also temporal indices are described which are of potential relevance as input for image or time series classification. The following sections describe the derivation of different temporal features which has been applied for the testing and benchmarking of methods for the grassland prototype production. The preliminary set of implemented features will be explained in the following chapters, along with feature selection results and a description of the consecutive classification workflow implementing the time features.

5.1.3.1 Annual Statistical SAR Composites (SAR)

Following annual features are generated using S-1 data and both polarisation signals (VV, VH) (Table 5-4) including 52 observations from 01.01.2017 till 30.11.2017 covering the demonstration site West.

Table 5-4: SAR annual statistical features.

feature	description
MIN	Minimum
MAX	Maximum
MEAN	Mean
STD	Standard deviation
CoV	Coefficient of Variation
DIFF	difference between the mean of the first three images and the mean of the last three images of the defined time period – useful for assessing phenological changes in seasonal/monthly image stacks or annual changes for low variance land cover classes (e.g. forests) in annual stacks

The SAR coefficients in VV and VH polarisation are used to differentiate different crop types from grassland areas. The highest dynamics are associated in agriculturally managed grasslands which are strongly managed in terms of fertilisation, irrigation, and mowing, differing from natural grasslands and meadows as well as other classes. As already tested in WP 33 [AD07] and shown in Figure 5-1 STD_VH, Mean_VV and CoV_VH are very promising for the grassland/cropland discrimination. Nevertheless, confusions of grassland occur with streets, waterbodies and orchards. Sparse and dry grasslands show spectral characteristics of bare soil.

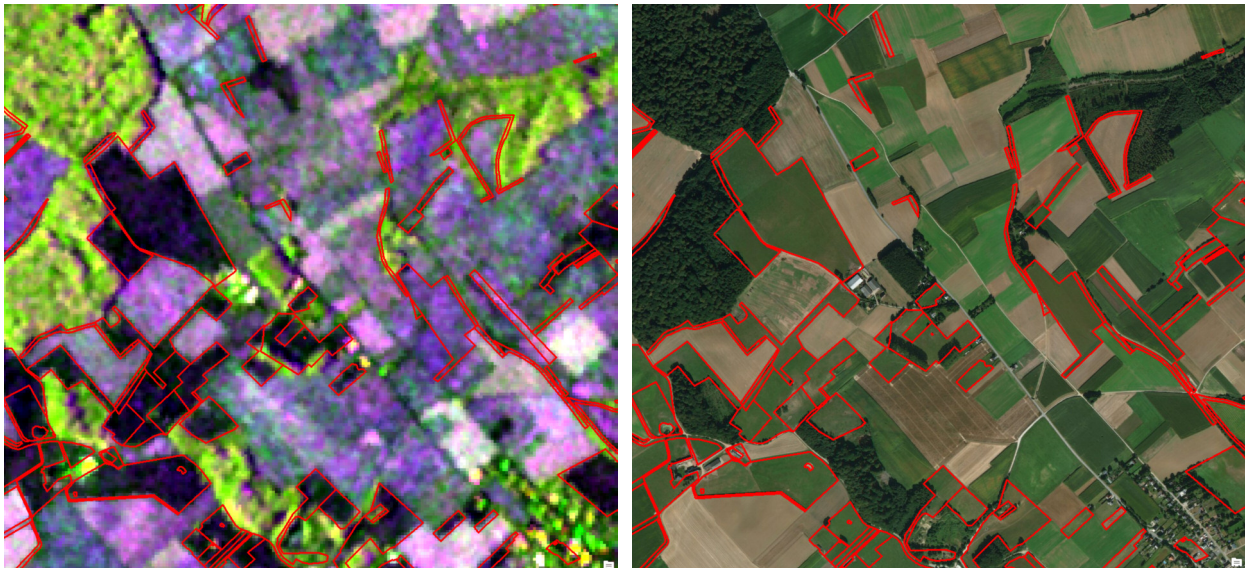


Figure 5-1: (left): Example of grassland areas in S-1 false colour composite of bands STD_VH (R), Mean_VV (G), and CoV_VH (B) of 2017 for Huldenberg. (right): ArcGIS Basemap (25.09.2016) with LGP grassland polygons in red (2016).

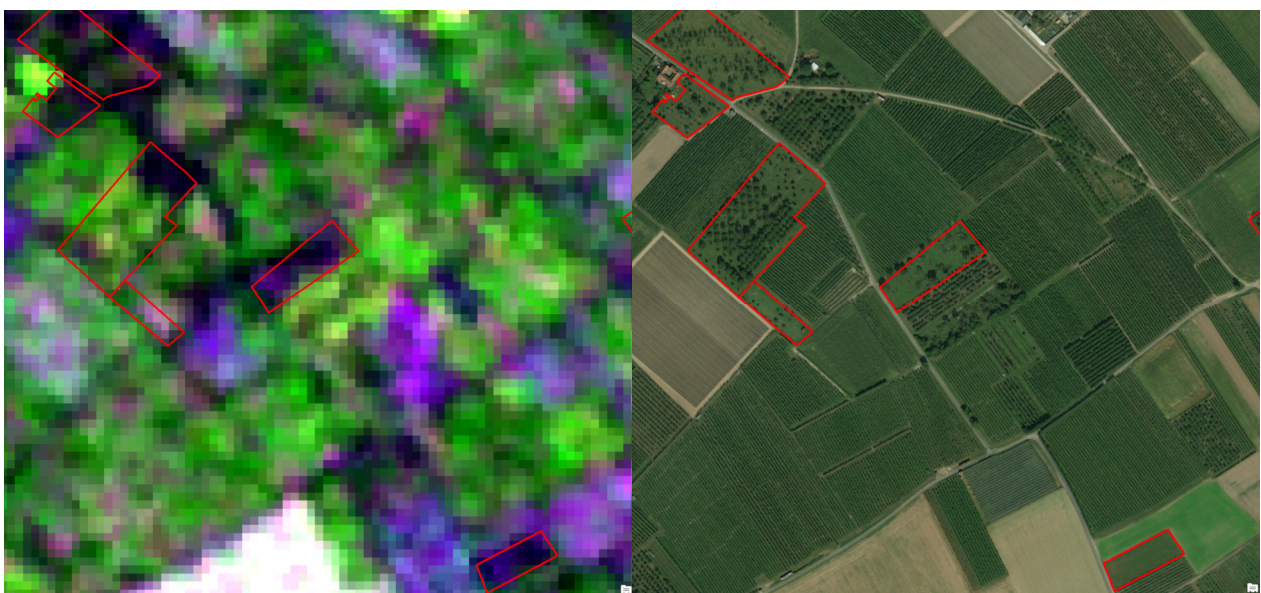


Figure 5-2: (left) Example of grassland areas in S-1 false colour composite of bands STD_VH (R), Mean_VV (G), and CoV_VH (B) of 2017 for area Huldenberg. (right) ArcGIS Basemap (25.09.2016) with LGP grassland polygons in red.

Figure 5-2 shows the potential of the annual SAR features considering the spectral separation of orchards from grassland features. In this example orchard patches with more than 10% trees which are comprised of a sparse canopy cover will be still classified as grassland. Nevertheless, the general separability of orchards features from grassland seems promising.

5.1.3.2 Annual Spectral Optical Indices Median Composites (VI + OPT)

A thorough list of envisioned indices has been reported in the WP 31 deliverable [AD06]. In the grassland context, the focus will be set on following indices (see Table 5-5), among the most used and described in WP 31, the NDVI, the EVI, and the SAVI index. Based on the derived vegetation indices for 2017 their statistical properties are computed in order to select the most relevant ones to study grassland cover.

Table 5-5: Used vegetation indices. (Xue and Su, 2017; Clevers et al., 2013; Wu et al., 2008).

Index abbreviation	Index name
CI_green	Green Chlorophyll Index
CI_red_edge	Red Edge Chlorophyll Index
EVI	Enhanced Vegetation Index
MCARI/OSAVI	Modified Chlorophyll Absorption Ratio Index / Optimized Soil-Adjusted Vegetation Index
MTCI	MERIS Terrestrial Chlorophyll Index
NBR	Normalized Burn Ratio
NDMI	Normalized Difference Moisture Index
NDRE1	Normalized Difference Red Edge Index (1)
NDRE2	Normalized Difference Red Edge Index (2)
NDVI	Normalized Difference Vegetation Index
TCARI/OSAVI	Transformed Chlorophyll Absorption Ratio Index / Optimized Soil-Adjusted Vegetation Index
REP	Red-Edge Position
SAVI	Soil-Adjusted Vegetation Index
TCB	Tasseled Cap Brightness
TCG	Tasseled Cap Greenness
TCW	Tasseled Cap Brightness

Based on the reflectance bands and derived vegetation indices annual median is calculated and analysed using the Mean Decrease Impurity (also known as Gini importance) measure. As described in WP 33 AD07 the Mean Decrease Impurity measure calculates the sum of the total impurity reductions at all tree nodes where the variable appears (Breiman, 2001). One major drawback is when the dataset is composed of correlating features, which can be assumed to have the same importance the first feature analysed reduces the importance of other correlating features (Louppe et al., 2013).

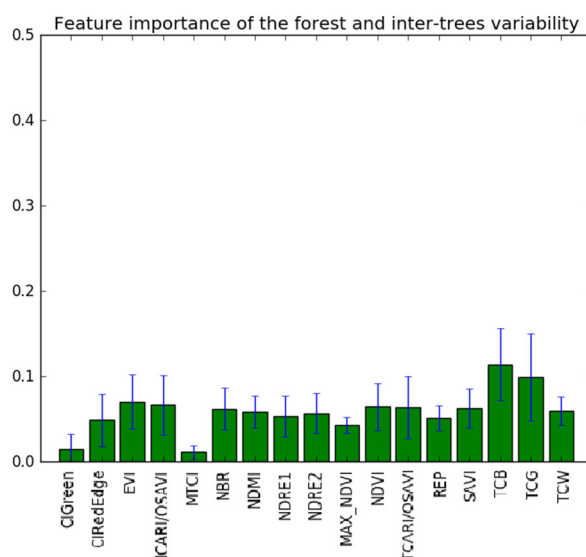


Figure 5-3: Feature importance of the forest for annual vegetation indices (median).

Regarding the feature selection TCB, TCG, EVI, MCARI, NDVI are identified as useful to enhance the grassland/non-grassland differentiation. Figure 5-3 also shows that most of the annual vegetation indices statistics provide similar information regarding the grassland/non-grassland differentiation.

The derivation of the optical annual reflectance bands composites (OPT) are described in detail in WP 33 [AD07]. The most promising optical annual reflectance bands composites are represented in Figure 5-4 and further used in the prototype generation.

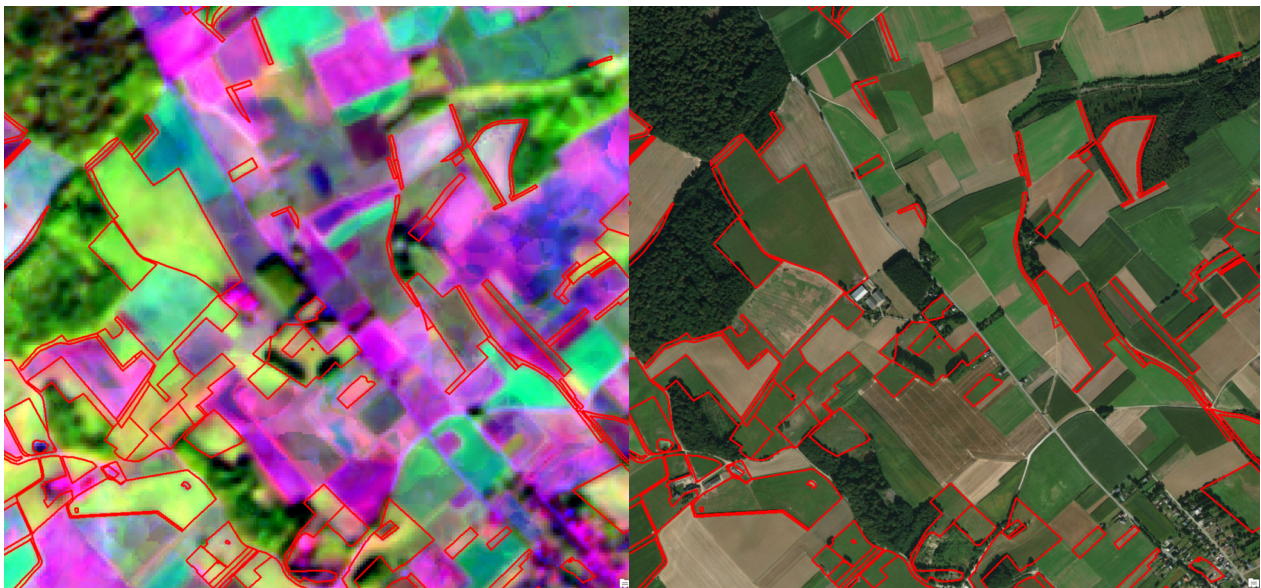


Figure 5-4: (left) Example of grassland areas in S-2 false colour composite of bands SWIR1 (R), NNIR (G), and Green (B) of 2017 for area Huldenberg. (right) ArcGIS Basemap (25.09.2016) with LGP grassland polygons in red.



Figure 5-5: (left) Example of grassland areas in S-2 false colour composite of bands EVI (R), TCB (G), and TCG (B) of 2017 for area Huldenberg. (right) ArcGIS Basemap (25.09.2016) with LGP grassland polygons in red.

The comparison of the S-2 false colour composite of bands SWIR1 (R), NNIR (G), and Green (B) (Figure 5-4) and the S-2 false colour composite of the indices EVI (R), TCB (G), and TCG (B) (Figure 5-5) show the higher potential of the most promising vegetation indices for the grassland discrimination with respect to only using annual temporal mosaic of spectral bands. However, it should be considered that these annual features vary for different biographic regions with the changing climate conditions and different management schemes.

5.1.3.3 Seasonal Optical Median Composites (seasonal)

The seasonal optical median composites are derived from the optical reflectance bands comprising different seasonal time periods including two months each. In a first analysis all time periods and all reflectance bands are analysed using the feature importance measurement and the results showed that the bands GREEN, NNIR and SWIR are more promising to differentiate between grassland and non-grassland than the other S-2 bands. In the second analysis all time periods with GREEN, NNIR and SWIR are analysed (see Figure 5-6).

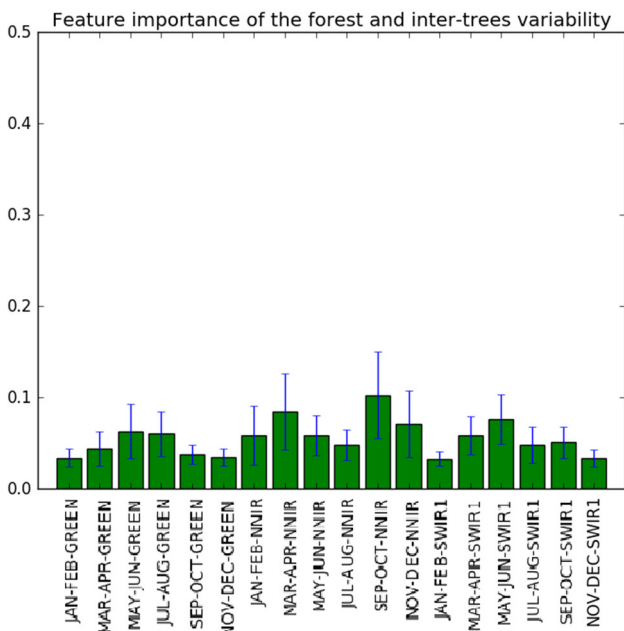


Figure 5-6: Feature importance of the forest for seasonal statistical reflectance features (median).

The results show that seasonal median composites, derived from the optical time series, up to the early growing season in combination with observations from the growing seasons are necessary for the grassland discrimination to cover observations of the vegetation cover over the year. Nevertheless, certain growing phases of crop types could possibly show similar reflectance characteristics as grassland features and are therefore hard to differentiate. The spring season (March-April), late summer (July – August) and autumn (September-October) seasons are found to be important to contribute to the grassland/cropland discrimination. Those time periods are found to be important to discriminate grassland from cropland and bare ground in the Belgium demo site taking into account agricultural management schemes.

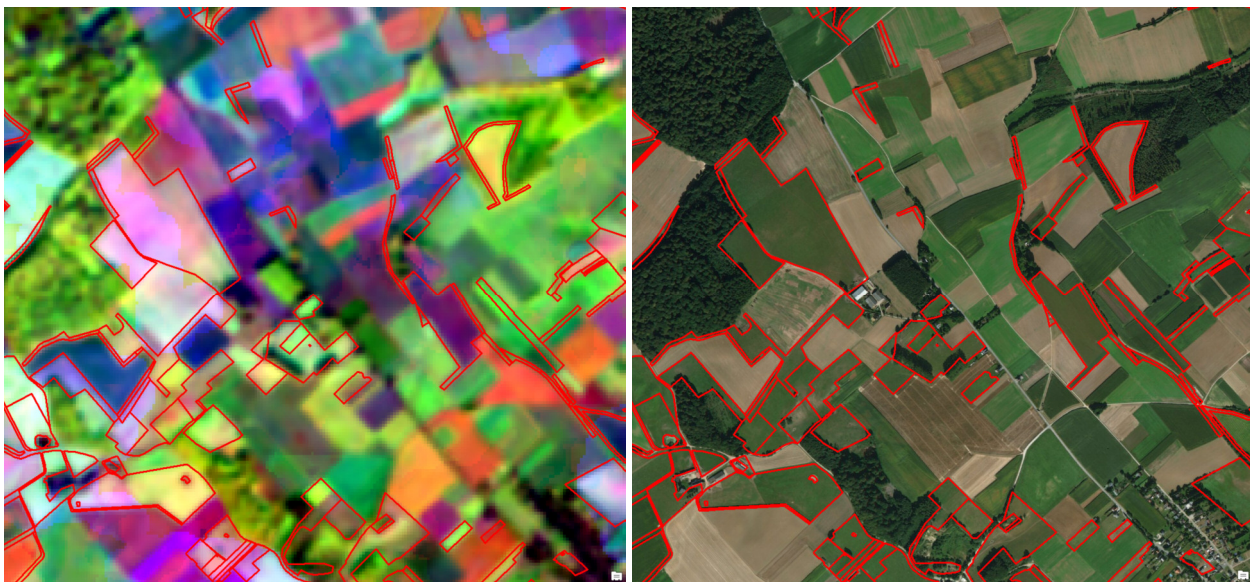


Figure 5-7: (left): Example of grassland areas in S-2 seasonal false colour composite of bands NNIR March-April (R), NNIR July-August (G), and NNIR September-October (B) of 2017 for area Huldenberg. (right): ArcGIS Basemap (25.09.2016) with LGP grassland polygons in red.

The comparison of the S-2 seasonal false colour composite of bands NNIR March-April (R), NNIR July-August (G), and NNIR September-October (B) and the VHR data as well as the reference polygons (Figure 5-7) shows the limited potential of the seasonal metrics for the grassland/cropland discrimination. Taking into account agricultural management schemes, the grassland features in Figure 5-7 show no harmonised spectral signature over the seasons due to different temporal appearance. Nevertheless, according to these results it seems promising to detect different grassland classes according to their temporal appearance. However, it should be considered that especially these seasonal features vary for different biographic regions with the changing climate conditions and different management schemes due to the higher temporal effect of seasonal compared to annual statistics.

5.1.4 Experimental Setup

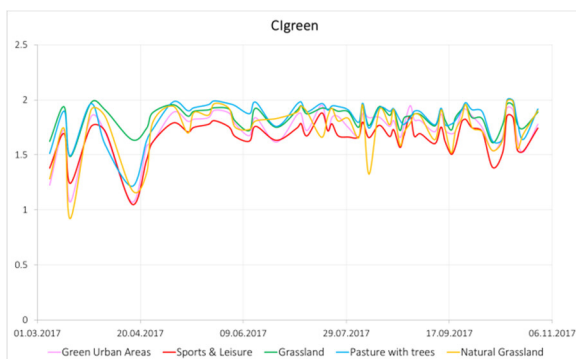
The aim of the prototype testing is to identify the most suitable phenological seasons and time series indicators from optical data and SAR data to get the best-trade-off between minimum numbers of individual features needed and the best corresponding classification accuracy. In this setup different data stacks are generated including several varying spectral composites, which are classified with the random forest algorithm in non-grass areas and grassy and non-woody vegetation. Intermediate validation results are calculated based on the 1/3 of the LUCAS points described in section 5.1.1 and used for an internal comparison without area weights, which are not fully comparable with the final validation (section 0). Additionally, the classification results are aggregated to 1ha taking into account 8 neighboring pixels to keep linear features which would be partially lost taking into account 4 neighboring pixels. Those aggregated results are used for a visual comparison between the resulting classifications.

5.1.4.1 Signature Analysis

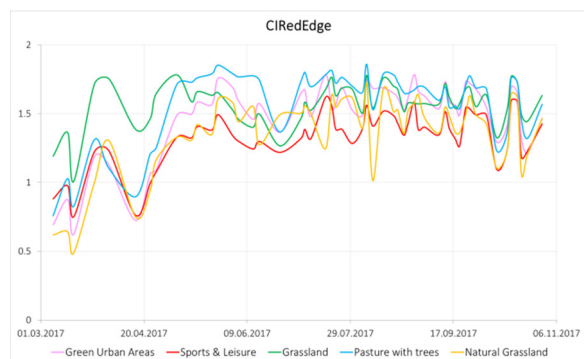
JECAM and Belgian reference data on grassland distribution with a variety of agricultural classes are available covering parts of the demonstration site (JECAM data covers 3 out of 6 S2 granules with in the demonstration site extent). Based on the Belgian reference datasets as well as the urban green classes of the Urban Atlas data set, a signature analysis has been performed on 16 spectral indices used to create the ECoLaSS HRL Grassland prototype 2017 (which are described into detail in chapter 4.2.1). These are in particular: (a) Clgreen, (b) CIRedEdge, (c) EVI, (d) MCARI/OSAVI, (e) MTCI, (f) NBR, (g) NDMI, (h) NDRE1, (i) NDRE2, (j) NDVI, (k) REP, (l) TCARI/OSAVI, (m) SAVI, (n) TCB, (o) TCG, and (p) TCW. The analysed grassland types are green urban areas, sports and leisure areas, grassland (agriculturally used), pastures with trees,

and natural grasslands. The results of this signature analysis are shown in Figure 5-8. As it can be seen, all five classes show a similar behaviour over the course of 2017 in all 16 indices. However, agricultural used grassland differs conspicuously at the beginning of the year from March to end of April. This can be seen as indicator for a possible separability of agricultural used grasslands and (semi-) natural grasslands, but needs a more into detail analysis.

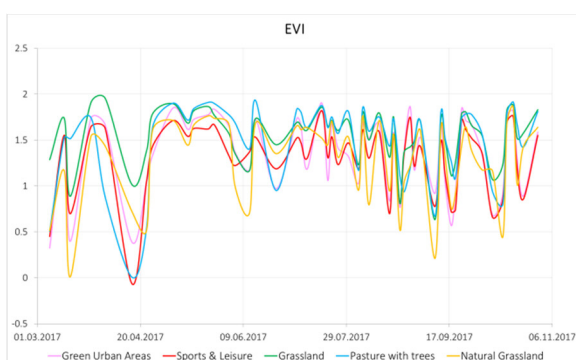
A detailed overview of the signal analysis of the five different grassland types present in the demo site WEST is provided in Annex 1.



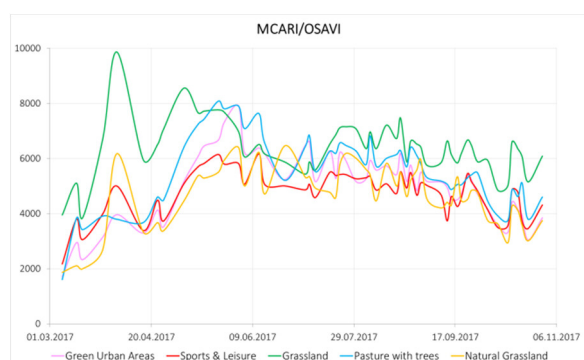
(a)



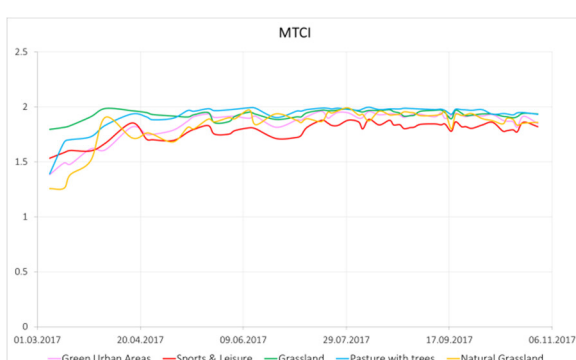
(b)



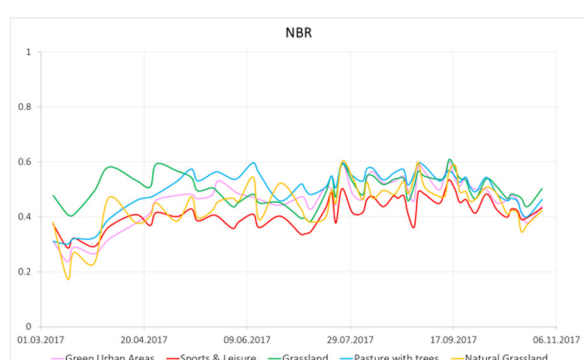
(c)



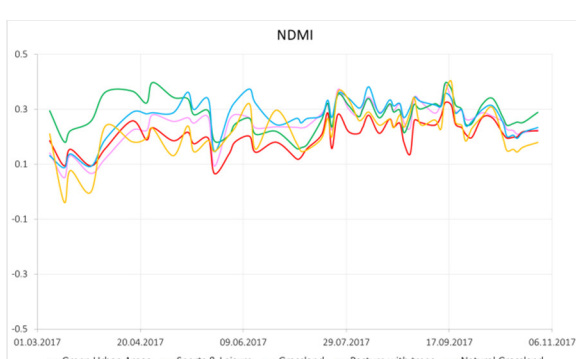
(d)



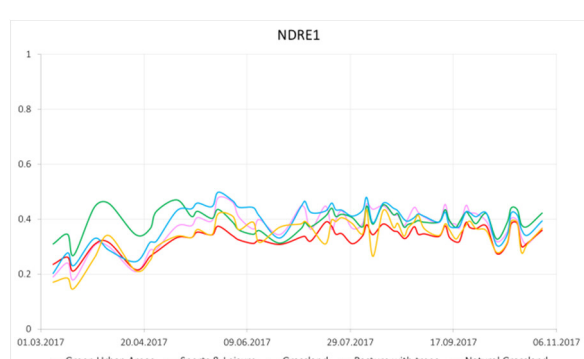
(e)



(f)



(g)



(h)



Figure 5-8: Spectral signatures of the 5 grassland types: green urban areas (rose) and sports and leisure areas (red) of the UA data set, as well as grassland (agriculturally used) (green), pastures with trees (blue), and natural grasslands (yellow) of the Belgian reference data set over the course of 2017 of the 16 indices: (a) Clgreen, (b) CIRedEdge, (c) EVI, (d) MCARI/OSAVI, (e) MTCI, (f) NBR, (g) NDMI, (h) NDRE1, (i) NDRE2, (j) NDVI, (k) REP, (l) TCARI/OSAVI, (m) SAVI, (n) TCB, (o) TCG, and (p) TCW.

5.1.4.2 SAR + seasonal features

Test case one includes annual statistical multi-temporal filtered SAR features (described in detail in section 5.1.3.1) in combination with seasonal optical features from March-April, July-August and September-October (described in detail in section 5.1.3.3). All feature composites are pre-processed and integrated as described in detail in section 5.1.1 and 5.1.2.

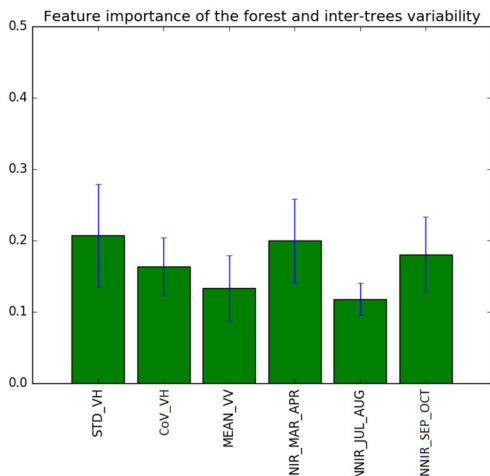


Figure 5-9: Feature importance for the combination of SAR and seasonal optical features.

The features importance represented in Figure 5-9 shows in detail which features are used in the classification approach and how they contribute to the grassland discrimination. The first three features can be summarized under annual SAR features (SAR) and the last three features are representing seasonal optical features (seasonal).



Figure 5-10: (left) Classification result of SAR + seasonal detailed view of 33UFS compared to (right) WV03 image (R:IR2;G:Red;B:Green) from 14.03.2017 with LGP grassland polygons in yellow (2016).

The comparison of the classification result with the LGP reference polygons in Figure 5-10 shows that the classification based on the combination of SAR features with seasonal optical features dataset has potential for the classification of grassland, considering, amongst others, the exclusion of cropland from the classification product.

To determine the accuracy of each classification and class the thematic accuracy assessment is performed including 1/3 of the points from the reference dataset, which were not included in the training process. These points are based on LUCAS points distributed over different locations in the demo site representing different land cover/use classes. Those classes were thematically aggregated to grassland/non-grassland classes. The error matrices are calculated from the not aggregated products due to the fact that the reference points are not considering the MMU of 1 ha. The overall, user's and producer's accuracy values of the grassland class are analysed to evaluate the classification accuracy.

Table 5-6: Error matrix (non-area-weighted) for SAR + seasonal features grassland mapping.

		Reference		
		Grassland	Others	Total
Classification	Grassland	174	51	225
	Others	59	832	891
	Total	233	883	1116
	PA [%]	74.68	94.22	

OA	90.14%
Delta OA	2.86



Figure 5-11: (left) aggregated classification result of SAR + seasonal detailed view of 33UFS compared to (right) WV03 image (R:IR2;G:Red;B:Green) from 14.03.2017 with LGP grassland polygons in yellow (2016).

The classification result in Figure 5-11 and Figure 5-10 illustrate that the grassland class could be successfully identified using both SAR multi-temporal filtered annual features and optical seasonal statistical reflectance features. The overall accuracy of the SAR and seasonal features classification is found as 90.14% (see Table 5-6 and Figure 5-10). Although the User's accuracy value is promising for the grassland class the Producer's values are comparatively indicating that some grass covered agricultural features are wrongly identified as grassland. Often, features containing a mixture of grass- and cropland or orchards were classified as grassland, contributing to the overall misclassification.

5.1.4.3 SAR + VI + seasonal features

Test case 2 uses annual statistical multi-temporal filtered SAR features (described in detail in section 5.1.3.1) in combination with the annual vegetation indices (described in detail in section 5.1.3.2) and seasonal optical features from March-April, July-August and September-October (described in detail in section 5.1.3.3) as input. All feature composites are pre-processed and integrated as described in detail in section 5.1.1 and 5.1.2.

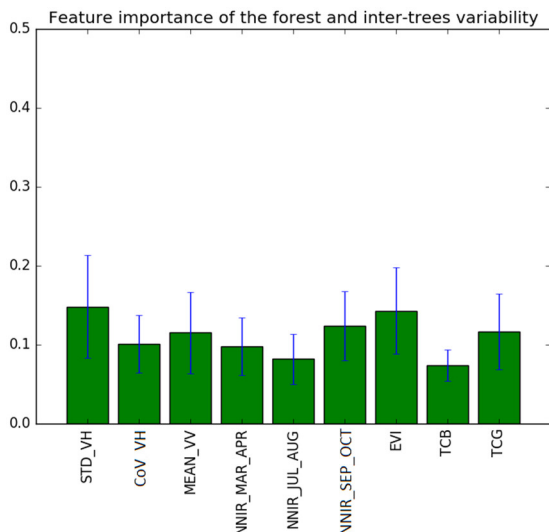


Figure 5-12: Feature importance for the combination of SAR, vegetation indices seasonal optical features.

The features importance represented in Figure 5-12 shows in detail which features are used and how they contribute to the grassland discrimination. The first three features can be summarized under annual SAR features (SAR), the next three features are representing seasonal optical features (seasonal); followed by the annual vegetation indices (VI).



Figure 5-13: (left) Classification result of SAR + VI + seasonal detailed view of 33UFS compared to (right) WV03 image (R:IR2;G:Red;B:Green) from 14.03.2017 with LGP grassland polygons in yellow (2016).

The comparison of the classification result with the reference polygons in Figure 5-13 shows that the inclusion of the annual vegetation also includes more wrongly classified grassland features like orchards. On the other hand, sparse dry grassland and intensively grazed pastures, which are sparsely covered with grass are mapped.

Table 5-7: Error matrix (non-area-weighted) for SAR + VI + seasonal features grassland mapping

		Reference			
		Grassland	Others	Total	UA [%]
Classification	Grassland	149	49	198	75.25
	Others	84	834	918	90.85
	Total	233	883	1116	
	PA [%]	63.95	94.45		

OA 88.08%

Delta OA 3.15



Figure 5-14: (left) Aggregated classification result of SAR + VI + seasonal detailed view of 33UFS compared to (right) WV03 image (R:IR2;G:Red;B:Green) from 14.03.2017 with LGP grassland polygons in yellow (2016).

The classification result in Figure 5-14 illustrates that the grassland class can be identified using both SAR multi-temporal filtered annual features and optical seasonal statistical reflectance features. The overall accuracy of the SAR and annual VI and seasonal features classification is found as 88.08% (seeTable 5-7). Compared with method one the overall accuracy is lower. This can be explained by the lower producer accuracy of 63.95% for the grassland class, which indicates that some grass covered agricultural features are wrongly identified as grassland.

5.1.4.4 SAR + OPT + seasonal features

Test case 3 includes annual statistical multi-temporal filtered SAR features (described in detail in section 5.1.3.1) in combination with annual optical features (described in detail in WP 33) and seasonal optical features from March-April, July-August and September-October (described in detail in section 5.1.3.3). All feature composites are pre-processed and integrated as described in detail in section 5.1.1 and 5.1.2.

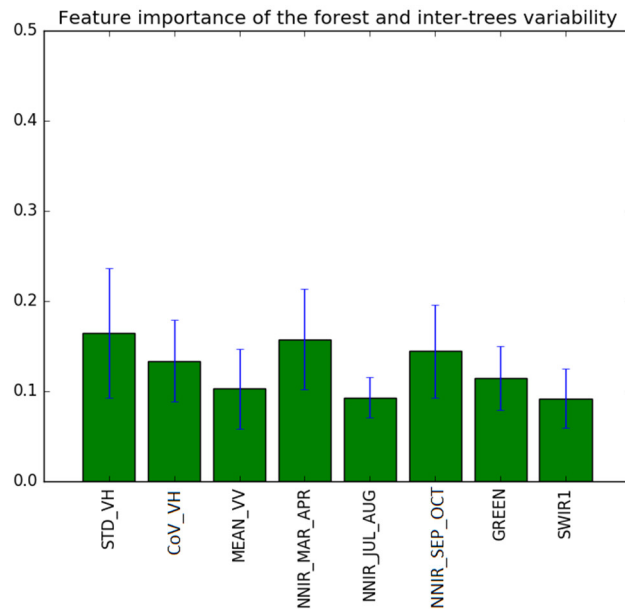


Figure 5-15: Feature importance for the combination of SAR, annual and seasonal optical features.

The features importance represented in Figure 5-15 shows in detail which features are used and how they contribute to the grassland discrimination. The first three features can be summarized under annual SAR features (SAR), the next three features are representing seasonal optical features (seasonal); followed by two annual optical reflectance band median composites (OPT).



Figure 5-16: (left) Classification result of SAR + OPT + seasonal detailed view of 33UFS compared to (right) WV03 image (R:IR2;G:Red;B:Green) from 14.03.2017 with LGP grassland polygons in yellow (2016).

The comparison of the classification result with the reference polygons in Figure 5-16 shows that the classification based on the combination of SAR features with annual and seasonal optical features datasets is characterized by more homogenous grassland patches including more grassland features compared to case one and two. The inclusion of the annual optical reflectance bands SWIR1 and Green also introduces

more wrongly classified grassland areas, such as orchards. On the other hand, sparse dry grassland and intensively grazed pastures, which are sparsely covered with grass, are also missed out. Overall the corresponding products of case 1 and 3 resemble.

Table 5-8: Error matrix (non-area-weighted) for SAR + OPT + seasonal features grassland mapping

		Reference			
		Grassland	Others	Total	UA [%]
Classification	Grassland	175	54	229	76.42
	Others	58	829	887	93.46
	Total	233	883	1116	
	PA [%]	75.11	93.88		

OA 89.96%

Delta OA 2.87



Figure 5-17: (left) Aggregated classification result of SAR + OPT + seasonal detailed view of 33UFS compared to (right) WV03 image (R:IR2;G:Red;B:Green) from 14.03.2017 with LGP grassland polygons in yellow (2016).

The classification result in Figure 5-17 illustrates that the grassland class could be successfully identified using SAR multi-temporal filtered annual features and optical annual and seasonal statistical reflectance features. The overall accuracy of this classification approach achieves an overall accuracy of 89.96% (see Table 5-8). User's and Producer's accuracy values of the grassland class are higher than 75% with this approach showing a more balanced product as with method 1 and 2.

5.1.4.5 SAR + OPT + VI + seasonal features

The best result could be achieved combining all in chapter 4.2 described features. Method four includes annual statistical multi-temporal filtered SAR features (described in detail in section 5.1.3.1) in combination with annual optical features (described in detail in WP 33) and seasonal optical features from March-April, July-August and September-October (described in detail in section 5.1.3.3) and annual vegetation indices (described in detail in section 5.1.3.2). All feature composites are pre-processed and integrated as described in detail in section 5.1.1 and 5.1.2.

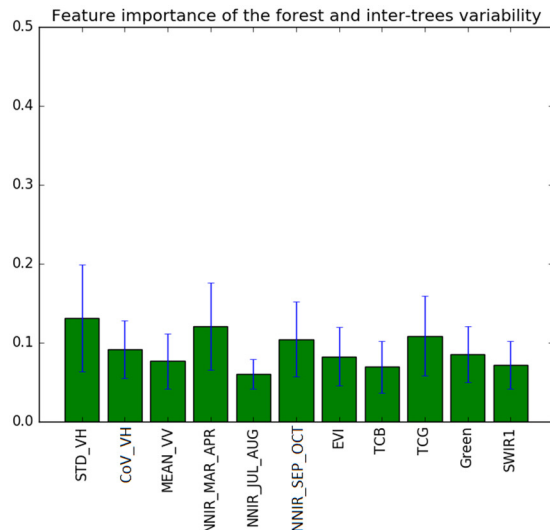


Figure 5-18: Feature importance for the combination of SAR, annual statistical vegetation indices, annual and seasonal optical features.

The features importance represented in Figure 5-18 shows in detail which features are used and how they contribute to the grassland discrimination. The first three features can be summarized under annual SAR features (SAR), the next three features are representing seasonal optical features (seasonal); followed by the annual vegetation indices (VI) and two annual optical reflectance bands (OPT).



Figure 5-19: (left) Classification result of SAR + OPT + VI + seasonal detailed view of 33UFS compared to (right) WV03 image (R:IR2;G:Red;B:Green) from 14.03.2017 with LGP grassland polygons in yellow (2016).

The comparison of the classification result with the reference polygons in Figure 5-19 shows that the classification based on the combination of combination, of SAR features with annual optical features, seasonal optical features datasets and annual optical vegetation indices median composites, has potential for the classification of grassland, considering, amongst others, the exclusion of cropland from the classification product.

Table 5-9: Error matrix (non-area-weighted) for SAR + VI + OPT + seasonal features grassland mapping

		Reference			
		Grassland	Others	Total	UA [%]
Classification	Grassland	180	49	229	78.6
	Others	53	834	887	94.02
	Total	233	883	1116	
	PA [%]	77.25	94.45		

OA 90.86%

Delta OA 2.77



Figure 5-20: (left) Aggregated classification result of SAR + OPT + VI + seasonal detailed view of 33UFS compared to (right) WV03 image (R:IR2;G:Red;B:Green) from 14.03.2017 with LGP grassland polygons in yellow (2016).

The classification result in Figure 5-20 illustrates that the grassland class can be identified using both SAR multi-temporal filtered annual features, optical annual and seasonal statistical reflectance features and annual vegetation indices. The overall accuracy of this approach is 90.86% (see Table 5-9). User's and Producer's accuracy values of the grassland class are higher than 75% with this approach showing a more balanced product as test 1 (section 5.1.4.2) and 2 (section 0). In comparison to test 3 (section 0) only a small product improvement could be observed. Grasslands might show similar spectral behaviour compared to certain crop types. As a matter of fact in the time series some needed observations are missing, which could foster the typical spectral behaviour of cropland, because in between ploughing practices create very distinct spectral response. This spectral response would be valuable for the differentiation from grassland. However, due to this lack of data it can happen that those crop types are wrongly classified.

5.2 Classification Results and Validation

This chapter presents the results of the feature selection (section 5.2.1) and the internal accuracy assessment of the ECoLaSS 2017 grassland prototype 2017 (section 0), followed by the comparison of the HRL Grassland 2015 with the VIRP as created in ECoLaSS, as well as a comparison between the HRL Grassland 2015 and the ECoLaSS grassland prototype 2017 (section 0).

5.2.1 Feature selection results

In this chapter the results of the section 5.1.4 Experimental Setup are summarised and compared to evaluated the most promising test case. To select an optimal feature set an accuracy assessment is performed including 1/3 of the points from the reference data set, which were not included in the trainings process. Please note, that this accuracy assessment was only used for the feature selection and not for the internal validation. The points are based on LUCAS sampling units distributed over different locations in the demonstration site representing different land cover / use classes. Those classes were thematically aggregated to grassland/non-grassland. Non-area-weighted based error matrices are calculated of the not aggregated products due to the fact that the reference points are not considering the MMU of 1 ha. The overall, user's and producer's accuracy values of the grassland class are analysed to evaluate the classification accuracy for the different feature sets as shown in below Table 5-10.

Table 5-10: Detailed class statistics for grassland mapping 2017 for different feature selections. Accuracy parameters are in percent (non-area-weighted).

Product/no aggregation	Overall Accuracy [%]	PA [%] - grassland	UA [%] - grassland	PA [%] – non grassland	UA [%] – non grassland
SAR + OPT*	89.26	69.40	76.67	94.46	92.17
SAR + seasonal	90.14	74.68	77.33	94.22	93.38
SAR + VI + seasonal	88.08	63.95	75.25	94.45	90.85
SAR + OPT + seasonal	89.96	75.11	76.42	93.88	93.46
SAR + OPT+ VI + seasonal	90.86	77.25	78.60	94.45	94.02

*results and detailed description of the classification setup for this test case are described in WP 33 [AD07]

As shown in Table 5-10 the most promising results over all test cases (described in detail in section 5.1.4) could be achieved combining annual statistical multi-temporal filtered SAR features (described in detail in section 5.1.3.1) in combination with annual (described in detail in WP 33) and seasonal optical features from March-April, July-August and September-October (described in detail in section 5.1.3.3) and annual vegetation indices (described in detail in section 5.1.3.2). Although the overall accuracy values for each experimental setup are higher than 88% the User's and Producer's accuracy range from 63% to 78% (see Table 5-10). The user's and producer's values are similar for the classifications SAR + seasonal, SAR + OPT + seasonal and SAR + OPT+ VI + seasonal, however user's and producer's accuracies show more differences compared with the classifications SAR + OPT and SAR + VI + seasonal. Among the five different classifications the highest accuracy has been obtained from the SAR + OPT+ VI + seasonal dataset.

The results identified several temporal statistical composites which significantly contribute to the grassland discrimination. Nevertheless, the usability of temporal statistical composites changes within different biogeographical regions and need to be tested individually for each region. Thus, a universal temporal feature set may never exist to satisfy the needs for a pan-European approach without differentiation between biogeographical regions.

5.2.2 Prototype Validation

The final internal validation has been carried out by the consortium partner SIRS for the most promising result of the feature selection (SAR + OPT+ VI + seasonal) as described in chapter 0. A detailed description of the prototype production (included features etc.) is given in chapter 5. The internal validation procedure and the area-weighted accuracy calculation are described in detail in section 4.4.

The result of the internal validation for the final prototype (SAR + OPT+ VI + seasonal) is presented in the below confusion matrix (Table 5-11) and in the following matrix from the blind approach (Table 5-12):

Table 5-11: Internal validation results for the SAR + OPT+ VI + seasonal product (area-weighted plausibility approach).

GRA_2017_010m_WEST_03035_V1_0		REFERENCE			User Accuracy	Confidence Interval
		Non-Grassland	Grassland	Total		
PRODUCT	Non-Grassland	596.4657	12.2143	608.6800	97.99%	0.98%
	Grassland	3.5812	87.7388	91.3200	96.08%	0.49%
	Total	600.0468	99.9532	700		
	Producer Accuracy	99.40%	87.78%		97.74%	Overall Accuracy
	Confidence Interval	0.90%	2.28%		0.93%	Confidence Interval

Table 5-12 - Validation results for the SAR + OPT+ VI + seasonal product (area-weighted blind approach)

GRA_2017_010m_WEST_03035_V1_0		REFERENCE			User Accuracy	Confidence Interval
		Non-Grassland	Grassland	Total		
PRODUCT	Non-Grassland	591.3764	17.3036	608.6800	97.16%	1.16%
	Grassland	8.0576	83.2624	91.3200	91.18%	0.72%
	Total	599.4340	100.5660	700		
	Producer Accuracy	98.66%	82.79%		96.38%	Overall Accuracy
	Confidence Interval	0.88%	2.63%		1.12%	Confidence Interval

The User Accuracy is particularly high and the results show very low level of commission errors with less than 4% and a confidence interval below 0.5%. Omissions errors are more numerous (12.22%) but remain in line with the product specifications approaching 90% accuracy. In addition, although the confidence interval for producer accuracy is higher than for user accuracy, it lies below 2.5% thus demonstrating the validity of the sampling and stratification approach.



Figure 5-21: (left) Classification result of SAR + OPT + VI + seasonal detailed view of 33UFS compared to (right) WV03 image (R:IR2;G:Red;B:Green) from 14.03.2017 with LGP grassland polygons in yellow (2016).

The final classification results are represented in Figure 5-21. Considering the characteristics of the demonstration site which is dominated by agriculture, there is no noticeable pattern in the omissions detected which are mostly in agricultural areas and within the urban fringe and some green spaces (e.g. sport and leisure facilities) within urban areas. Commission patterns are detected including cultivated and managed areas.



Figure 5-22: Example of orchards. Aggregated (MMU = 1ha) classification result (left) detailed view of 33UFS for SAR + OPT + VI + seasonal compared to (right) ArcGIS Basemap (25.09.2016).

Critical grassland features that could not be captured adequately with this approach are sparse and dry grasslands and small orchard parcels. Further, the distinction of grassland and shrubs in abandoned regions is challenging. As Figure 5-22 shows that vegetation classes such as small orchard parcels, with more than 10% tree cover are misclassified as grassland, because they show a rather low spectral dynamic over the year compared to other dynamic classes e.g. cropland.

5.2.3 HRL2015 Comparison with an Independent Data Source

For a better understanding of the quality of the pan-European HRL Grassland 2015 layer and to be able to quantify the improvements achieved by the methodological developments of the present project, it was intended to test the HRL Grassland 2015 against the training and validation data used by the ECoLaSS project: the Visually Interpreted Reference Points (VIRP). The analysis should confirm the overall thematic accuracy of the HRL Grassland layer 2015 of more than 85% and provide information on most relevant omission and commission errors with other land cover classes as a basis for further methodological enhancements.

As described in chapter 5.1.1 the VIRP have been extracted from the LUCAS point database and visually interpreted on Sentinel-2 time series from 2016 till 2017 and by using VHR data (like Bing maps) as additional data source. The points extracted represent main land cover classes and features with a minimum mapping unit of at least 900m². To be able to use the VIRP for analysing the quality of the HRL grassland classification, the database was initially adapted to the characteristics of the HRL data set. Each point representing grassland was reviewed and classified as grassland or non-grassland by applying the HRL grassland definition and respective minimum mapping unit of 1ha. The result was a data set with 597 grassland and 2811 non-grassland points that was subsequently combined with the classification of the HRL layer for further analysis. The result of the comparison is presented in the Table 5-13 below. While the majority of 525 grassland points could be confirmed, 72 grassland points have been assigned to non-grassland in the HRL layer. Moreover, 100 out of 2811 non-grassland VIRP turned out to be grassland in the HRL Grassland layer.

Table 5-13: Comparison between the HRL Grassland layer 2015 and the adapted VIRP 2017

Class		VIRP 2017		Totals
		No GRA	GRA	
HRL Grassland 2015		0	1	
No GRA	0	2711	100	2811
GRA	1	72	525	597
	Totals	2783	625	3408

Table 5-14: Accuracies for HRL Grassland using the adapted VIRP 2017 as Reference

Class Name	Producer's Accuracy	95% Confidence Interval		User's Accuracy	95% Confidence Interval	
No GRA/No GRA	97,41%	96,81%	98,02%	96,44%	95,74%	97,15%
GRA/GRA	84,00%	81,05%	86,95%	87,94%	85,24%	90,64%

Overall Accuracy: 94,95%

Based on these results, a confusion matrix (see Table 5-14) was calculated to evaluate the overall thematic accuracy and respective user's and producer's accuracies. The result confirms a high overall thematic accuracy of approx. 95% for the HRL Grassland layer. While the producer's accuracy is slightly below 85%, the user's accuracy provides satisfying values with approx. 88% thematic accuracy.

When analysing the wrong class assignments of the HRL data set, confusions between cropland and managed (mowed) grassland could be identified as the most important reason. Special attention should therefore be paid to this effect in the ECoLaSS project. The Grassland HRL 2015 was also tested against the first outcome of the ECoLaSS prototype. The ECoLaSS grassland prototype was created for the reference year 2017 and was trained on the VIRP (see section 5.2.1). This is a first version of this comparison. The tests and all presented results are still preliminary and will be continued in project phase 2.

The area figures for grassland and non-grassland for both layers are quite similar; however, in general the ECoLaSS grassland prototype layer shows some more grassland than the HRL GRA 2015. Reasons for that will be discussed in the following paragraphs. An overall grassland statistic can be found in Table 5-15.

Table 5-15: Comparative Grassland statistic (HRL 2015, ECoLaSS 2017) for the demonstration site West

Class	HRL GRA 2015	ECoLaSS grassland prototype 2017
Grassland	10,365 km ² / 83.9 %	10,943 km ² / 83.2 %
Non-Grassland	53,957 km ² / 16.1 %	54,083 km ² / 16.8 %
Clouds/Cloud-Shadows	2 km ² / 0.0%	0 km ² / 0.0 %
Overall	64,324 km ²	65,023 km ²

The slight difference in the overall area is due to the estuary of Westerschelde, which was classified as non-grassland in the ECoLaSS prototype but excluded from the HRL 2015.

Figure 5-23 shows a visual comparison of both layers highlighting the differences. Patches classified as grassland in both layers are shown in green, whereas additional grassland patches in the ECoLaSS prototype are highlighted in red and additional grassland patches in the HRL 2015 are highlighted in blue.

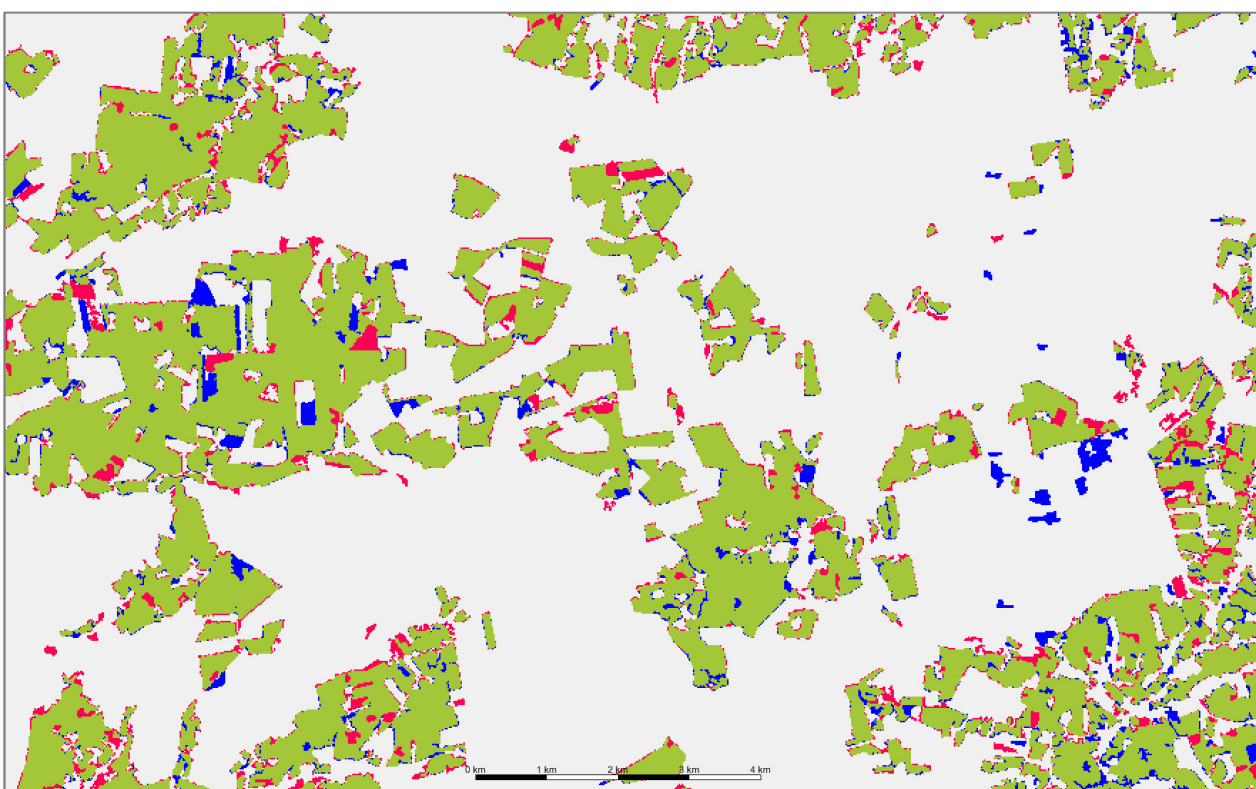


Figure 5-23: Unfiltered comparison of the HRL GRA 2015 and the ECoLaSS prototype 2017: grassland in both layers (green), grassland only in the ECoLaSS prototype (red), and only in the HRL GRA 2015 (blue).

To compare both datasets the ECoLaSS prototype in 10 m spatial resolution was resampled to the 20 m resolution of the HRL GRA 2015. It is obvious that differences appear continually at the border of grasslands, which is mainly due to the different geometric resolution and the resampling. Another reason could be the different input base data source, which is mainly Sentinel-1 and Sentinel-2 but acquired in different years. Slight geometric differences as well as illumination differences can lead to a different delineation of patches. Moreover, the different classification processes can provoke these deviances. The HRL GRA 2015 included an object-based approach with a segmentation of patches, while the ECoLaSS prototype is constricted to a pixel-based classification approach. Another issue is the MMU of the HRL GRA 2015 of 1 ha which was not applied in the same way to the ECoLaSS prototype. The HRL GRA 2015 allowed only pixel which share a direct border to another pixel (4 neighboring pixels are taken into account) and groups of pixel needed to be at least 1 ha of size. The ECoLaSS prototype allowed also pixel which do not share a direct border but a corner of an adjacent pixel (8 neighboring pixels are taken into account).

Therefore the ECoLaSS prototype includes also single (diagonal) pixels, as compared to the HRL 2015 which does not.

In the first step of comparison the difference between both layers was calculated but on purpose not yet filtered, to check (i) if also very small grassland patches could have been correctly detected and (ii) if very small patches are mainly noise and misclassifications of mixed pixels in the base data source. These resulting differences, described above, are therefore not real changes, just technical issues, and are not topic of the following interpretation of the differences between both data sets.

As a second step this difference map between the ECoLaSS prototype 2017 and the HRL GRA 2015 was also filtered to the MMU of the HRL grassland layer 2015 of 1 ha. The outcome is shown in Figure 5-24: Filtered comparison of the HRL GRA 2015 and the ECoLaSS prototype 2017: grassland in both layers (green), grassland only in the ECoLaSS prototype (blue), and only in the HRL GRA 2015 (red). Most of the technical differences related to single pixel and lines of pixel at borders of grassland patches were removed. Resulting compact patches are a proxy for a possible grassland change product. The following analyses will show that due to different classification approaches the filtered map-to-map difference can still not be considered as a change layer, as it is mainly highlighting misclassifications in one or the other of the two layers.

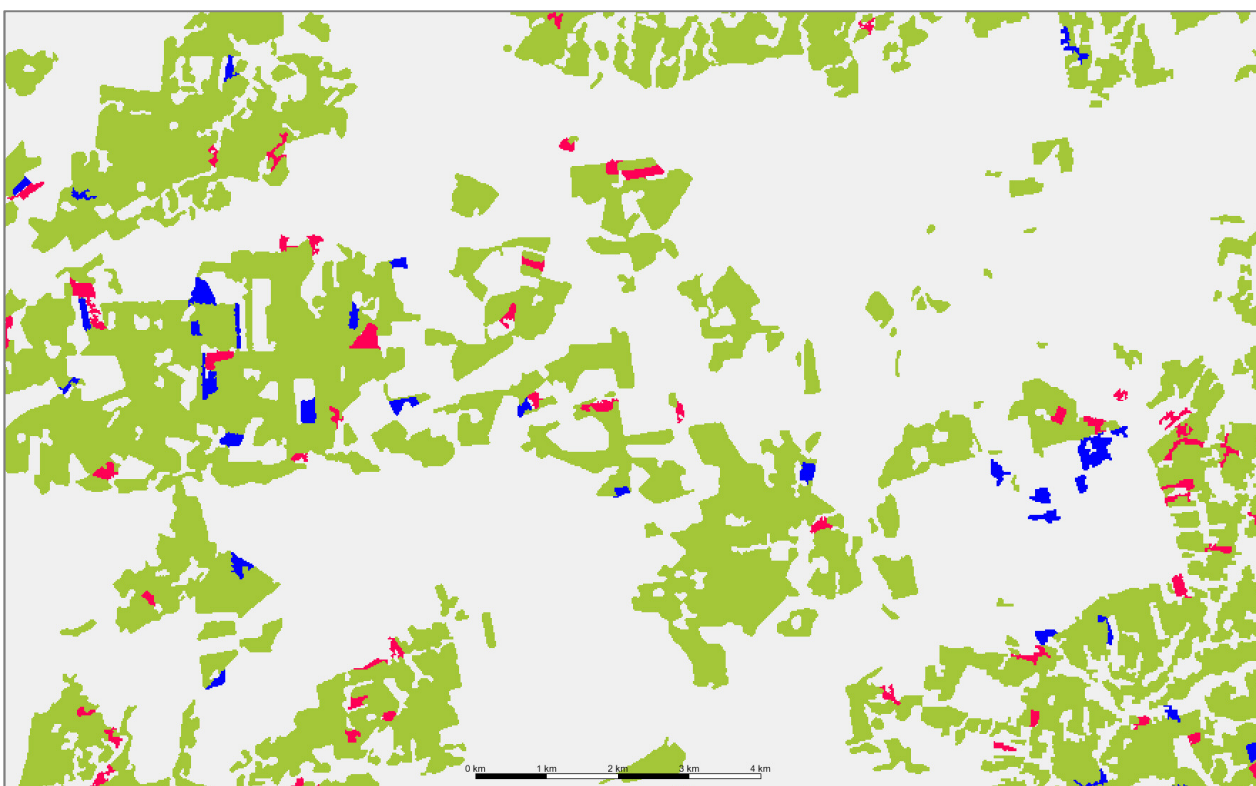


Figure 5-24: Filtered comparison of the HRL GRA 2015 and the ECoLaSS prototype 2017: grassland in both layers (green), grassland only in the ECoLaSS prototype (blue), and only in the HRL GRA 2015 (red).

The following description of misclassifications included a comparison of both datasets and a cross-check against VHR data from GoogleEarth and BingMaps.

SPECIFIC TYPES OF GRASSLAND THAT WERE MISSED OUT IN ONE OF THE LAYERS (OMISSION ERRORS)

Table 5-16 shows types of grassland which were left out and therefore not detected by the classifier in one or the other layer.

Table 5-16: Types of omission errors for HRL GRA 2015 and the ECoLaSS prototype 2017

Grassland Type	HRL GRA 2015	ECoLaSS prototype 2017
Urban green areas like sport fields, parks and residential areas	Partly missing	Partly missing
Natural Grassland on military sites	Partly missing	Missing

Reasons for these omissions in the ECoLaSS 2017 layer could be missing reference samples of these classes (in the VIRP). Reasons for omissions in the HRL GRA 2015 for urban areas are mainly related to the MMU, as urban green areas are very often mixed with trees, buildings etc. and do therefore often not fulfill the MMU of the HRL GRA 2015 of at least 1 ha. It was expected that the ECoLaSS prototype will show some more urban green areas due to the better resolution. This was partly the case, however, not valid for all urban areas. Even without filtering no systematic caption of small urban green areas could be determined.

The Omissions of natural grassland on military sites are related to confusion of this land cover feature with low density shrub and forest areas, but the results for this land cover type are much more compact within the HRL GRA 2015 than in the ECoLaSS prototype 2017. Compact patches better represent the natural grassland features on the military sites and therefore it will be targeted to improve the capturing of such sites.

SPECIFIC TYPES OF NON-GRASSLAND THAT ARE WRONGLY OVERREPRESENTED IN ONE OF THE LAYERS (COMMISSION ERRORS)

Table 5-17Figure 5-17 shows types of non-grassland by definition, which are overrepresented in the grassland mask in one or the other layer.

Table 5-17: Types of commission errors for HRL GRA 2015 and the ECoLaSS prototype 2017

Grassland Type	HRL GRA 2015	ECoLaSS prototype 2017
Low density urban areas	Not detected	Misclassification of garden plots with certain percentage of buildings and urban infrastructures (relevant for the whole demonstration site).
Cultivated and managed areas of agricultural use	Not detected	Misclassification of e.g. Orchards and managed grassland with fruit trees (southern part of the demonstration site).
Moore and heathland	Not included in Grassland by definition, but still included in the HRL GRA 2015 at least in some areas over Europe.	Successfully excluded from the grassland mask of the ECoLaSS grassland prototype (especially northern part of the demonstration site)

Reasons for these commissions in the ECoLaSS 2017 layer could be missing reference samples of these classes (in the VIRP). Reasons for commissions in the HRL GRA 2015 for moor and heathland are mainly related to spectral confusion with wet grassland. The successful exclusion of these land cover features is a great improvement of the ECoLaSS prototype 2017.

The misclassifications present in the ECoLaSS prototype 2017 related to orchards and garden plots were successfully avoided within the HRL GRA 2015 project, in particular by the implementation of SAR EO data. As the ECoLaSS 2017 prototype layer is based on dense time series of both, optical and SAR data, the

removal of these commissions should be further investigated in the second project phase, and is to be tested with a focus on SAR data.

DIFFERENCES BETWEEN THE TWO LAYERS RELATED TO REAL CHANGES BETWEEN THE YEARS 2015 AND 2017, WHICH CAN BE AN INDICATION ABOUT APPROPRIATE UPDATE CYCLES OF SUCH A PRODUCT

Based on inspection of selected change patches it can be concluded that most of the detected differences between the two products (omissions and commissions) are mainly related to technical changes. E.g., within the demonstration site no agricultural site was found where a change of the actual land use to grassland took place. Likewise, no conversion from grassland into other land covers such as urban areas was found. Therefore the differences between the two layers are mainly caused by the classification errors described above or due to the differences of the MMU. As not every single patch was reviewed, it could still be the case that also several real changes are included in such a proxy for a possible change product. In the second phase it will be investigated how such a simple map-to-map difference layer could be separated into (i) real change classes, to derive a real change layer and (ii) technical changes, which could be used to improve the former and consequently, the grassland mask for future improved HRL products.

APPROPRIATE MMU FOR A 10 M PRODUCT

Regarding the appropriate MMU for future 10m resolution grassland products, further testing shall follow in phase two of ECoLaSS. Though not all green urban areas were included in the ECoLaSS prototype 2017, some improvements, with respect to the HRL GRA 2015, have been found. These revealed that patches even smaller than the HRL GRA 2015 MMU of 1 ha could have been detected. The appropriate MMU size of a new 10 m product still is under investigation and will be further explored in the second project phase.

5.3 Prototype Specifications

The raster products of the ECoLaSS prototypes are delivered as GeoTIFF (*.tif) with world file (*.tfw), pyramids (*.ovr), attribute table (*.dbf) and statistics (*.aux.xml), enabling an instant illustration and analysis of the products within Geographic Information System (GIS) software. Each product is accompanied with a product-specific colour table (*.clr) and INSPIRE-compliant metadata in XML format. Metadata are provided together with the products as INSPIRE-compliant XML files according to the EEA Metadata Standard for Geographic Information (EEA-MSGI). EEA-MSGI has been developed by EEA to meet needs and demands for inter-operability of metadata. EEA's standard for metadata is a profile of the ISO 19115 standard for geographic metadata and contains more elements than the minimum required to comply the INSPIRE metadata regulation. Detailed conceptual specifications on EEA-MSGI and other relevant information on metadata can be found at <http://www.eionet.europa.eu/gis>.

The consortium has developed a standardised and harmonised product file naming convention for all prototypes produced as part of ECoLaSS based on the file naming convention of the CLMS High Resolution Layers. This file naming convention will be applied to all raster prototypes and associated reference files and is documented in the Deliverables of Task 4.

The file names generally contain the following 7 main aspects:

THEME YEAR RESOLUTION EXTENT EPSG TYPE VERSION

THEME

3 letter abbreviation for main products: DLT (dominant leaf type), TCC (tree cover change), GRA (grassland), IMD, IMC (imperviousness degree, imperviousness degree change), CRT (crop type), CRM (crop mask) and new land cover products, to be decided.

REFERENCE YEAR

2017 in four digits

Change products in four digits (e.g. 1517)

RESOLUTION

Four-digit (020m and 010m)

EXTENT

2-digit code for demonstration-sites (CE (central), NO (north), WE (west), SW (southwest), SE (southeast), SA (South Africa), ML (Mali))

EPSG

5-digit EPSG code (geodetic parameter dataset code by the European Petroleum Survey Group) "03035" for the European LAEA projection

TYPE

prototype

VERSION

3-digit code "v01"

EXAMPLE:

"GRA_2017_010m_WE_03035_prototype_v01.tif" stands for: Grassland, 2017 reference year, 10m, Demonstration-site West, European projection (EPSG: 3035), prototype, version 01

The product specifications of the ECoLaSS grassland prototype 2017 are shown in Table 5-18.

Table 5-18: Grassland prototype specifications.

Grassland 10m	Acronym	Product category			
	GRA	Improved Primary Status Layer			
Reference year					
2017					
Geometric resolution					
Pixel resolution 10m x 10m, fully conform with the EEA reference grid					
Coordinate Reference System					
European ETRS89 LAEA projection					
Geometric accuracy (positioning scale)					
Less than half a pixel. According to ortho-rectified satellite image base delivered by ESA.					
Thematic accuracy					
Minimum 85% overall accuracy					
Data type					
8bit unsigned raster with LZW compression					
Minimum Mapping Unit (MMU)					
Pixel-based (1ha)					
Necessary attributes					
Raster value, count, class name, area (in km2), area percentage (taking outside area not into account)					
Raster coding (thematic pixel values)					
0: all non-grass areas					
1: Grassy and non-woody vegetation					
254: unclassifiable (no satellite image available, or clouds, or shadows)					
255: outside area					
Metadata					
XML metadata files according to INSPIRE metadata standards					
Delivery format					
Geotiff					
Colour table					
ArcGIS *.clr format					
<hr/>					
Class Code	Class Name	Red	Green	Blue	
0	all non-grass areas	240	240	240	
1	Grassy and non-woody vegetation	70	158	74	
254	unclassifiable (no satellite image available, or clouds, or shadows)	153	153	153	
255	outside area	0	0	0	

6 Conclusion and Outlook

The objective of WP43 Permanent Grassland Identification is an improved identification of grassland areas using Sentinel satellite image time series with the aim to develop a prototype of a next-generation European HR Grassland Layer with high thematic accuracy.

With the availability of dense optical and SAR time series from Sentinel satellites, grassland mapping can profit from the increased information content provided by temporal measurements of the reflectance. A supervised classification approach using the Random Forest classifier based on dense time series data from Sentinel-1 and Sentinel-2 has been successfully applied. Using time features of Sentinel-2 and Sentinel-1 data and reference samples based on visually reinterpreted LUCAS samples, a new classification of grassland for the year 2017 was retrieved. A Random Forest classifier has been applied in four experiments using different combinations of time features including annual SAR and optical features, seasonal optical features and annual spectral optical indices to assess their usability as described in chapter 5.1.4. The accuracy of grassland classification depends on the number of valid optical observations in the time series, covering the growing period, to derive accurate seasonal and annual statistical composites without gaps. The best result could be achieved combining all in chapter 4.2 described features. Among five experiments the one with the best performance was selected which includes annual statistical multi-temporal filtered SAR features (described in detail in section 5.1.3.1) in combination with annual and seasonal optical features from March-April, July-August and September-October (described in detail in section 5.1.3.3) and annual vegetation indices (described in detail in section 5.1.3.2).

The results show the potential of SAR annual features and optical seasonal features in combination with optical annual features to identify grasslands. The combination of multi-temporal and multi-sensoral data allows improving the classification accuracy due to observations of phenological effects and (temporal) grassland management patterns. The optical data proved to be more suitable to characterize the vegetation status and to exclude water covered objects and urban objects, while SAR imagery proved to support the separation of grassland from cropland areas. The combination of data of the Sentinel fleet shows great potential in terms of consistency and enhancement for the grassland classifications. The automated feature selection (section 5.2.1) revealed that the highest accuracy is achieved by the combined use of optical and SAR temporal features.

Misclassifications are partly caused by gaps in optical time-series. Further, small orchard parcels, with more than 10% tree cover, show a rather low spectral dynamic over the year compared to other classes, e.g. cropland, and could be therefore misclassified as grassland. On the other hand, sparse dry grassland and intensively grazed pastures, which are rather sparsely covered with grass, are also mistakenly excluded from the grassland class in some cases, due to showing similar spectral characteristics as open areas.

For the identification of grasslands on a pan-European level, complementary information derived from S-1 annual statistical parameters in addition to S-2 can improve the thematic classification.

An internal validation of the ECoLaSS 2017 grassland layer showed a high overall accuracy of 97.74% and high user and producer accuracies (UA: 96.08% ; PA: 87.78%). Compared with the grassland HRL2015 the main improvements are:

- Increase of the thematic accuracy
- Seamless, wall-to-wall coverage (without “no data” gaps)
- Fully automated approach based on dense S-1 and S-2 time series
- Improved spatial resolution of 10m.

In the second Reporting Period of the ECoLaSS project, the focus will be on analysis with further curve fitting and outlier-detection approaches, to optimally utilize the information content of temporal trajectories. Dense Sentinel-1 SAR and Sentinel-2 optical time series data will be used in phase 2 to derive

temporal parameters with the aim to distinguish between intensively and extensively managed grasslands. A signature analysis showed the potential for this separation, especially during the early stages of the phenological cycle in spring. However, further more into detail analysis is necessary. The highest dynamics in SAR backscatter is associated with intensively used grasslands which are strongly managed in terms of fertilisation, irrigation, and mowing, differing from natural grasslands and pastures.

In WP34 [AD08] first steps in this direction are made with regression model fitting and trend analysis of grassland areas in comparison with agricultural areas to lay the focus on the grassland management intensity and separation between grasslands and croplands. Comparative analyses will be undertaken in phase 2 of the project for distinguishing different types of grasslands and different grassland management intensities as illustrated in below figure.

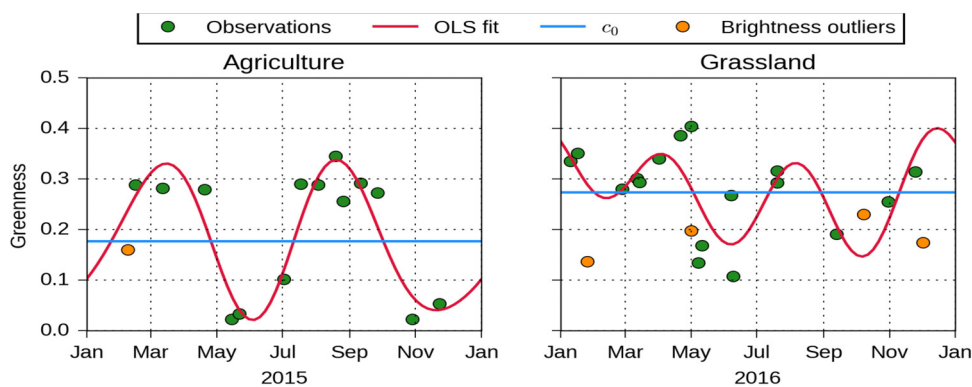


Figure 6-1: Comparison of an agricultural pixel to a grassland pixel.

Several differences between the fitted curves can be observed, for example the value of the trend parameter c_0 , the composition of the seasonal pattern with respect to the amplitudes of the different frequencies, and the minimal value and range (difference max, min) of the fitted curve (see Figure 6-1). Further analysis will be undertaken in phase 2 of the project, e.g. related to outlier detection in selected features (such as e.g. greenness vs. brightness etc., see Figure 6-2), and signature anomaly detection related to changes such as between agriculture and grassland land cover.

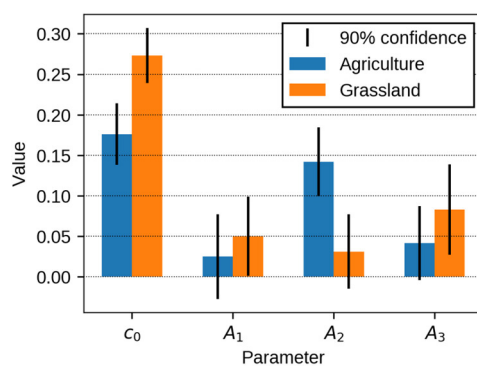


Figure 6-2: Greenness trend and amplitudes of an agriculture and grassland pixel.

Additional to the parameter values, also the covariance matrix of the estimates can be calculated, which can be further used to derive the uncertainty of the amplitude values. Figure 6-2 contrasts the trend and amplitude parameters for distinguishing between cropland and grassland. This represents a promising approach also for discrimination of grassland management regimes. To allow accurate signal trend analysis based on dense time series, the current data density of optical time series from Sentinel-2 is not fully appropriate for 2016 to 2017, as Sentinel-2B data is available from July 2017 onwards only. Therefore, the testing will be continued on dense Sentinel-2 and Sentinel-1 time series in phase 2. Improvement of the minimum mapping unit from currently 1ha to 0.5ha or below will be analysed for both the status as well as grassland change layers in phase 2.

Further, in phase 2 the developed processing line on grassland identification will be implemented on other more challenging Mediterranean and Alpine biographic regions. Moreover, approaches for deriving grassland change between two status layers or as an incremental update will be tested in project phase 2.

References

- Barnes, E. M., Clarke, T. R., Richards, S. E., Colaizzi, P. D., Haberland, J., Kostrzewski, M., ... & Lascano, R. J. (2000, July). Coincident detection of crop water stress, nitrogen status and canopy density using ground based multispectral data. In *Proceedings of the Fifth International Conference on Precision Agriculture, Bloomington, MN, USA* (Vol. 1619).
- Breiman, L. (2001). Random Forests. *Machine Learning*, 4(1), 5-32.
- Büttner G., Kosztra B., Maucha G., Pataki R. (2012): Implementation and achievements of CLC2006, ETC-LUSI, EEA, 65p.
- Cho, M. A., & Skidmore, A. K. (2009). Hyperspectral predictors for monitoring biomass production in Mediterranean mountain grasslands: Majella National Park, Italy. *International Journal of Remote Sensing*, 30(2), 499-515.
- Clevers, J. G., & Gitelson, A. A. (2013). Remote estimation of crop and grass chlorophyll and nitrogen content using red-edge bands on Sentinel-2 and-3. *International Journal of Applied Earth Observation and Geoinformation*, 23, 344-351.
- Clevers, J. G., & Kooistra, L. (2012). Using hyperspectral remote sensing data for retrieving canopy chlorophyll and nitrogen content. *IEEE Journal of Selected Topics in Applied Earth Observations and Remote Sensing*, 5(2), 574-583.
- Daughtry, C. S. T., Walthall, C. L., Kim, M. S., De Colstoun, E. B., & McMurtrey Iii, J. E. (2000). Estimating corn leaf chlorophyll concentration from leaf and canopy reflectance. *Remote sensing of Environment*, 74(2), 229-239.
- Dymond, C. C., Mladenoff, D. J., & Radeloff, V. C. (2002). Phenological differences in Tasseled Cap indices improve deciduous forest classification. *Remote Sensing of Environment*, 80(3), 460-472.
- Fernández-Manso, A., Fernández-Manso, O., & Quintano, C. (2016). Sentinel-2A red-edge spectral indices suitability for discriminating burn severity. *International journal of applied earth observation and geoinformation*, 50, 170-175.
- EEA (2015). Biogeographical regions dataset. Available: <http://www.eea.europa.eu/data-and-maps/data/biogeographical-regions-europe-3#tab-gis-data>. European Environment Agency (EEA).
- Foody, G. M., & Dash, J. (2007). Discriminating and mapping the C3 and C4 composition of grasslands in the northern Great Plains, USA. *Ecological Informatics*, 2(2), 89-93.
- Gallego, F. J. (1995). *Sampling frames of square segments*. Office for Official Publ. of the European Communities.
- Gallego, J. and JRC-IES, I. I. (2004). Area Frames for Land Cover Estimation: Improving the European LUCAS Survey. Presented at the Proceedings of the 3rd World Conference on Agricultural and Environmental Statistical Application, Cancun, Mexico, 2–4.
- Gao, B. C. (1996). NDWI—A normalized difference water index for remote sensing of vegetation liquid water from space. *Remote sensing of environment*, 58(3), 257-266.
- Gitelson, A. A., Vina, A., Ciganda, V., Rundquist, D. C., & Arkebauer, T. J. (2005). Remote estimation of canopy chlorophyll content in crops. *Geophysical Research Letters*, 32(8).

Gitelson, A., & Merzlyak, M. N. (1994). Spectral reflectance changes associated with autumn senescence of *Aesculus hippocastanum* L. and *Acer platanoides* L. leaves. Spectral features and relation to chlorophyll estimation. *Journal of Plant Physiology*, 143(3), 286-292.

Henrich, V., Krauss, G., Götze, C., Sandow, C. (2012). IDB. URL: <http://www.indexdatabase.de> (Entwicklung einer Datenbank für Fernerkundungsindizes. AK Fernerkundung, Bochum).

Heute, A. R., Liu, H. Q., Batchily, K., & Van Leeuwen, W. (1997). A comparison of vegetation indices over a global set of TM images for EOS-MODIS. *REMOTE SENSING OF ENVIRONMENT-NEW YORK-*, 59, 440-451.
Horler, D. N. H., DOCKRAY, M., & Barber, J. (1983). The red edge of plant leaf reflectance. *International Journal of Remote Sensing*, 4(2), 273-288.

Huete, A. R. (1988). A soil-adjusted vegetation index (SAVI). *Remote sensing of environment*, 25(3), 295-309.

Kawamura, K., Akiyama, T., Yokota, H. O., Tsutsumi, M., Yasuda, T., Watanabe, O., & Wang, S. (2005). Comparing MODIS vegetation indices with AVHRR NDVI for monitoring the forage quantity and quality in Inner Mongolia grassland, China. *Grassland Science*, 51(1), 33-40.

Keil, M., Esch, T., Divanis, A., Marconcini, M., Metz, A., Ottinger, M., Voinov, S., Wiesner, M., Wurm, M. & Zeidler, J. (2015). Updating the Land Use and Land Cover Database CLC for the Year 2012-„Backdating“ of DLM-DE of the Reference Year 2009 to the Year 2006.

Magiera, A., Feilhauer, H., Waldhardt, R., Wiesmair, M., & Otte, A. (2017). Modelling biomass of mountainous grasslands by including a species composition map. *Ecological Indicators*, 78, 8-18.

Olofsson, P., Foody, G. M., Stehman, S. V., and Woodcock, C. E. (2013). Making better use of accuracy data in land change studies: Estimating accuracy and area and quantifying uncertainty using stratified estimation. *Remote Sensing of Environment*, 129, 122–131.

Rossini, M., Migliavacca, M., Galvagno, M., Meroni, M., Cogliati, S., Cremonese, E., ... & Siniscalco, C. (2014). Remote estimation of grassland gross primary production during extreme meteorological seasons. *International Journal of Applied Earth Observation and Geoinformation*, 29, 1-10.

Rüetschi, M., Schaepman, M. E., & Small, D. (2017). Using Multi-temporal Sentinel-1 C-band Backscatter to Monitor Phenology and Classify Deciduous and Coniferous Forests in Northern Switzerland. *Remote Sensing*, 10(1), 55.

Samadzadegan, F. (2004). Data integration related to sensors, data and models. In *XXth ISPRS Congress. Istanbul, Turkey, ISPRS*.

Schmidt, T., Schuster, C., Kleinschmit, B., & Förster, M. (2014). Evaluating an Intra-Annual Time Series for Grassland Classification—How Many Acquisitions and What Seasonal Origin Are Optimal?. *IEEE Journal of Selected Topics in Applied Earth Observations and Remote Sensing*, 7(8), 3428-3439.

Selkowitz, D. J. and Stehman, S. V. (2011). Thematic accuracy of the National Land Cover Database (NLCD) 2001 land cover for Alaska. *Remote Sensing of Environment*, 115 (6), 1401–1407.

Stehman, S. V. and Czaplewski, R. L., (1998). Design and analysis for thematic map accuracy assessment: fundamental principles. *Remote Sensing of Environment*, 64 (3), 331–344.

Suhet (2015). *Sentinel-2 User Handbook*. E. S. Agency, Ed.,1.2 ed.

Turner, D. P., Cohen, W. B., Kennedy, R. E., Fassnacht, K. S., & Briggs, J. M. (1999). Relationships between leaf area index and Landsat TM spectral vegetation indices across three temperate zone sites. *Remote sensing of environment*, 70(1), 52-68.

Vicente, L. E., LOEBMANN, D. D. S., Zillmann, E., González, A., Vicente, A. K., de OLIVEIRA, B. P., & de Araújo, L. S. Assessment of vegetational indices applied to sugarcane monitoring using Rapideye images. In *Embrapa Meio Ambiente-Artigo em anais de congresso (ALICE)*. In: SIMPÓSIO BRASILEIRO DE SENSORIAMENTO REMOTO, 18., 2017, Santos. Anais Santos: Inpe, 2017. Trabalho 59847.

Wang, C., Jamison, B. E., & Spicci, A. A. (2010). Trajectory-based warm season grassland mapping in Missouri prairies with multi-temporal ASTER imagery. *Remote sensing of environment*, 114(3), 531-539.

Waske, B., & van der Linden, S. (2008). Classifying multilevel imagery from SAR and optical sensors by decision fusion. *IEEE Transactions on Geoscience and Remote Sensing*, 46(5), 1457-1466.

Woodhouse, I. H. (2017). *Introduction to Microwave Remote Sensing*. CRC press.

Wu, C., Niu, Z., & Gao, S. (2012). The potential of the satellite derived green chlorophyll index for estimating midday light use efficiency in maize, coniferous forest and grassland. *Ecological Indicators*, 14(1), 66-73.

Wu, C., Niu, Z., Tang, Q., & Huang, W. (2008). Estimating chlorophyll content from hyperspectral vegetation indices: Modeling and validation. *Agricultural and forest meteorology*, 148(8-9), 1230-1241.

Xu, D., Guo, X., Li, Z., Yang, X., & Yin, H. (2014). Measuring the dead component of mixed grassland with Landsat imagery. *Remote Sensing of Environment*, 142, 33-43.

Xue, J., & Su, B. (2017). Significant remote sensing vegetation indices: a review of developments and applications. *Journal of Sensors*, 2017.

Yang, X., Smith, A. M., & Hill, M. J. (2017). Updating the Grassland Vegetation Inventory Using Change Vector Analysis and Functionally-Based Vegetation Indices. *Canadian Journal of Remote Sensing*, 43(1), 62-78.

Yang, Y. H., Fang, J. Y., Pan, Y. D., & Ji, C. J. (2009). Aboveground biomass in Tibetan grasslands. *Journal of Arid Environments*, 73(1), 91-95.

Zillmann, E., Gonzalez, A., Herrero, E. J. M., van Wolvelaer, J., Esch, T., Keil, M., ... & Garzón, A. M. (2014). Pan-European grassland mapping using seasonal statistics from multisensor image time series. *IEEE Journal of selected topics in applied Earth Observations and Remote Sensing*, 7(8), 3461-3472.

Zillmann, E., Weichelt, H., Herrero, E. M., Esch, T., Keil, M., & van Wolvelaer, J. (2013, June). Mapping of grassland using seasonal statistics derived from multi-temporal satellite images. In *Analysis of Multi-temporal Remote Sensing Images, MultiTemp 2013: 7th International Workshop on the* (pp. 1-3). IEEE.

Annexe 1

In the following, a detailed overview of the signal analysis of the five different grassland types present in the demo site WEST is given showing besides the MEAN spectral signature of the different indices for all five grassland types together also the MEAN +/- the standard deviation for the five grassland types separately.

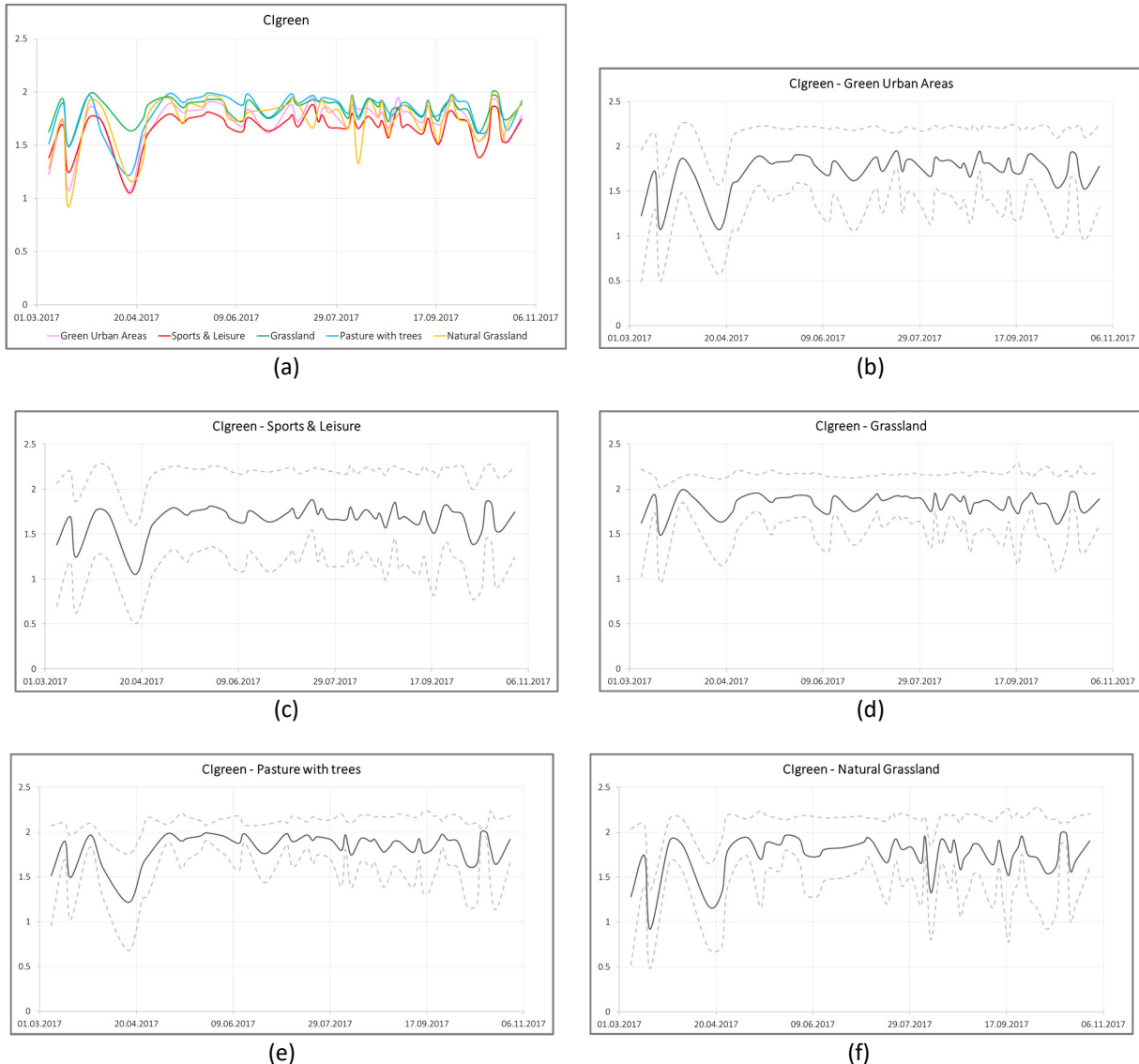


Figure 6-3: Overview of the MEAN spectral signature of the index Clgreen for all five grassland types (a) as well as the MEAN +/- the standard deviation for the single five grassland types: (b) green urban areas, (c) sports and leisure areas, (d) pastures with trees, (e) grassland (agriculturally used), and (f) natural grasslands.

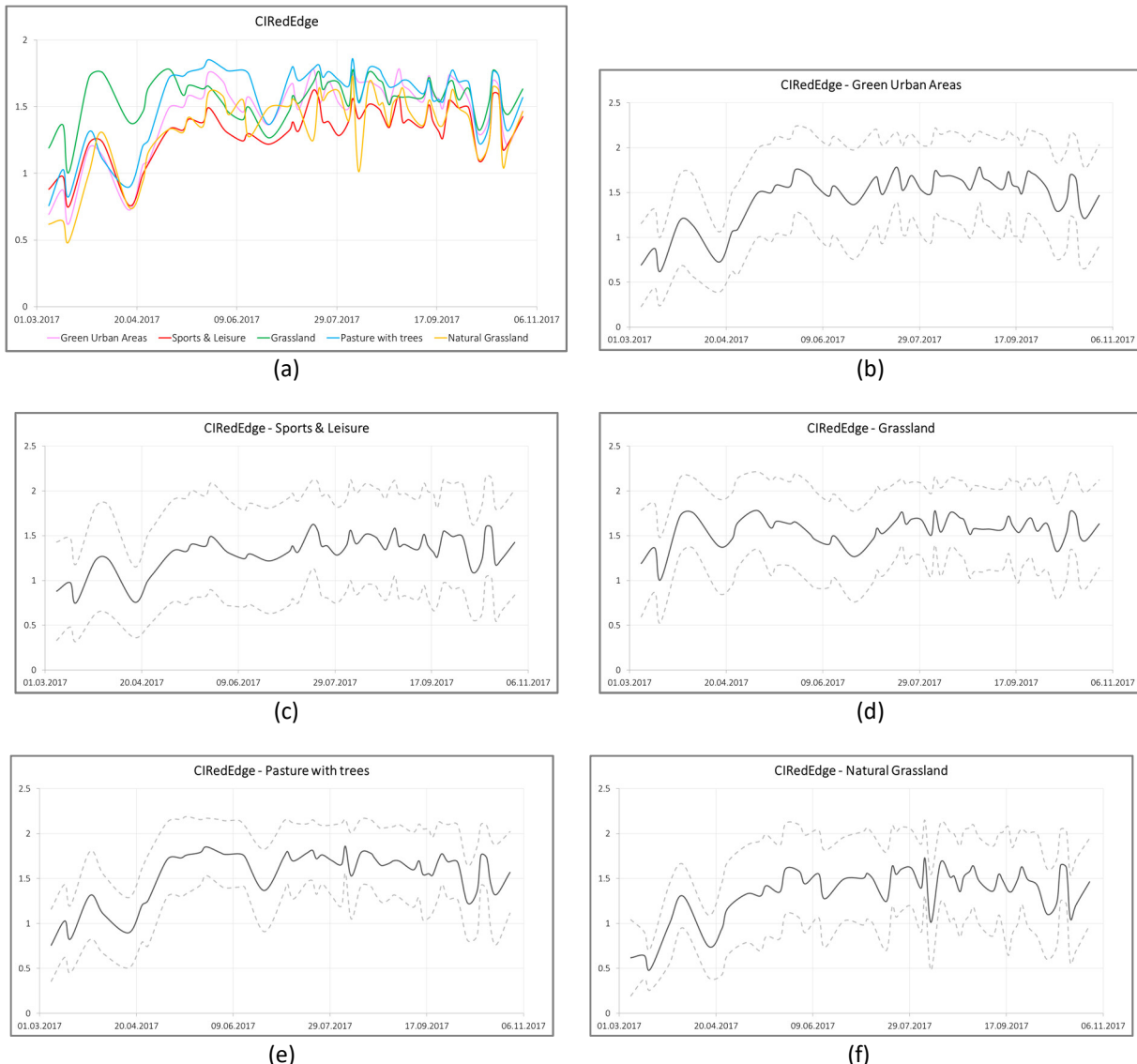
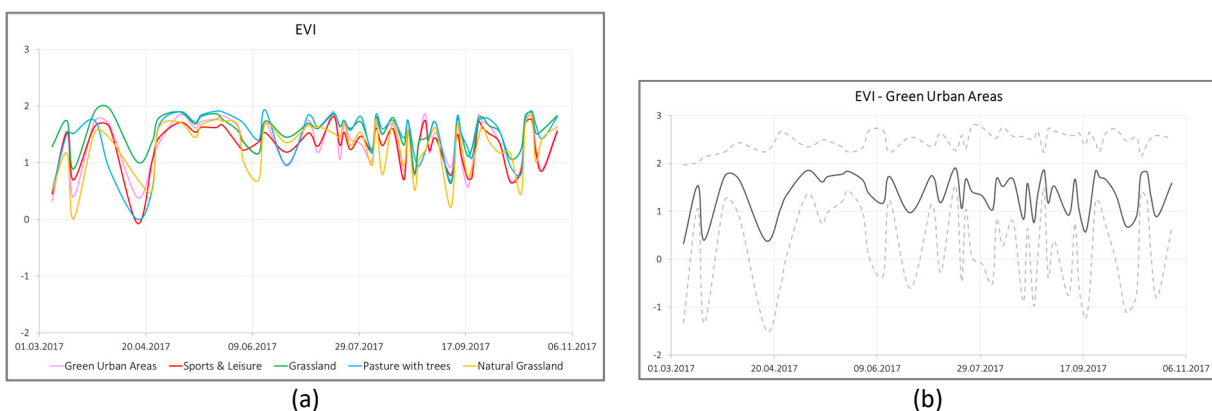


Figure 6-4: Overview of the MEAN spectral signature of the index CIRedEdge for all five grassland types (a) as well as the MEAN +/- the standard deviation for the single five grassland types: (b) green urban areas, (c) sports and leisure areas, (d) pastures with trees, (e) grassland (agriculturally used), and (f) natural grasslands.



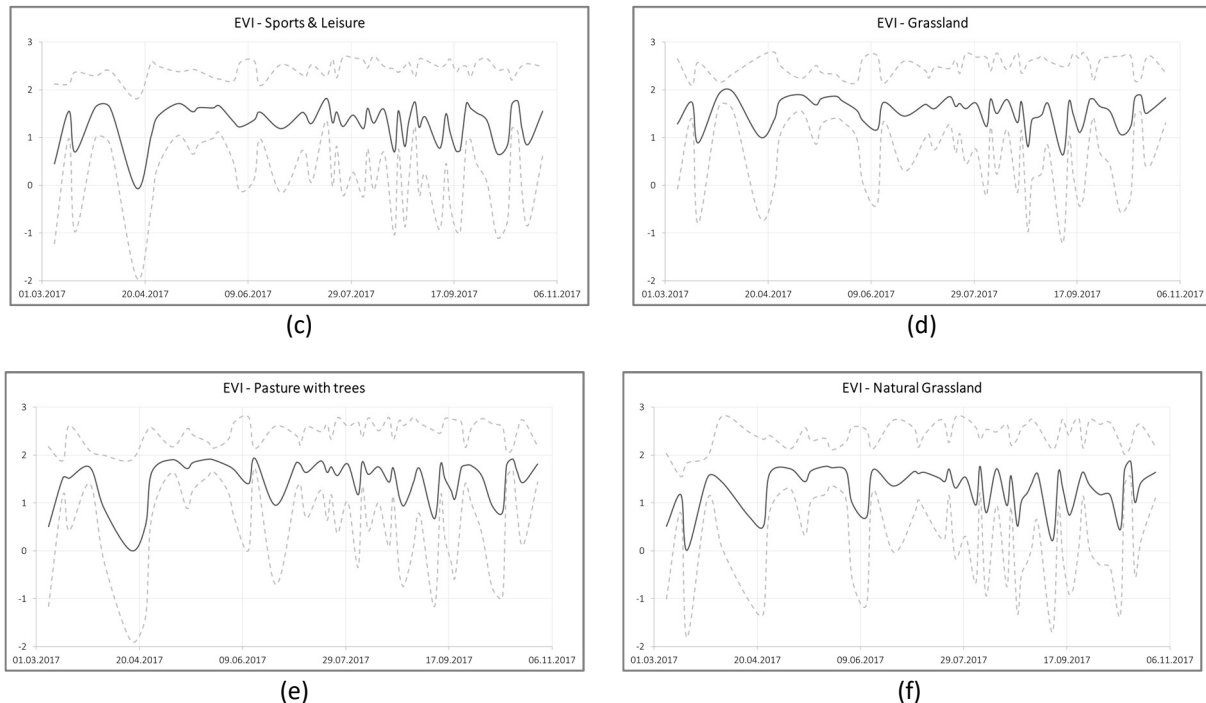
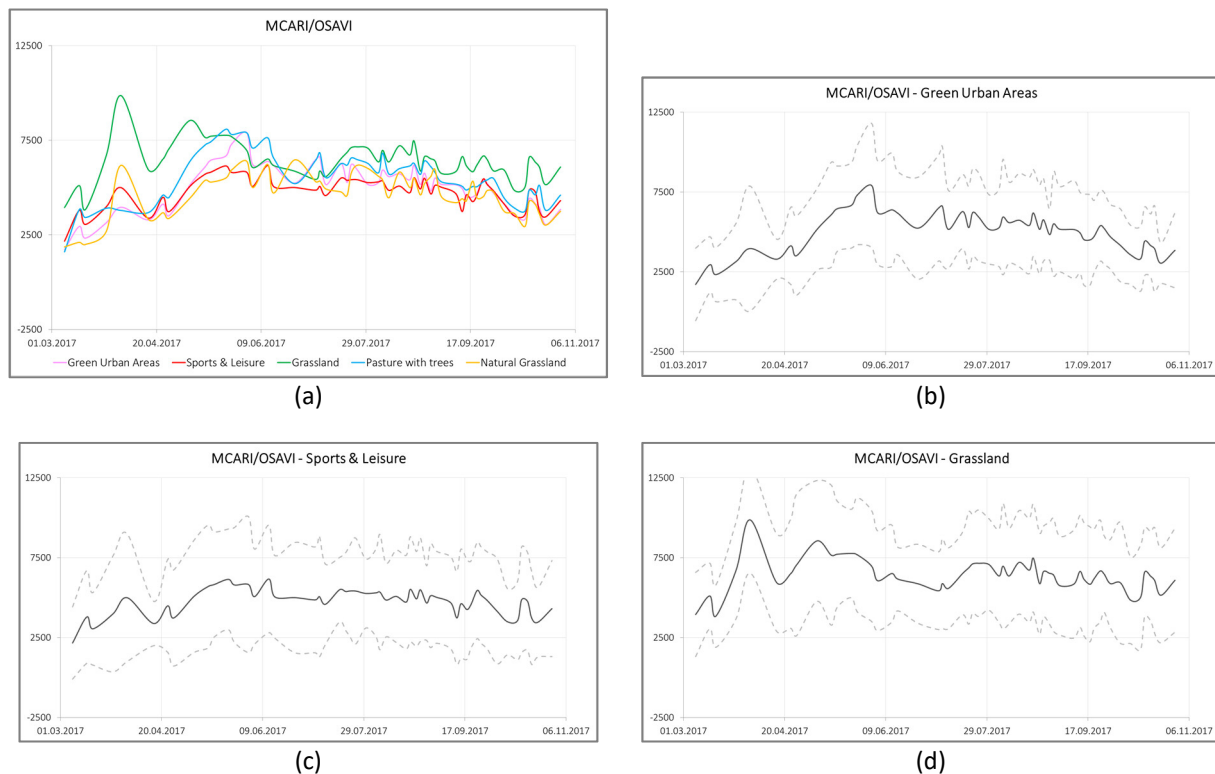


Figure 6-5: Overview of the MEAN spectral signature of the index EVI for all five grassland types (a) as well as the MEAN +/- the standard deviation for the single five grassland types: (b) green urban areas, (c) sports and leisure areas, (d) pastures with trees, (e) grassland (agriculturally used), and (f) natural grasslands.



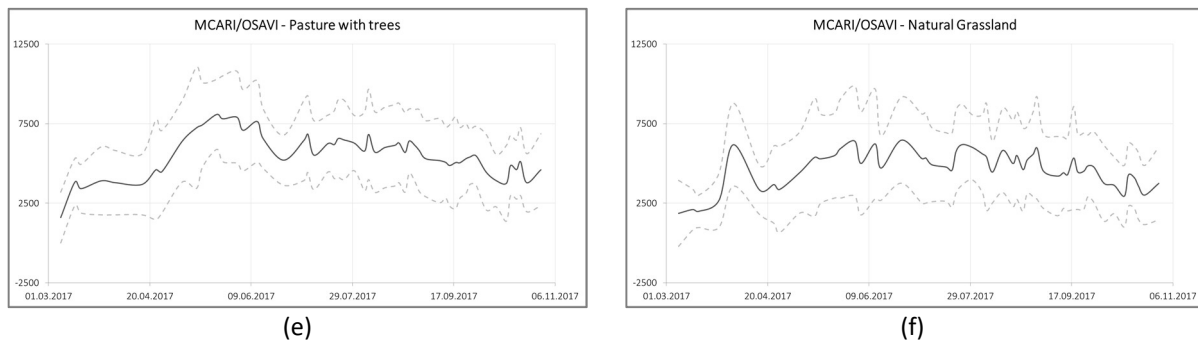


Figure 6-6: Overview of the MEAN spectral signature of the index MCARI/OSAVI for all five grassland types (a) as well as the MEAN +/- the standard deviation for the single five grassland types: (b) green urban areas, (c) sports and leisure areas, (d) pastures with trees, (e) grassland (agriculturally used), and (f) natural grasslands.

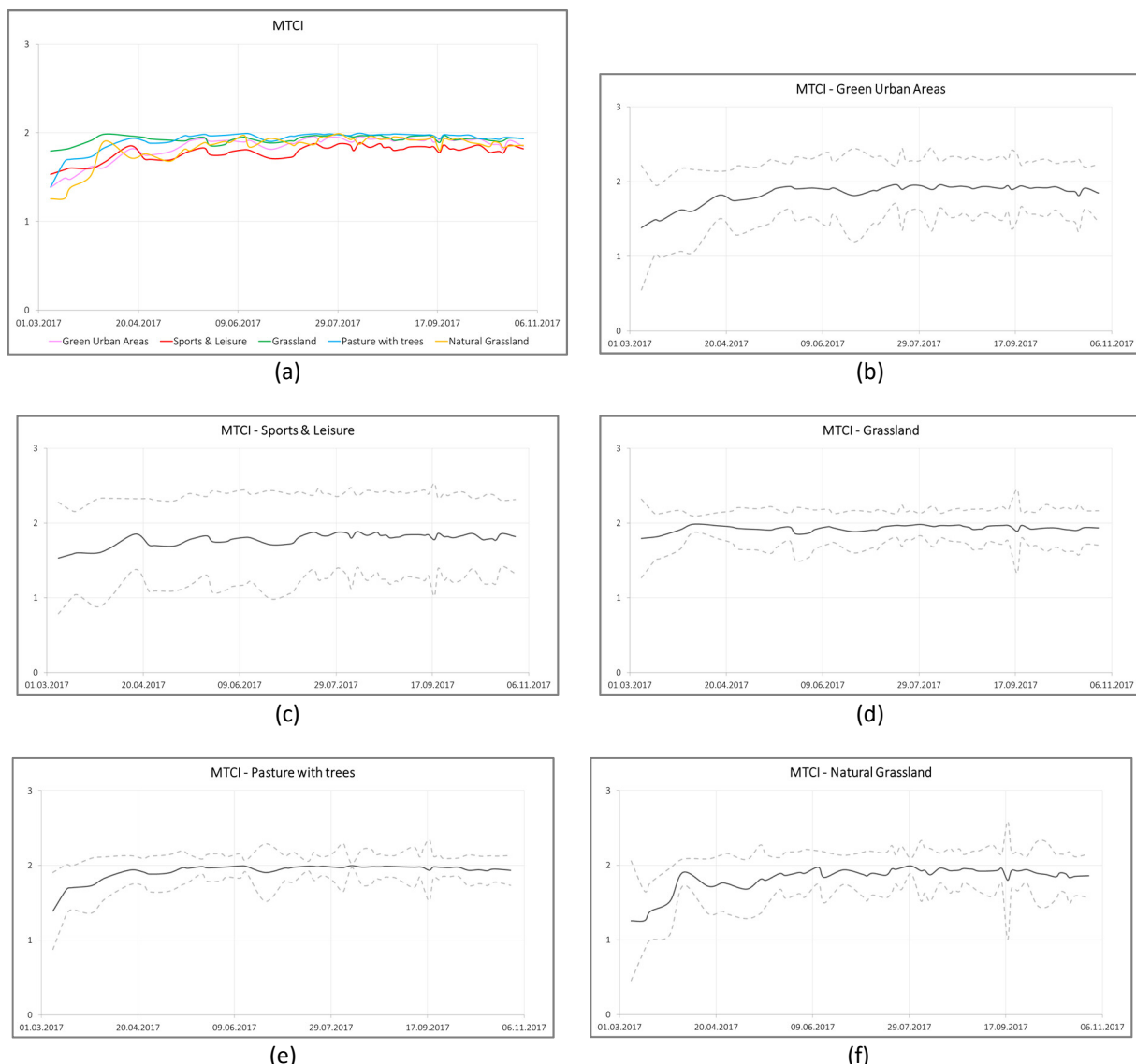


Figure 6-7: Overview of the MEAN spectral signature of the index MTCI for all five grassland types (a) as well as the MEAN +/- the standard deviation for the single five grassland types: (b) green urban areas, (c) sports and leisure areas, (d) pastures with trees, (e) grassland (agriculturally used), and (f) natural grasslands.

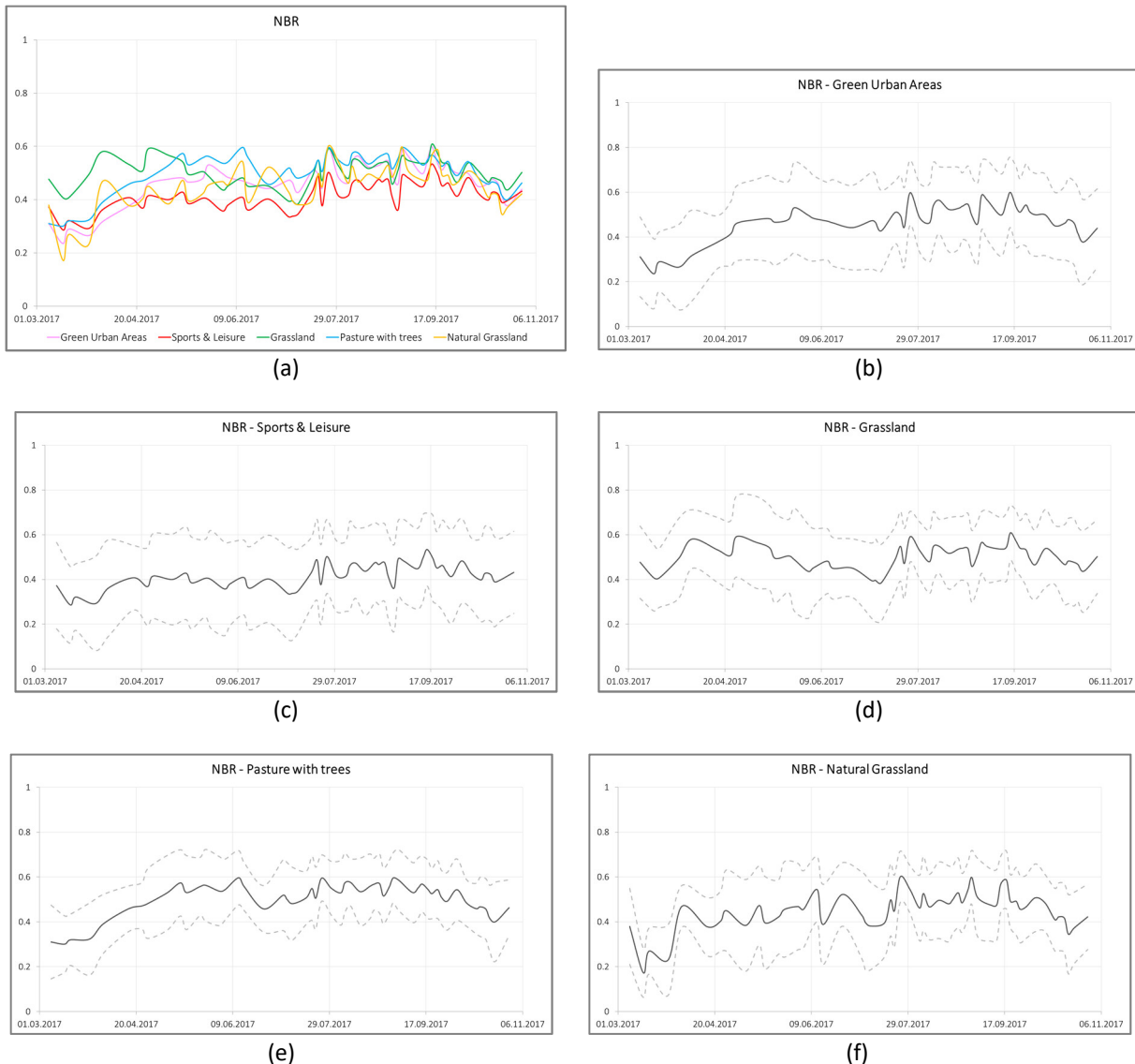
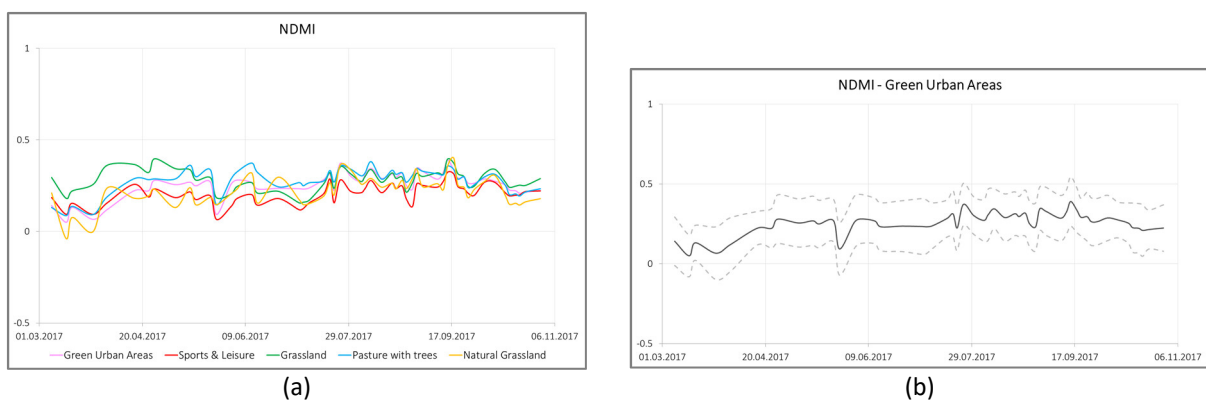


Figure 6-8: Overview of the MEAN spectral signature of the index NBR for all five grassland types (a) as well as the MEAN +/- the standard deviation for the single five grassland types: (b) green urban areas, (c) sports and leisure areas, (d) pastures with trees, (e) grassland (agriculturally used), and (f) natural grasslands.



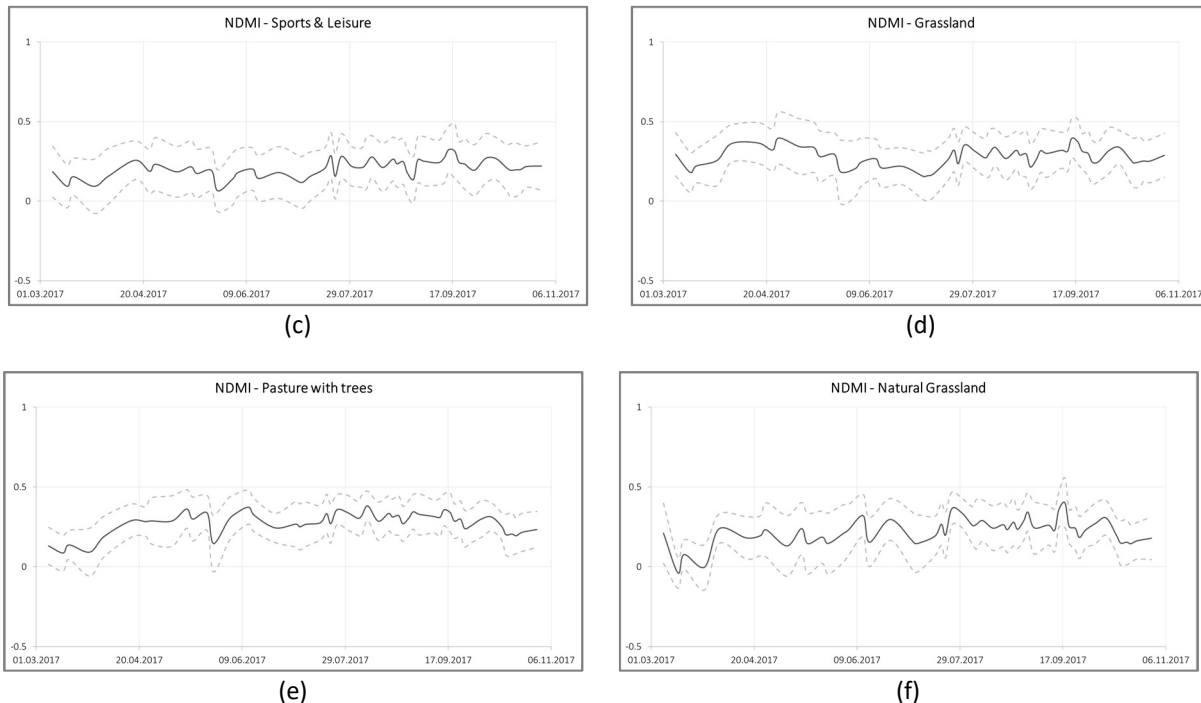
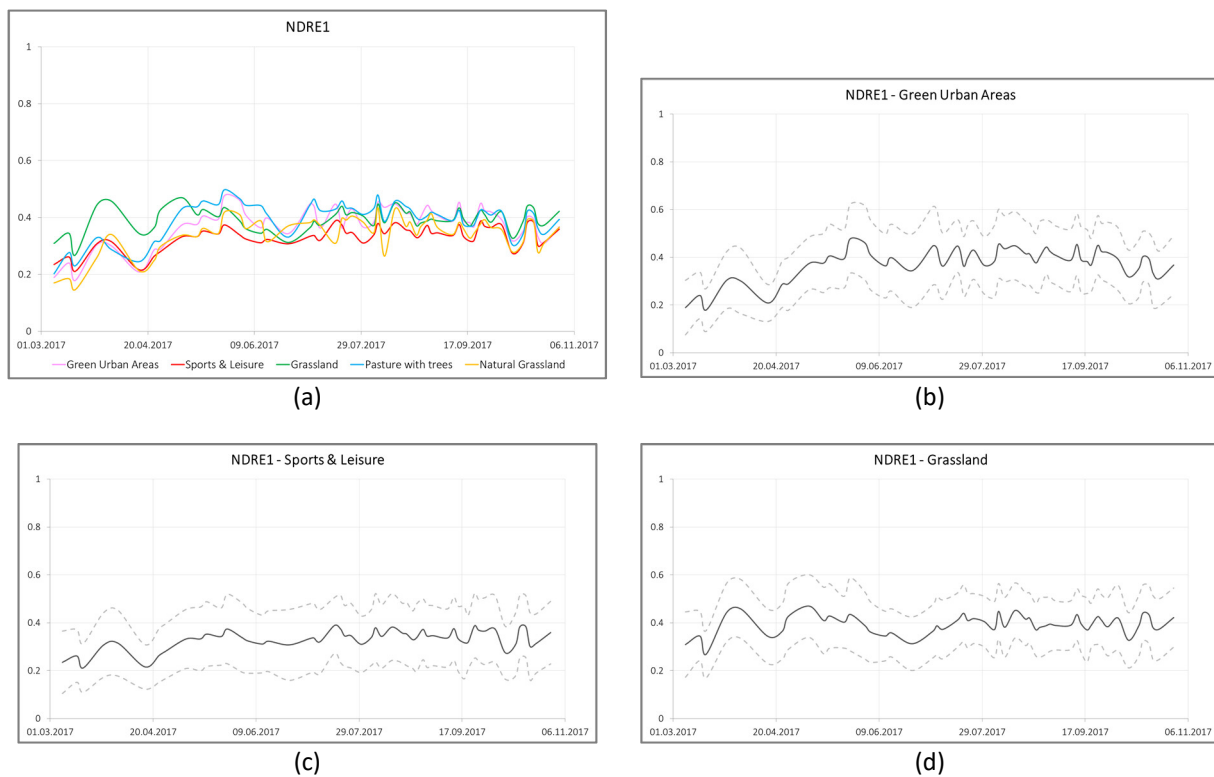


Figure 6-9: Overview of the MEAN spectral signature of the index NDMI for all five grassland types (a) as well as the MEAN +/- the standard deviation for the single five grassland types: (b) green urban areas, (c) sports and leisure areas, (d) pastures with trees, (e) grassland (agriculturally used), and (f) natural grasslands.



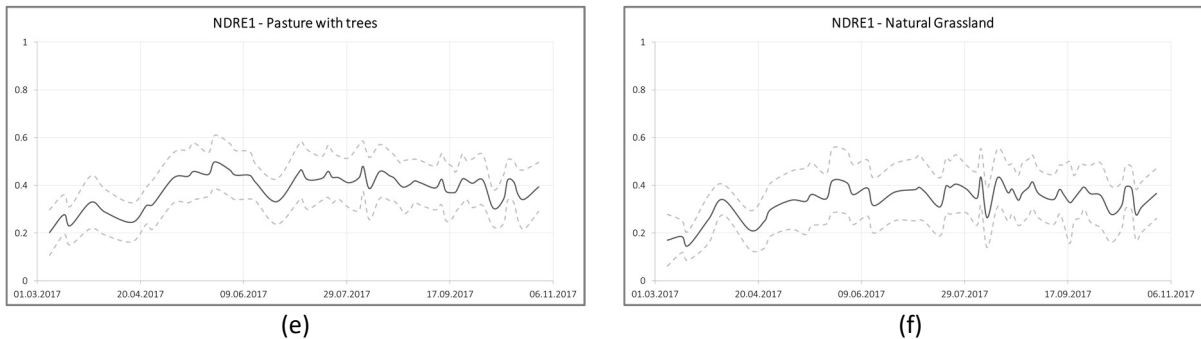


Figure 6-10: Overview of the MEAN spectral signature of the index NDRE1 for all five grassland types (a) as well as the MEAN +/- the standard deviation for the single five grassland types: (b) green urban areas, (c) sports and leisure areas, (d) pastures with trees, (e) grassland (agriculturally used), and (f) natural grasslands.

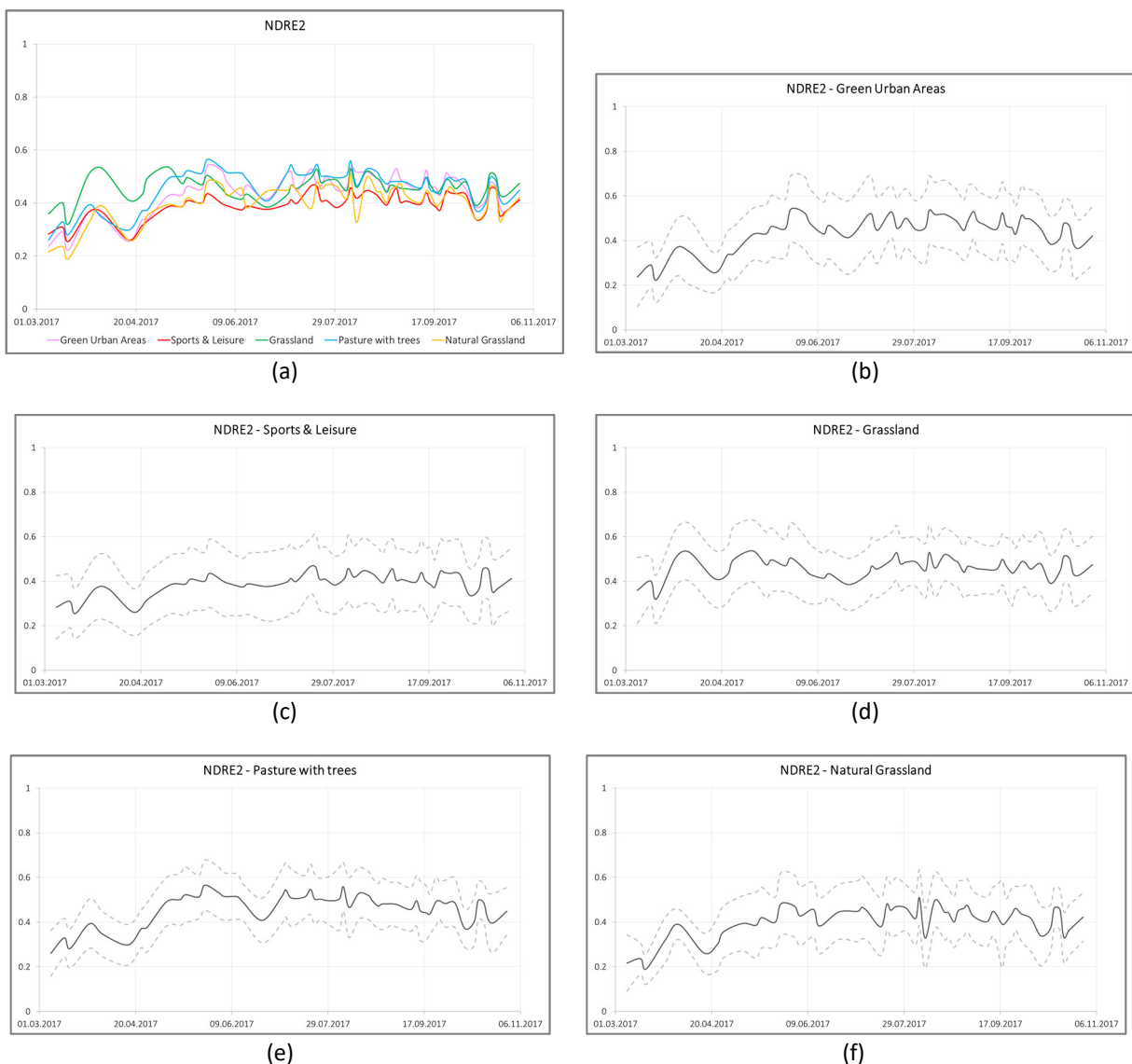


Figure 6-11: Overview of the MEAN spectral signature of the index NDRE2 for all five grassland types (a) as well as the MEAN +/- the standard deviation for the single five grassland types: (b) green urban areas, (c) sports and leisure areas, (d) pastures with trees, (e) grassland (agriculturally used), and (f) natural grasslands.

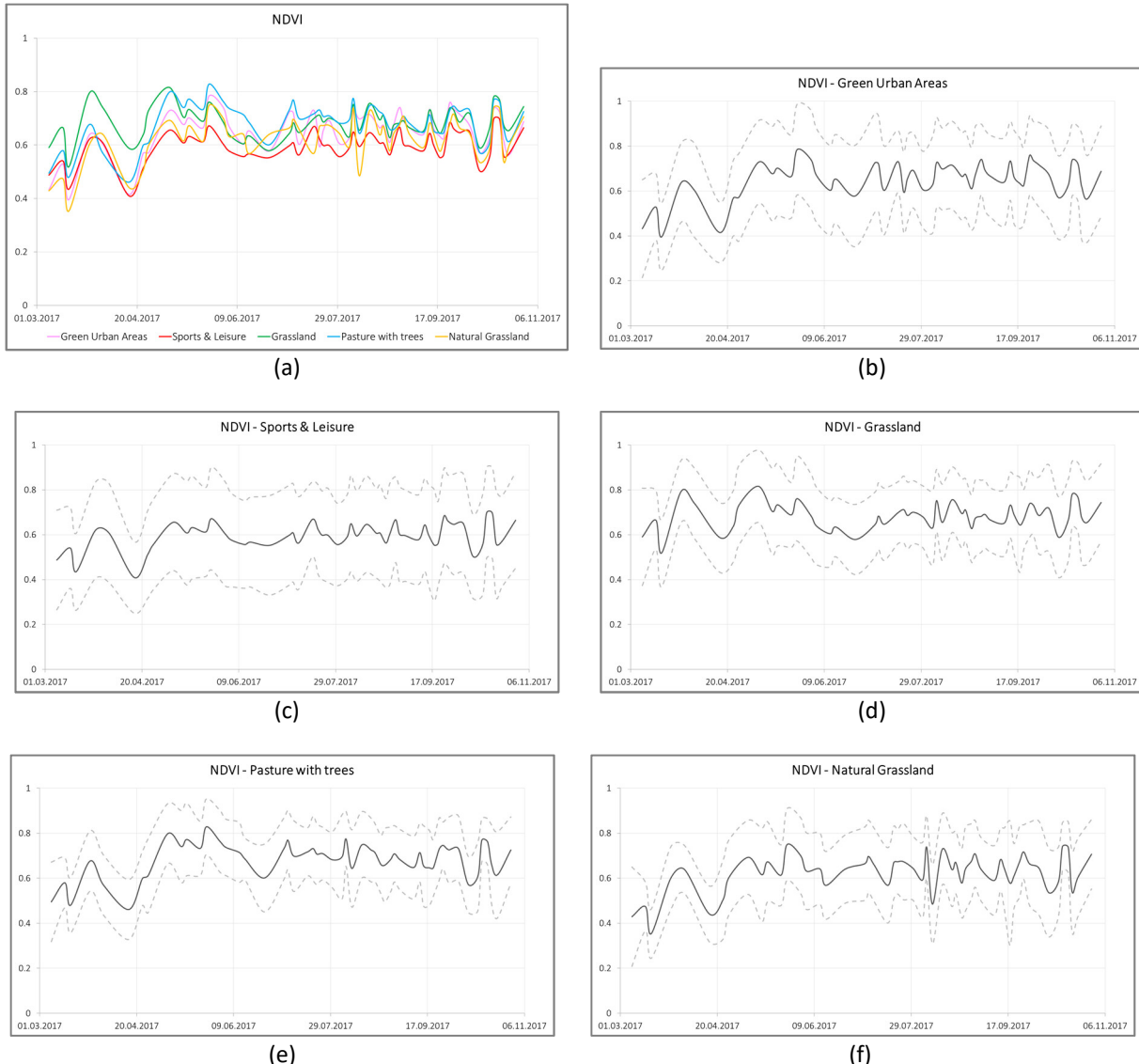
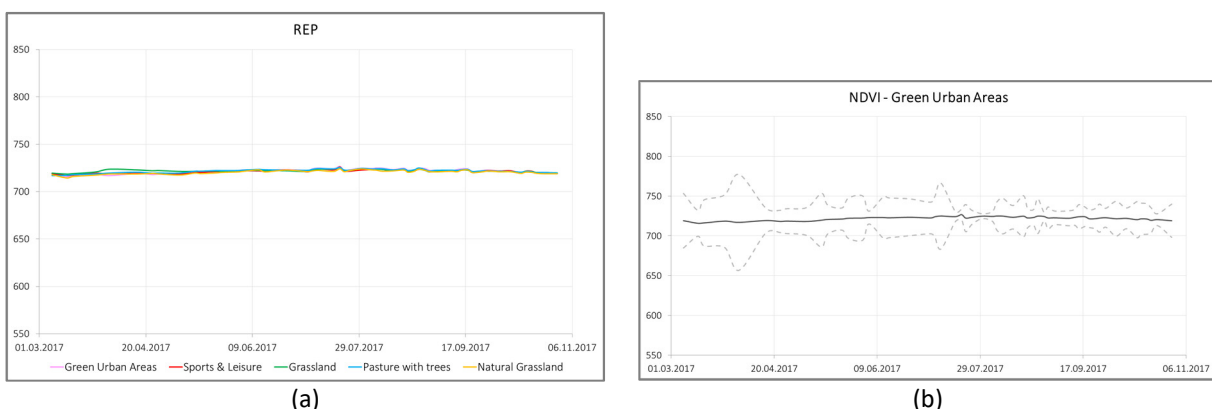


Figure 6-12: Overview of the MEAN spectral signature of the index NDVI for all five grassland types (a) as well as the MEAN +/- the standard deviation for the single five grassland types: (b) green urban areas, (c) sports and leisure areas, (d) pastures with trees, (e) grassland (agriculturally used), and (f) natural grasslands.



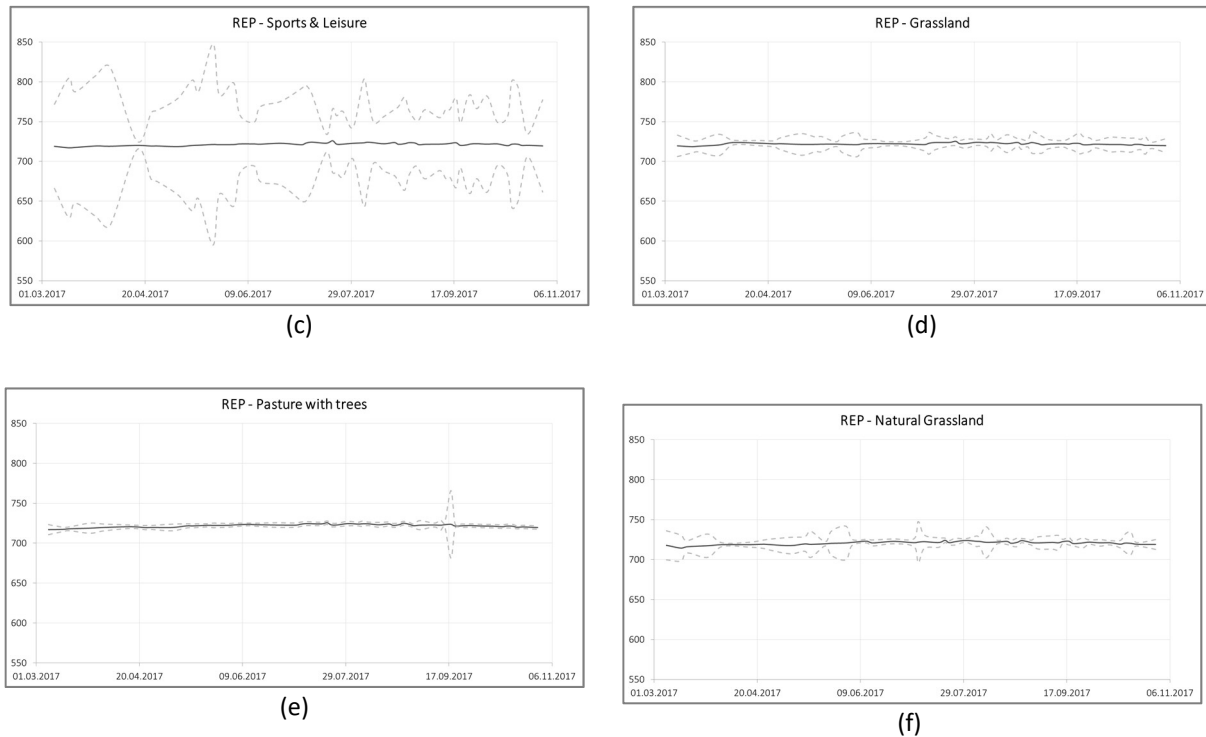
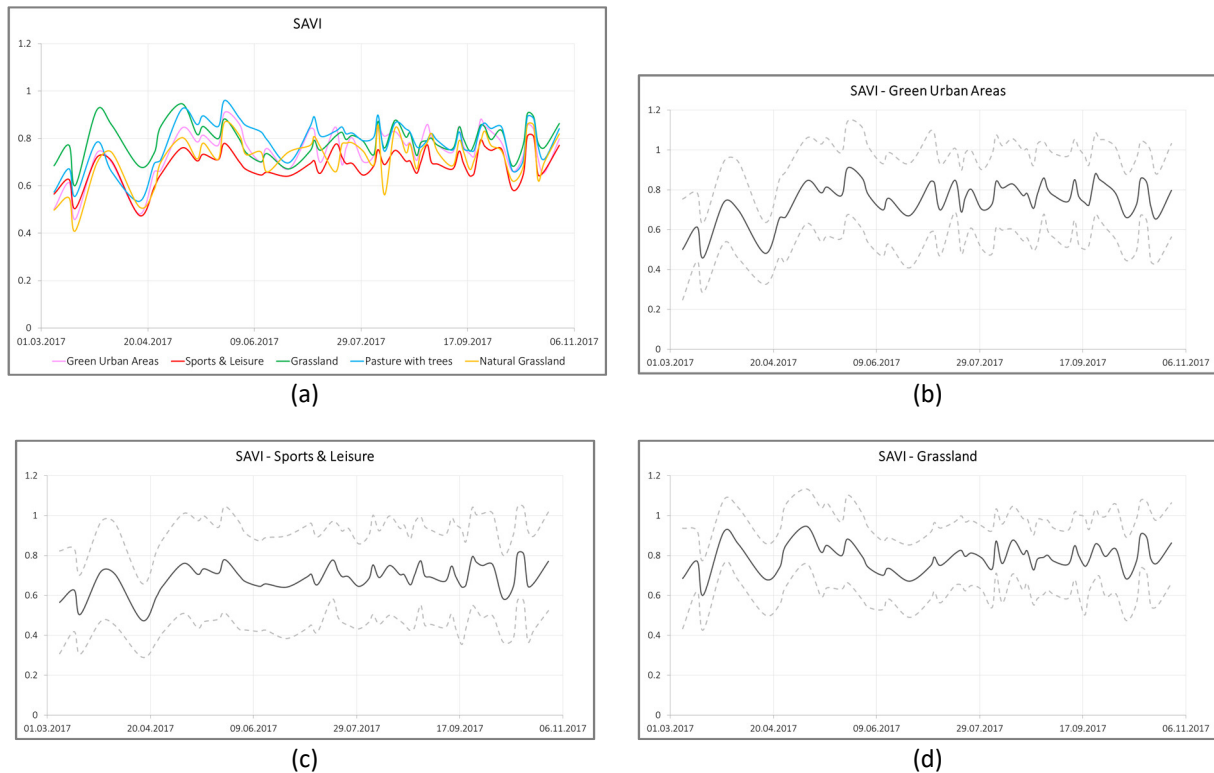


Figure 6-13: Overview of the MEAN spectral signature of the index REP for all five grassland types (a) as well as the MEAN +/- the standard deviation for the single five grassland types: (b) green urban areas, (c) sports and leisure areas, (d) pastures with trees, (e) grassland (agriculturally used), and (f) natural grasslands.



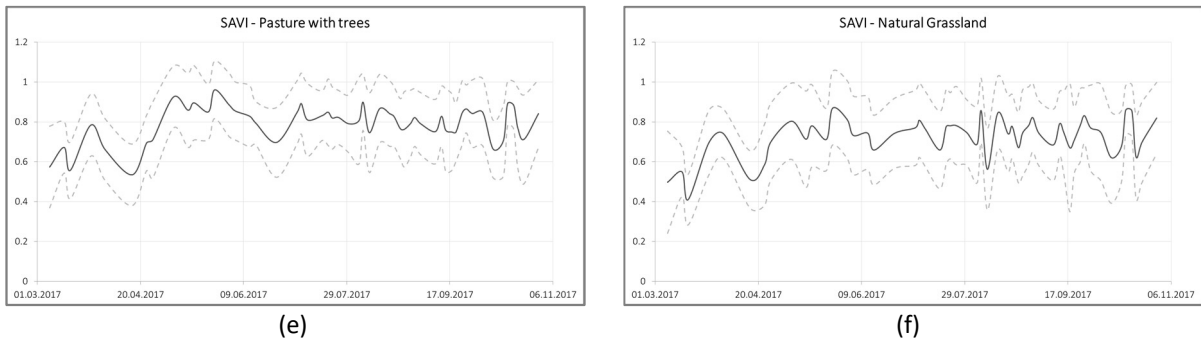


Figure 6-14: Overview of the MEAN spectral signature of the index SAVI for all five grassland types (a) as well as the MEAN +/- the standard deviation for the single five grassland types: (b) green urban areas, (c) sports and leisure areas, (d) pastures with trees, (e) grassland (agriculturally used), and (f) natural grasslands.

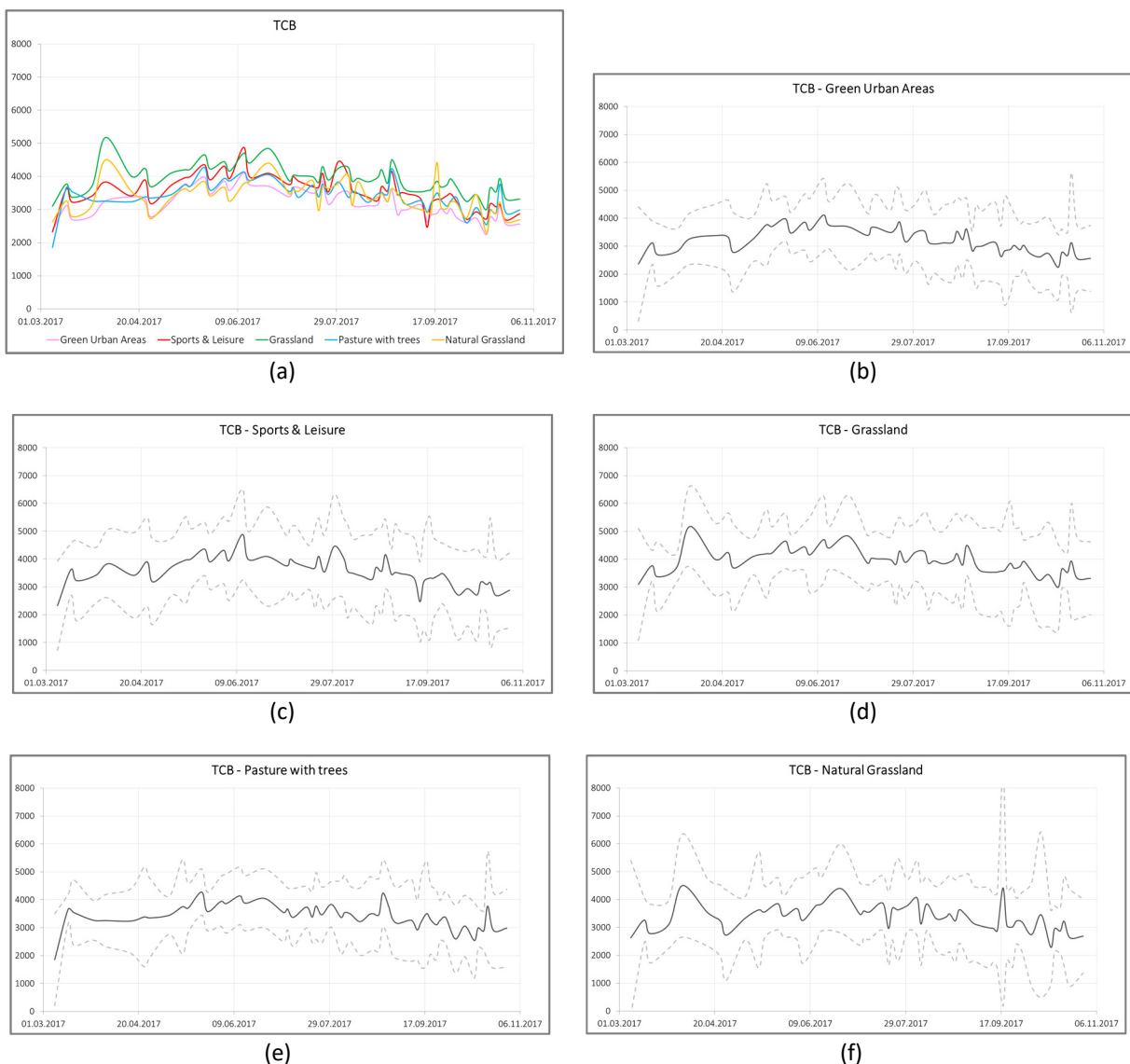


Figure 6-15: Overview of the MEAN spectral signature of the index TCB for all five grassland types (a) as well as the MEAN +/- the standard deviation for the single five grassland types: (b) green urban areas, (c) sports and leisure areas, (d) pastures with trees, (e) grassland (agriculturally used), and (f) natural grasslands.

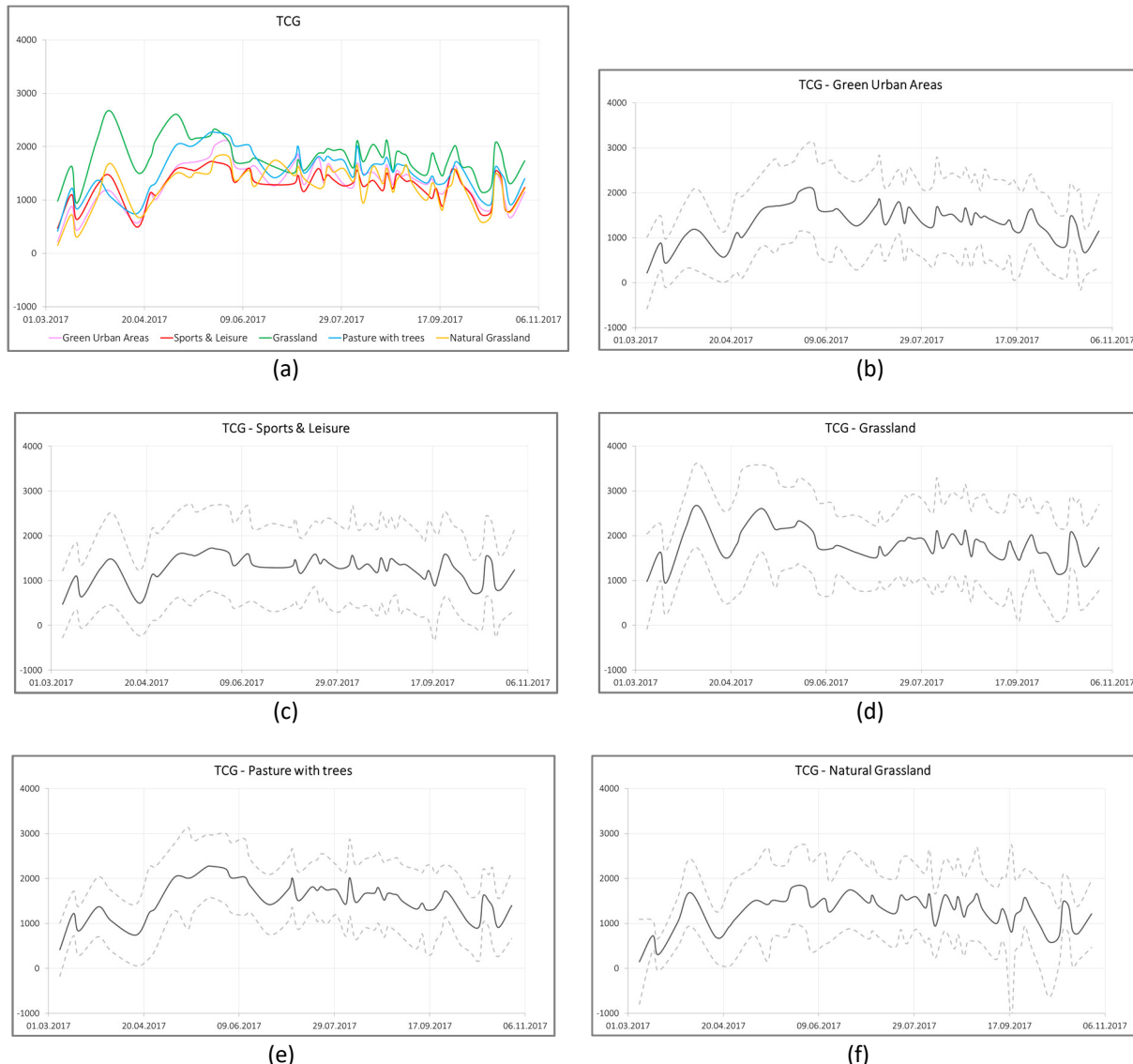
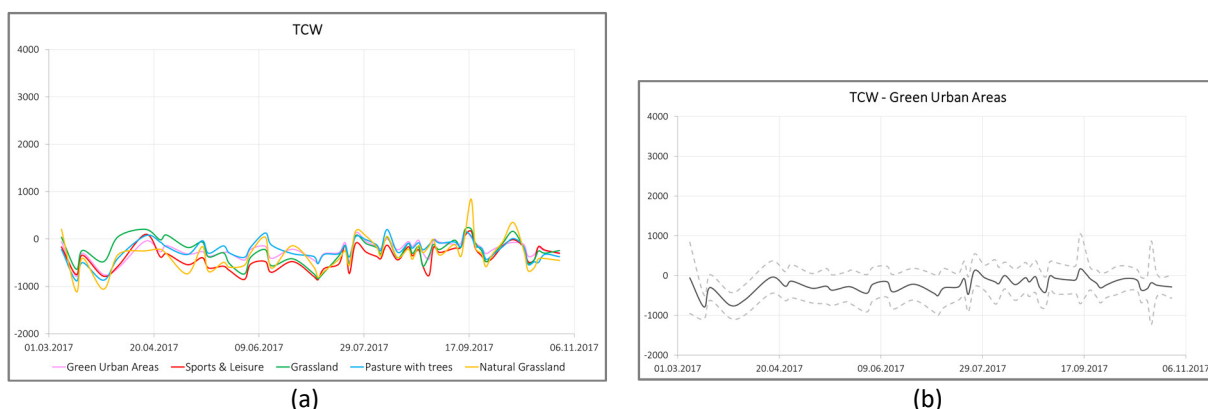


Figure 6-16: Overview of the MEAN spectral signature of the index TCG for all five grassland types (a) as well as the MEAN +/- the standard deviation for the single five grassland types: (b) green urban areas, (c) sports and leisure areas, (d) pastures with trees, (e) grassland (agriculturally used), and (f) natural grasslands.



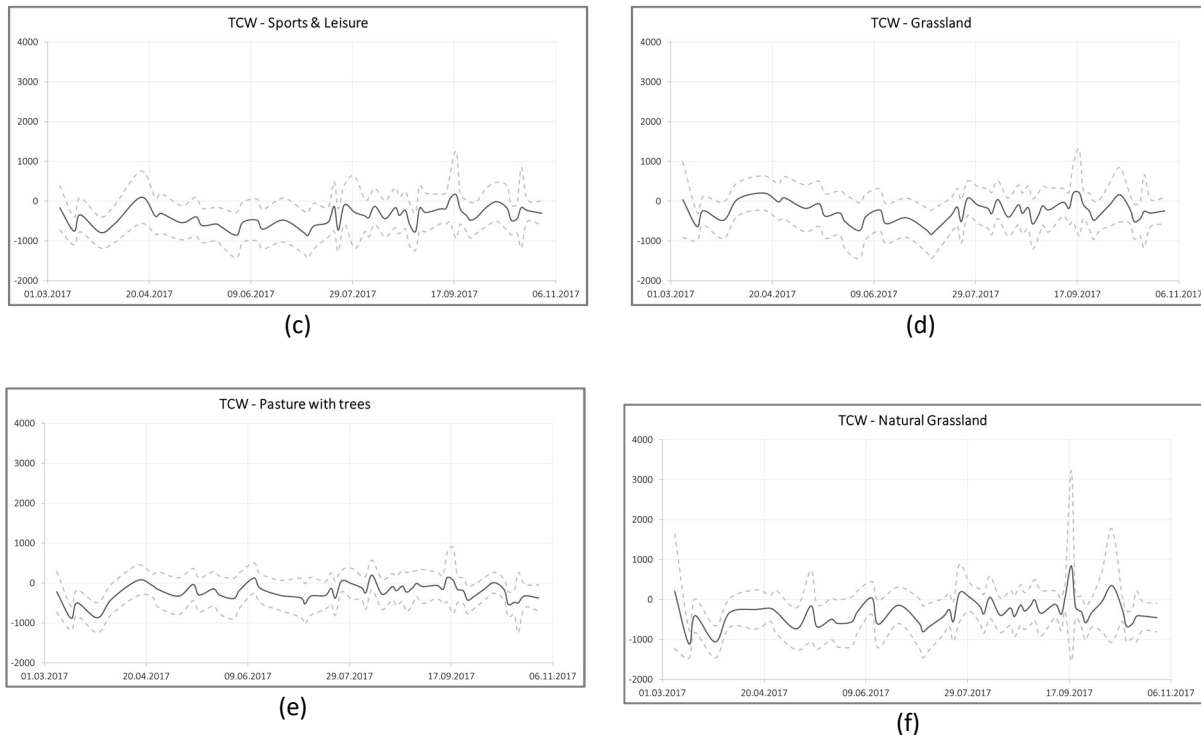


Figure 6-17: Overview of the MEAN spectral signature of the index TCW for all five grassland types (a) as well as the MEAN +/- the standard deviation for the single five grassland types: (b) green urban areas, (c) sports and leisure areas, (d) pastures with trees, (e) grassland (agriculturally used), and (f) natural grasslands.